

# NOTE TO USERS

This reproduction is the best copy available.

**UMI<sup>®</sup>**



The Cretaceous rocks of the Orpheus Graben, offshore Nova Scotia

By

Shawna L. Weir-Murphy

B.Sc., Saint Mary's University, 2002

A Thesis Submitted in Partial Fulfillment of  
The Requirements For The Degree of Master of Science

In

The Faculty of Graduate Studies

Department of Geology

Saint Mary's University

June, 2004

© Shawna L. Weir-Murphy, 2004



Library and  
Archives Canada

Bibliothèque et  
Archives Canada

Published Heritage  
Branch

Direction du  
Patrimoine de l'édition

395 Wellington Street  
Ottawa ON K1A 0N4  
Canada

395, rue Wellington  
Ottawa ON K1A 0N4  
Canada

*Your file* *Votre référence*

*ISBN: 0-612-93678-3*

*Our file* *Notre référence*

*ISBN: 0-612-93678-3*

The author has granted a non-exclusive license allowing the Library and Archives Canada to reproduce, loan, distribute or sell copies of this thesis in microform, paper or electronic formats.

L'auteur a accordé une licence non exclusive permettant à la Bibliothèque et Archives Canada de reproduire, prêter, distribuer ou vendre des copies de cette thèse sous la forme de microfiche/film, de reproduction sur papier ou sur format électronique.

The author retains ownership of the copyright in this thesis. Neither the thesis nor substantial extracts from it may be printed or otherwise reproduced without the author's permission.

L'auteur conserve la propriété du droit d'auteur qui protège cette thèse. Ni la thèse ni des extraits substantiels de celle-ci ne doivent être imprimés ou autrement reproduits sans son autorisation.

---

In compliance with the Canadian Privacy Act some supporting forms may have been removed from this thesis.

Conformément à la loi canadienne sur la protection de la vie privée, quelques formulaires secondaires ont été enlevés de cette thèse.

While these forms may be included in the document page count, their removal does not represent any loss of content from the thesis.

Bien que ces formulaires aient inclus dans la pagination, il n'y aura aucun contenu manquant.

**Canada**

## **Cretaceous rocks of Orpheus Graben, offshore Nova Scotia**

S.L. Weir Murphy

June 2004

### **Abstract**

The Orpheus Graben is an offshore Mesozoic basin along the trace of the Cobequid - Chedabucto fault system, along strike from the Lower Cretaceous Chaswood Formation of central Nova Scotia. Orpheus Graben contains up to 10 km of Upper Triassic and Lower Jurassic strata, including the Argo salt, overlain by a relatively thin succession of Upper Jurassic to Lower Tertiary strata. The Missisauga Formation is divisible into its Middle and Upper members and the Logan Canyon Formation is divisible into the Naskapi, Cree, Sable and Marmora members in the Orpheus Graben. The sediments are most likely those of delta plain to shoreface environments, which experienced two episodes of open marine conditions. Two volcanic intervals and one pyroclastic unit are also observed.

All observed detrital lithic clasts of both formations in Orpheus Graben could have been derived from the Meguma and Avalon terranes. The detrital mineral grains observed suggest that they are likely from a distant source. Rather different detrital petrology in the Chaswood Formation and Sable Subbasin suggests they had a different fluvial supply than the Orpheus Graben. The sediments of the Orpheus Graben are interpreted to have an important local provenance, originating from the North of the graben with an additional source from metamorphic rocks of the Taconic Orogen and Canadian Shield. Early diagenetic cements include siderite (principally in mudstone), calcite, ankerite, pyrite, hematite, glauconite, limonite and francolite. Later diagenetic minerals include kaolinite, illite, sepioclorite, chlorite, siderite and barite. Basalt cuttings are found to alter to stilpnomelane, chlorite, siderite and calcite.

At least five unconformities are observed in the Orpheus Graben, the last three of which are thought to correspond to the last three erosional events that make up the multi-phase "Avalon Unconformity", formed by the progressive rifting of Iberia and the Grand Banks and movement along the Cobequid-Chedabucto-SW Grand Banks transform fault system. There appear to be four types of faults in the Orpheus Graben: ENE-WSW trending faults that define the graben; faults possibly associated with the breakup of Grand Banks and Iberia; ENE-WSW trending faults in the northernmost part of the northeastern section of the graben; and faults related to salt tectonics. In the Cretaceous-Tertiary interval, older Lower Cretaceous syn-depositional faulting probably corresponds to syn-sedimentary tectonism in the onshore Chaswood Formation, whereas younger (Oligocene-Miocene?) faulting is interpreted to relate to the uplift and erosion of the inferred 700 m thick post-Chaswood sediments of the onshore region.

## **ACKNOWLEDGMENTS**

I would like to thank NSERC, Exxon Mobil Sable Project, PR-AC and Saint Mary's University for funding, S. Ingram for conducting the well logging, sampling and sample preparation for the probe thin sections, C. Albert for petrographically describing all cuttings > 2 mm, and O. Suleyman for performing the carbonate analyses on the marl samples. I would also like to thank G. Brown for making the probe thin sections, P. Stoffyn and R. MacKay for their assistance with the electron micro-probe analysis, F. Thomas for his help with the ESEM, J. Shimeld for the use of his scanner, Seismic Micro Technologies for the Kingdom Suite software, D. Mosher for conducting the 2D-3D seismic interpretation course, M.J. Verrall and N. Williams from the Canada Offshore Petroleum Board for their help with the sidewall cores and well history reports and R. Corney for his computer expertise.

Without the help of Georgia Pe-Piper, Pierre Jutras, Andrew MacRae, and David Piper this project would not have been as successful. Thank you Georgia for being a combination of supervisor and mom and Andrew for reminding me that it is ok to say "I don't know" when I don't know the answer, to ask for help when I need it, and to have confidence in myself and my work. I would also like to thank my family for their support, my friends (especially Angela Ford) for their patience and pampering during times of stress, and my husband Scott for knowing that I could do it even when I thought I couldn't, and for loving me through the crankiest and whiniest times.

## TABLE OF CONTENTS

<b>ABSTRACT</b> .....	<b>2</b>
<b>ACKNOWLEDGMENTS</b> .....	<b>3</b>
<b>TABLE OF CONTENTS</b> .....	<b>4</b>
<b>LIST OF FIGURES</b> .....	<b>7</b>
<b>LIST OF TABLES</b> .....	<b>9</b>
<b>CHAPTER 1</b> .....	<b>10</b>
<b>INTRODUCTION AND BACKGROUND</b> .....	<b>10</b>
1.1 Introduction.....	10
1.2 Objectives of This Study.....	13
Previous Work .....	14
1.3.1 Tectonic History of the Scotian Margin.....	14
1.3.2 Depositional History of the Orpheus Graben.....	15
1.3.3 Mic Mac, Missisauga, Logan Canyon and Dawson Canyon formations.....	18
1.3.4 Volcanic Rocks .....	24
<b>CHAPTER 2</b> .....	<b>25</b>
<b>METHODS</b> .....	<b>25</b>
2.1 Petrographic study .....	25
2.1.1 Conventional cores.....	25
2.1.2 Sidewall cores .....	25
2.1.3 Cutting sample preparation .....	25
2.1.4 Identification of cuttings > 2 mm.....	26
2.1.5 Identification of heavy fraction of cuttings < 2 mm .....	26
2.1.6 Microprobe analysis.....	27
2.1.7 Scanning electron microscopy .....	27
2.1.8 Carbonate analyses.....	28
2.2 Lithostratigraphic Interpretations.....	28
2.3 Seismic Reflection Data.....	29
2.3.1 Data preparation.....	31
2.3.2 Data interpretation .....	31
2.3.4 Synthetic seismograms.....	32
<b>CHAPTER 3</b> .....	<b>34</b>
<b>LITHOSTRATIGRAPHY</b> .....	<b>34</b>
3.1 Introduction.....	34
3.2 Fox I-22 (D23) .....	37
3.3 Crow F-52 (D20).....	42
3.4 Argo F-38 (D17) .....	48
3.5 Jason C-20 (D131) .....	55
3.6 Eurydice P-36 (D034) .....	62
3.7 Hercules G-15 (D130).....	66
3.8 Adventure F-80 (D144).....	69
<b>CHAPTER 4</b> .....	<b>72</b>
<b>SEISMIC MARKERS AND CORRELATION WITH THE</b>	
<b>LITHOSTRATIGRAPHY</b> .....	<b>72</b>
4.1 Introduction.....	72

4.1.1 The U1 Marker.....	74
4.1.2 The U2 Marker.....	74
4.1.3 The Petrel Marker .....	74
4.1.4 The Green Marker.....	77
4.1.5 The U3 Marker.....	77
4.1.6 The Volcanic Marker .....	79
4.1.7 The U4 Marker.....	81
4.1.8 The Mic Mac Marker .....	81
4.1.9 The U5 Marker.....	83
4.1.10 Other Markers .....	83
4.2 Regional distribution of the lithostratigraphic units from seismic data.....	86
<b>CHAPTER 5.....</b>	<b>89</b>
<b>SEISMIC INTERPRETATIONS AND STRUCTURE.....</b>	<b>89</b>
5.1 Introduction.....	89
5.2 Acoustic Facies .....	89
5.2.1 Facies A .....	89
5.2.2 Facies B.....	90
5.2.3 Facies C.....	91
5.2.4 Facies D .....	91
5.2.5 Facies E.....	92
5.3 Salt acoustic facies and structure .....	93
5.4 Faults.....	99
<b>CHAPTER 6.....</b>	<b>106</b>
<b>PETROLOGICAL STUDY .....</b>	<b>106</b>
6.1 Introduction.....	106
6.2 Petrography of grains .....	106
6.2.1 Mic Mac Formation .....	106
6.2.2 Missisauga Formation.....	107
6.2.3 Cree Member .....	108
6.2.4 Sable Member .....	108
6.2.5 Marmorata Member .....	109
6.2.6 Trends observed between wells, formations, and members .....	109
6.3 Provenance.....	113
6.3.1 Detrital mineral provenance.....	113
6.3.2 Lithic clast provenance .....	114
6.4 Diagenetic minerals .....	115
6.4.1 Francolite .....	117
6.4.2 Septochlorites.....	121
6.4.3 Stilpnomelane .....	123
6.5 Contaminants .....	124
<b>CHAPTER 7.....</b>	<b>127</b>
<b>DISCUSSION AND CONCLUSIONS.....</b>	<b>127</b>
7.1 Introduction.....	127
7.2 Correlation between wells.....	127
7.2.1 Hercules Biostratigraphy .....	130
7.2.2 Base Cretaceous unconformity (U5).....	131

7.2.3 Missisauga Formation.....	132
7.2.4 Top Missisauga unconformity (U4).....	135
7.2.5 Naskapi Member.....	137
7.2.6 Volcanic interval of the Cree Member.....	139
7.2.7 Cree Member .....	143
7.2.8 Top Cree Unconformity.....	144
7.2.9 Sable Member .....	145
7.2.10 Marmora Member .....	146
7.3 Comparison with the Sable Subbasin and the onshore Chaswood Formation.....	148
7.3.1 Comparison with the Chaswood Formation onshore.....	148
7.3.2 Comparison with the Sable Subbasin .....	149
7.4 Tectonic evolution .....	150
7.5 Conclusions.....	157
<b>REFERENCES.....</b>	<b>163</b>
 <b>APPENDICES.....</b>	 refer to CD
Appendix 1 - Fox I-22.....	169
Appendix 2 - Crow F-52.....	245
Appendix 3 - Argo F-38.....	294
Appendix 4 - Jason C-20.....	356
Appendix 5 - Seismic Interpretations.....	408
Appendix 6 - Petrography of Grains > 2 mm.....	441
Appendix 7 - Petrographic Summary Tables.....	471

## LIST OF FIGURES

<b>Figure 1.1.</b> Map showing the location of the Orpheus Graben and the onshore Chaswood Formation.....	11
<b>Figure 1.2.</b> Map of study area showing the basement contours and the location of the wells and seismic lines studied (a in Figure 1.1).....	12
<b>Figure 1.3.</b> Generalized stratigraphic diagram for the eastern Scotian Shelf.....	16
<b>Figure 1.4.</b> Type section of the Missisauga Formation and its members (modified from Wade and MacLean, 1990).....	20
<b>Figure 1.5.</b> Type section of the Logan Canyon Formation and its members (modified from Wade and MacLean, 1990).....	21
<b>Figure 2.1.</b> Map showing the location of the interpreted seismic lines and wells studied in the Orpheus Graben.....	30
<b>Figure 2.2.</b> Enlargement of a in Figure 1.1 showing seismic lines interpreted in this study.....	30
<b>Figure 3.0.</b> General legend for lithostratigraphic plots.....	39
<b>Figure 3.1.</b> Lithostratigraphic plot for Fox I-22 showing formation, member and age boundaries and gamma, velocity and density wireline logs.....	40
<b>Figure 3.2.</b> Lithostratigraphic plot for Crow F-52 showing formation, member and age boundaries and gamma, velocity and density wireline logs.....	45
<b>Figure 3.3.</b> Lithostratigraphic plot for Argo F-38 showing formation, member and age boundaries and gamma, velocity and density wireline logs.....	51
<b>Figure 3.4.</b> Lithostratigraphic plot for Jason C-20 showing formation, member and age boundaries and gamma, velocity and density wireline logs.....	57
<b>Figure 3.5.</b> Lithostratigraphic plot for Eurydice P-36 showing formation, member and age boundaries and gamma, velocity and density wireline logs.....	64
<b>Figure 3.6.</b> Lithostratigraphic plot for Hercules G-15 showing formation, member and age boundaries and gamma, velocity and density wireline logs.....	67
<b>Figure 3.7.</b> Lithostratigraphic plot for Adventure F-80 showing formation, member and age boundaries and gamma, velocity and density wireline logs.....	70
<b>Figure 3.8.</b> Correlation diagram showing the members of the Logan Canyon (Marmora, Sable, Cree, and Naskapi) and Missisauga (Middle and Upper) formations.....	71
<b>Figure 4.1.</b> Line 390-B showing the correlation between the inferred lithostratigraphy at the Argo F-38 well and the corresponding seismic response (refer to Figure 2.1 for well and line location).....	75
<b>Figure 4.2.</b> Map showing the extent of the U2 marker.....	76
<b>Figure 4.3.</b> Map showing the extent of the Petrel marker.....	78
<b>Figure 4.4.</b> Map showing the extent of the Volcanic marker.....	80
<b>Figure 4.5.</b> Map showing the extent of the U4 marker.....	82
<b>Figure 4.6.</b> Map showing the extent of the U5 marker.....	84
<b>Figure 4.7.</b> Illustration of the typical chronological order of the key reflection markers in the seismic profiles. Also depicts the general regional (east-west) distribution of the lithostratigraphic units within the Orpheus Graben.....	87

<b>Figure 5.1.</b> Line 81-415 shows the acoustic character of the Argo Formation below the top Argo marker.....	94
<b>Figure 5.2.</b> Line 81-413 showing withdrawal minibasins that are thought to be filled with sediment of the Mohican and Mic Mac formations. ....	96
<b>Figure 5.3.</b> Line 4133-83 illustrating the typical salt structures and faulting observed in the northeastern part of the graben and in parts of the central graben.....	97
<b>Figure 5.4.</b> Line 390-B showing fault offsetting the Mohican marker to Petrel marker due to salt withdrawal to the north-northeast direction (to the right). ....	98
<b>Figure 5.5.</b> Map showing the top of Agro salt marker with contours.....	100
<b>Figure 5.6.</b> Isochron map for the top of Agro salt marker to the Basement marker showing the location of salt diapirs in the deepest parts of the graben.....	101
<b>Figure 5.7.</b> Isochron map for the top of Agro salt marker to Eurydice marker showing the location of salt diapirs.....	102
<b>Figure 5.8</b> A schematic cross section showing the four types of faults graben.....	103
<b>Figure 5.9.</b> A tie line between seismic lines 4123-83A, 4130-83 and 4127-83 showing the typical fault structures observed in the northeastern most part of the graben.....	105
<b>Figure 6.1.</b> Electron microprobe back-scattered electron image of a bone fragment....	110
<b>Figure 6.2.</b> Back-scattered electron images of cuttings containing francolite from Argo F-38.....	118
<b>Figure 6.3.</b> Back-scattered electron images of cuttings containing francolite from Argo F-38.....	119
<b>Figure 6.4.</b> Back-scattered electron images of cuttings containing francolite from Crow F-52. ....	120
<b>Figure 6.5.</b> Back-scattered electron images of cuttings containing septochlorite diagenetic minerals.....	122
<b>Figure 6.6.</b> Back-scattered electron images of cuttings containing septochlorite diagenetic minerals.....	123
<b>Figure 6.7.</b> Back-scattered electron images of some cuttings containing stilpnomelane diagenetic minerals.....	124
<b>Figure 6.8.</b> Back-scattered electron images of contaminants.....	126
<b>Figure 7.1.</b> Generalized W-E stratigraphic column.....	128
<b>Figure 7.2.</b> Correlation diagram for the Lower Cretaceous sediments within the seven wells in the Orpheus Graben.....	back pocket
<b>Figure 7.3.</b> Line 3604-1 showing the location of the volcanic interval at the Hesper P-52 well, south of the Orpheus Graben.....	140
<b>Figure 7.4.</b> Generalized W-E stratigraphic column with an interpretation of the tectonic evolution and timing of fault and salt movement within the Orpheus Graben.....	151
<b>Figure 7.5.</b> Isochron map for the U4 marker to top of Argo salt marker.....	153
<b>Figure 7.6.</b> Isochron map for the U1 to U4 marker .....	154
<b>Figure 7.7.</b> Plate tectonic map.....	155
<b>Figure 7.8.</b> Plate tectonic map.....	156
<b>Figure 7.9.</b> Isochron map for the U2 marker to Volcanic marker.....	158

## LIST OF TABLES

<b>Table 1.1.</b> Depth to the top of formations for each well in the Orpheus Graben.....	17
<b>Table 2.1.</b> Company and year of acquisition of seismic projects used in this study.....	29
<b>Table 3.1.</b> Descriptions of the nine lithotypes, the character of the cuttings and the well log response.....	36
<b>Table 3.2.</b> Analyses of percent carbonate in samples from the Fox I-22 well.....	39
<b>Table 3.3.</b> Sidewall core descriptions for the Eurydice P-36 well .....	62
<b>Table 4.1.</b> Key seismic markers, their attributes and the attributes of the reflections above and below.....	73
<b>Table 5.1.</b> Acoustic facies of the Cretaceous seen in the seismic profiles of the Orpheus Graben.....	90
<b>Table 6.1.</b> Detrital minerals and lithic clasts identified.....	111
<b>Table 6.2.</b> Component minerals of contaminants identified in the cuttings from the Fox I-22 well.....	116
<b>Table 6.3.</b> Diagenetic minerals identified .....	125

# **CHAPTER 1**

## **INTRODUCTION AND BACKGROUND**

### **1.1 Introduction**

The Orpheus Graben (Figures 1.1 and 1.2) is located on the northeast corner of the Scotian Shelf between latitudes  $45^{\circ} 20'N$  and  $45^{\circ} 40'N$  and longitudes  $58^{\circ} W$  and  $61^{\circ} W$ . The Orpheus Graben plunges and widens east from the Chedabucto Bay of mainland Nova Scotia to the Laurentian Channel (Jansa and Wade, 1975a). Structurally, the graben is surrounded by a series of discontinuous subparallel faults. It is bounded to the north by the Scatarie Ridge and to the south by the Canso Ridge.

The offshore east coast of Canada is divided into three major continental shelves, the Labrador Shelf in the north, the Grand Banks, and the Scotian Shelf in the south. The Scotian Shelf exceeds 1000 km in length and 400 km in width. Its subsurface structure is dominated by the Scotian Basin. The Scotian Basin is then subdivided into the Sable, Shelburne, and Abenaki Subbasins, and the Orpheus Graben. The Orpheus Graben is more “proximal” sedimentologically than productive areas of the Sable Subbasin; it also appears to be structurally rather different (although there may be similarities to the Abenaki Subbasin). Information from the Cretaceous rocks of the Orpheus Graben may reveal information about the paleogeography and structural setting and therefore help us understand the overall history of the graben and the Scotian Basin.

From reviewing previous work conducted in the Orpheus Graben, it is clear that several questions about the Cretaceous rocks remain to be answered or can be further refined.

These include: what is the detailed lithostratigraphy, what is the provenance of these rocks, what sedimentary architecture and tectonic structures are present, what is the timing of faults and salt movement, and did the offshore rocks have connectivity to rocks of the Chaswood Formation onshore or to the Sable Subbasin, and if so, to which unit (s)?

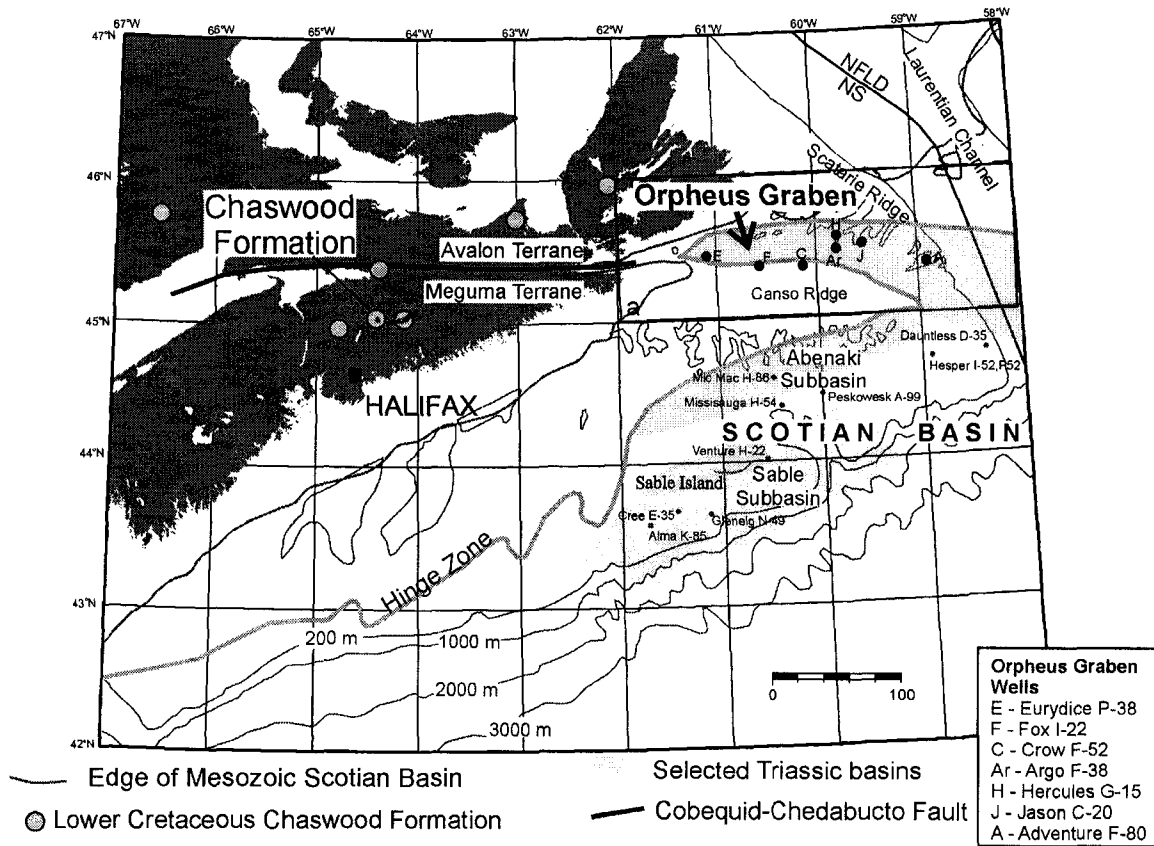


Figure 1.1. Map showing the location of the Orpheus Graben and the onshore Chaswood Formation. Labeled box shows the location of the study area and the area shown in more detail in Figure 1.2. Bathymetry and Mesozoic edge are from MacLean (1991). Chaswood Formation localities are from Stea and Pullan (2001). The UTM zone 20 map was plotted with Generic Mapping Tools (GMT) by Wessel and Smith (1992).

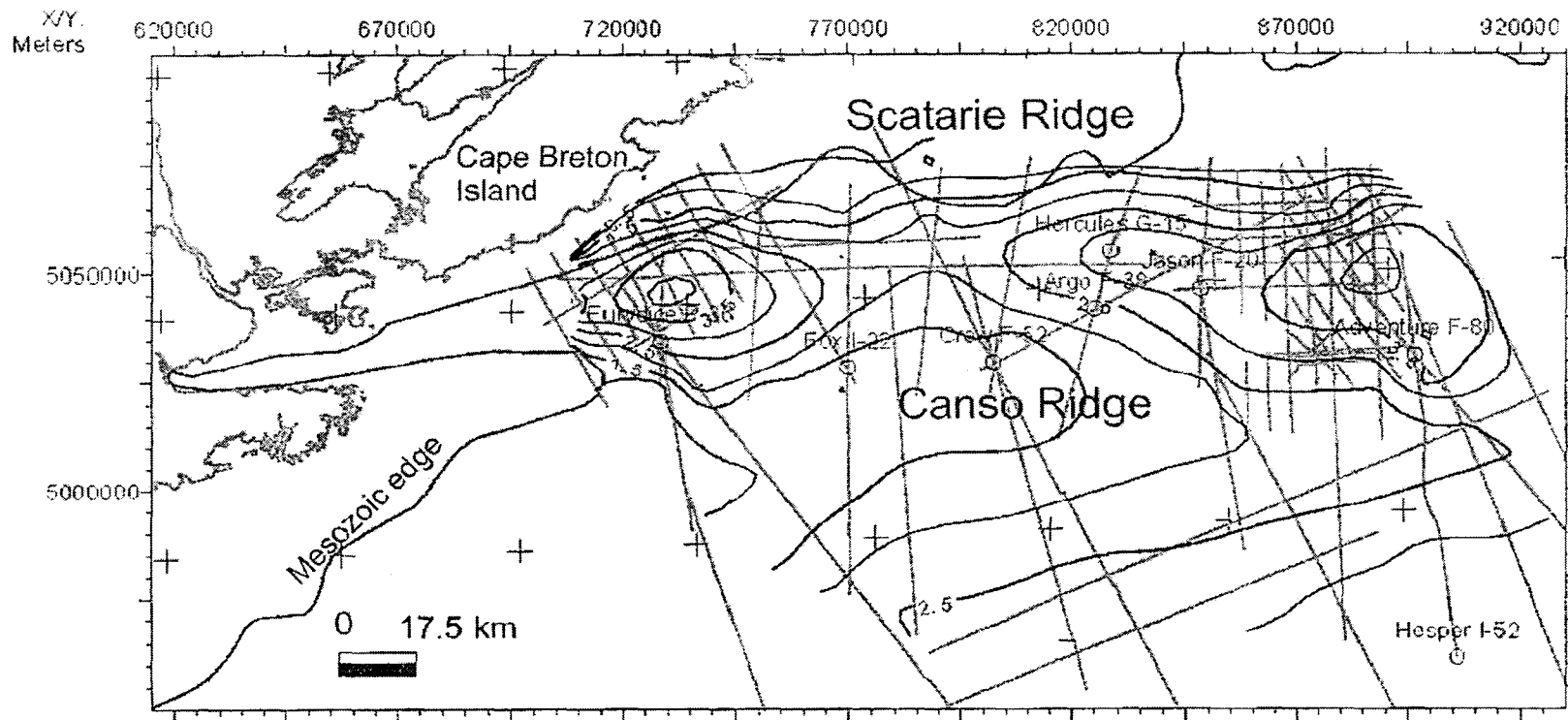


Figure 1.2 Map of study area showing the basement contours and the location of the wells and seismic lines studied (A in Figure 1.1). Contours of basement were generated using the algorithm “inverse distance to a power” with a grid spacing of 5 km, maximum distance of 100 km, weight of 2 and low smoothing. Bathymetry and Mesozoic edge are from MacLean (1991). Map plotted using The KINGDOM Suite with UTM Zone 20N (66° W to 60° W) and WGS 1984 datum.

The objective of this thesis is to answer these questions, which are presented in more detail below. The second part of this chapter will discuss the previous work conducted in the Orpheus Graben as well as the tectonic and depositional history of the Scotian Basin.

## **1.2 Objectives of This Study**

### *Short term:*

- 1) To determine the sedimentary petrology and sedimentology of the Lower Cretaceous deposits using grain size analysis, optical microscopy, and the electron microprobe.
- 2) To determine possible sediment sources for the Orpheus Graben deposits by comparing the detrital petrology with possible source rock locations.
- 3) To determine the timing of fault and salt movement that deformed Cretaceous sediments within the graben.
- 4) To refine the lithostratigraphy of the 7 wells and subdivide the Missisauga and Logan Canyon formation into member, not previously done in this area, by integrating previous interpretations, well log data, and sedimentary petrography.
- 5) To correlate the 7 wells with the help of an improved lithostratigraphy and seismic ties.

### *Long Term:*

- 1) To determine the paleofluvial relationship, if any, between the Chaswood Formation, Sable Subbasin and the Orpheus Graben, and to define sediment provenance and pathways.
- 2) To better characterize offshore Cretaceous reservoirs and to acquire a better understanding of where productive reservoirs, if any, may be.
- 3) To better understand the timing and relationship between local tectonic events, both salt and non-salt, and broader Eastern Canada tectonic history.

## **Previous Work**

In 1971, the first exploration well (Argo F-38) was drilled in the Orpheus Graben by Shell Canada Resources. Within the same year, Shell drilled 2 more wells (Crow F-52, and Fox I-22) and in 1972 they drilled Eurydice P-36. In 1974 Union *et al.* drilled the Hercules G-15 and Jason C-20 wells in the Orpheus Graben. Stratigraphic work on the graben has been conducted by McIver (1972), Jansa and Wade (1975a, 1975b), Given (1977), and Wade and MacLean (1990) based on the data obtained from the wells. King and MacLean (1970) conducted a continuous seismic reflection study of the Orpheus Graben gravity anomaly.

Lyngberg (1984) studied the palynology, organic geochemistry, and maturation of the sediments to produce a time-temperature history for the Orpheus Graben. Pe-Piper and Jansa (1985, 1987, and 1999), Pe-Piper *et al.* (1994), and Jansa and Pe-Piper (1985 and 1988) have studied the geology and geochemistry of the Cretaceous igneous rocks on the eastern North American margin and the implications for plate tectonics during that time. Holser *et al.* (1988) discussed evaporite deposits of the Argo Formation in the Orpheus Graben.

### **1.3.1 Tectonic History of the Scotian Margin**

During the Acadian Orogeny (Devonian), the Late Precambrian to Silurian metasedimentary and igneous rocks of the Avalon Terrane were juxtaposed against the Cambro-Ordovician low-grade metasedimentary strata of the Meguma Group and overlying Silurian units (MacLean and Wade, 1992). The Cobequid/Chedabucto Fault Zone, onshore and offshore, sharply separates these two terranes. The Scotian Basin

developed during the Triassic when the super continent of Pangaea began to break up (MacLean and Wade, 1992). Sinistral transtensional forces caused the rock of the Meguma basement to be broken up into a complex of northeast- and east-trending horsts, grabens and half-grabens (MacLean and Wade, 1992). During the latest Jurassic and Early Cretaceous, the eastern margin of Canada continued to rift and eventually formed oceanic crust further north, this time between the Grand Banks and Iberia (western Europe) (MacLean and Wade, 1992). This episode generated the Avalon Uplift, which resulted in significant erosion of Jurassic and older sediments to form the Late Aptian Avalon Unconformity at the top of the Avalon Formation on the Grand Banks (MacLean and Wade, 1992). The Avalon Uplift sourced large amounts of sediment into the Scotian Basin during the Early Cretaceous (MacLean and Wade, 1992).

### **1.3.2 Depositional History of the Orpheus Graben**

The basement rocks of the Scotian Shelf are composed of Precambrian-Devonian metasedimentary and igneous rocks (Jansa and Wade, 1975a, Pe-Piper and Jansa, 1999). The oldest sediments encountered in the graben are the Triassic continental redbeds of the Eurydice Formation (Table 1.1) (Jansa and Wade, 1975a). These sediments are present only in the deeper parts of the graben. The Eurydice Formation is overlain by thick evaporites of the Triassic to Lower Jurassic Argo Formation. They are separated by the break-up unconformity from the overlying Mesozoic and Cenozoic clastic and minor carbonate deposits of the Mohican and Iroquois formations (Jansa and Wade, 1975a). The thick, dominantly massive sandstone units of the fluvio-deltaic Missisauga and Logan Canyon formations overlie the clastic and carbonate facies of the Mic Mac

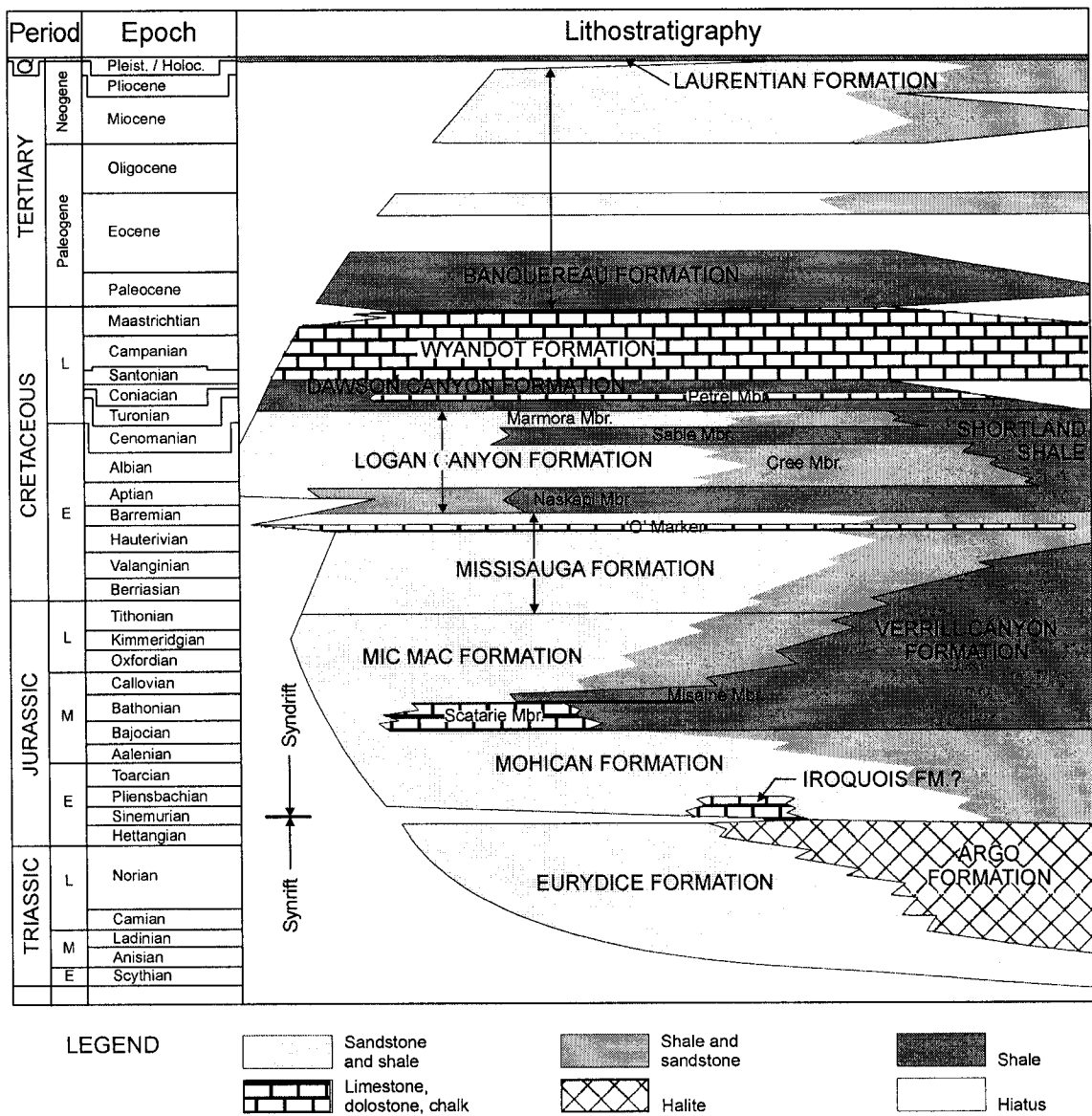


Figure 1.3. Generalized stratigraphic diagram for the eastern Scotian Shelf (modified after Wade *et al.*, 1995).

Well	Eurydice P-36		Fox I-22		Crow F-52		Argo F-38		Hercules G-15		Jason C-20		Adventure F-80	
	(ft)	(m)	(ft)	(m)	(ft)	(m)	(ft)	(m)	(ft)	(m)	(ft)	(m)	(ft)	(m)
Rotary table	98.1	29.9	103.0	31.4	85.0	25.9	103.0	31.4	98.1	29.9	98.1	29.9	98.1	29.9
Water depth	539.9	164.6	274.9	83.8	310.0	94.5	234.8	71.6	379.8	115.8	370.0	112.8	?	?
Start of logs	652.7	199.0	390.3	119.0	419.8	128	931.5	284.0	1059.4	323.0	1062.7	324.0	941.4	287.0
Banquereau Fm	-	-	-	-	-	-	-	-	-	-	-	-	IC	IC
Wyandot Fm	-	-	-	-	-	-	-	-	-	-	-	-	1302	397
Dawson Canyon Fm	-	-	-	-	IC	IC	IC	IC	-	-	IC	IC	1706	520
Petrel Mbr	-	-	-	-	?	?	1474	443	?	?	1994	608	2402	732
Logan Canyon Fm	-	-	<b>550</b>	<b>168</b>	<b>1140</b>	<b>348</b>	<b>1495</b>	<b>456</b>	<b>1059</b>	<b>323</b>	<b>2135</b>	<b>651</b>	<b>2720</b>	<b>829</b>
Marmora Mbr	-	-	<b>550</b>	<b>168</b>	<b>1140</b>	<b>348</b>	<b>1495</b>	<b>456</b>	<b>1059</b>	<b>323</b>	<b>2135</b>	<b>651</b>	<b>2720</b>	<b>829</b>
Sable Mbr	-	-	<b>1160</b>	<b>353</b>	<b>1900</b>	<b>579</b>	<b>2637</b>	<b>804</b>	<b>1891</b>	<b>576</b>	<b>3000</b>	<b>914</b>	-	-
Top Cree unconformity	-	-	<b>1300</b>	<b>396</b>	<b>2022</b>	<b>616</b>	<b>2775</b>	<b>845</b>	<b>2085</b>	<b>635</b>	<b>3169</b>	<b>965</b>	-	-
Cree Mbr	-	-	<b>1300</b>	<b>396</b>	<b>2022</b>	<b>616</b>	<b>2775</b>	<b>845</b>	<b>2085</b>	<b>635</b>	<b>3169</b>	<b>965</b>	-	-
Pyroclastic unit	-	-	-	-	-	-	-	-	<b>2085-2332</b>	<b>635-711</b>	<b>4008-4325</b>	<b>1246-1318</b>	-	-
Volcanic unit	-	-	-	-	-	-	<b>3210-3280</b>	<b>978-1000</b>	<b>2474-2465</b>	<b>744-752</b>	<b>4462-4471</b>	<b>1359-1363</b>	-	-
Volcanic unit	-	-	-	-	-	-	<b>3360-3419</b>	<b>1024-1042</b>	<b>2485-2539</b>	<b>758-774</b>	<b>4484-4512</b>	<b>1367-1376</b>	-	-
Naskapi Mbr	-	-	<b>1818</b>	<b>554</b>	2500	762	<b>3582</b>	<b>1091</b>	-	-	-	-	-	-
Top Missisauga unconformity	-	-	<b>1940</b>	<b>591</b>	<b>2545</b>	<b>776</b>	<b>3685</b>	<b>1124</b>	<b>2539</b>	<b>774</b>	<b>4512</b>	<b>1376</b>	-	-
Missisauga Fm	889	200	1940	591	2545	776	3685	1124	-	-	4512	1376	-	-
Upper Mbr	<b>889</b>	<b>200</b>	<b>1940</b>	<b>591</b>	<b>2545</b>	<b>776</b>	<b>3685</b>	<b>1124</b>	-	-	-	-	-	-
Middle Mbr	<b>840</b>	<b>256</b>	<b>2060</b>	<b>628</b>	<b>2700</b>	<b>823</b>	<b>3880</b>	<b>1183</b>	-	-	<b>4512</b>	<b>1376</b>	-	-
Volcanic unit	-	-	-	-	-	-	<b>4410-4430</b>	<b>1344-1350</b>	-	-	-	-	-	-
Volcanic unit	-	-	-	-	-	-	<b>4567-4588</b>	<b>1392-1398</b>	-	-	-	-	-	-
Avalon unconformity	<b>1650</b>	<b>503</b>	-	-	-	-	-	-	-	-	-	-	-	-
Mic Mac Fm	-	-	2282	697	3275	998	<b>5018</b>	<b>1529</b>	<b>2539</b>	<b>774</b>	<b>5955</b>	<b>1815</b>	-	-
Mohican Fm	-	-	-	-	4272	1302	5488	1673	3044	927	7094	2162	-	-
Breakup unconformity	?	?	?	?	?	?	7563	2305	?	?	?	?	?	?
Iroquois	<b>1650</b>	<b>503</b>	-	-	<b>4511</b>	<b>1375</b>	<b>6810</b>	<b>2076</b>	<b>3312</b>	<b>1009</b>	7835	2389	3256	992
Argo	2610	796	-	-	-	-	7563	2305	3460	1055	8036	2449	3393	1034.2
Eurydice	7850	2393	-	-	-	-	10122	3080	?	?	?	?	?	?
Meguma basement	?	?	2573	784	4938	1501	10926	3331	?	?	?	?	?	?
Bottom of the well	9728	2965	2722	830	4943	1507	11107	3386	3547	1081	8146	2483	6559	1999.2

Table 1.1. The depth (in feet and metres measured depth) to the tops of formations for each well in the Orpheus Graben. Wells are listed west to east. IC = in casing, ? = starting depth unknown and - = not present (after MacLean and Wade, 1993; bold and italicized numbers have been modified as a result of this study).

Formation (Wade and MacLean, 1990). Thin basalt beds occur above near the base of the Logan Canyon Formation in three wells (Argo F-38, Jason C-20, and Hercules G-15) in the Orpheus Graben (MacLean and Wade, 1990; MacLean and Wade, 1993). The transgressive Upper Cretaceous marine shales of the Dawson Canyon Formation and the marl and chalk deposits of the Wyandot Formation overlie the Logan Canyon Formation (Jansa and Wade, 1975a). Salt movement in the graben during the deposition of the Mohican-Iroquois formations has created salt pillows and diapirs (MacLean and Wade, 1993).

### **1.3.3 Mic Mac, Missisauga, Logan Canyon and Dawson Canyon formations**

This thesis focuses on the Missisauga and Logan Canyon formations of the Orpheus Graben. Therefore most detail is provided for these two formations and lesser amounts on the overlying Dawson Canyon Formation and underlying Mic Mac Formation.

The Mic Mac Formation is composed of mostly shale with some very fine to fine grained silica- or calcite-cemented sandstone and limestone beds. On the Scotian margin the formation is thought to be Bathonian-Callovian to Tithonian (Ascoli, 1976) and was deposited in a shallow marine, in part nearshore, environment with strong inputs of terrigenous sediments from the north and northwest (Jansa and Wade, 1975a). The type section for the Mic Mac Formation is in Shell Mic Mac H-86 between 10125 ft (3086 m) and 14375 ft (4382 m) (McIver, 1972).

McIver (1972) defined the overlying Missisauga Formation and subdivided it into the “updip” and “downdip” facies based on the percent of sand found in the type sections

(Figure 1.3). Wade and MacLean (1990) divided the Missisauga Formation into three members after drilling in 1979 revealed a third facies. The lower member of Wade and MacLean (1990) (type section between 5100 m (16728 ft) and 4149 m (13609 ft) in Venture H-22) equates to McIver's downdip facies and the middle (type section in Missisauga H-54 is between 3537 m (11601 ft) and 2740 m (8987 ft)) and upper members (type section in Missisauga H-54 is between 2740 m and 2414 m (7918 ft)) are included in McIver's updip facies (Figure 1.4). The lower member consists of a series of fine grained to pebbly sandstones that often coarsen upwards, and minor limestone beds within a marine shale unit. The lower unit is thought to be not present on the eastern Scotian Shelf (Wade and MacLean, 1990). The lower unit is overlain by the middle member, which is characterized by thick, mature fine to coarse sandstone. The "O" Marker, a transgressive limestone unit within the Missisauga Formation, separates the middle and upper units. The "O" Marker was not deposited in the Orpheus Graben because it onlaps the "Avalon Unconformity" on the Canso Ridge (Wade and MacLean, 1990). The Missisauga Formation's upper member is a thick section of dominantly sandstone and is characterized by a much higher sand-shale ratio than the lower and middle members (Wade and MacLean, 1990). The Missisauga Formation is thought to have been deposited in a lower delta plain to inner neritic environment (Wade and MacLean, 1990). The age of the Missisauga Formation is Berriasian to Barremian (Williams, 1975; Wade and MacLean, 1990).

The Aptian to Late Cenomanian (Williams, 1975; Ascoli, 1973) or Aptian to Early Cenomanian (Barss *et al.*, 1979) Logan Canyon Formation is described by McIver (1972)

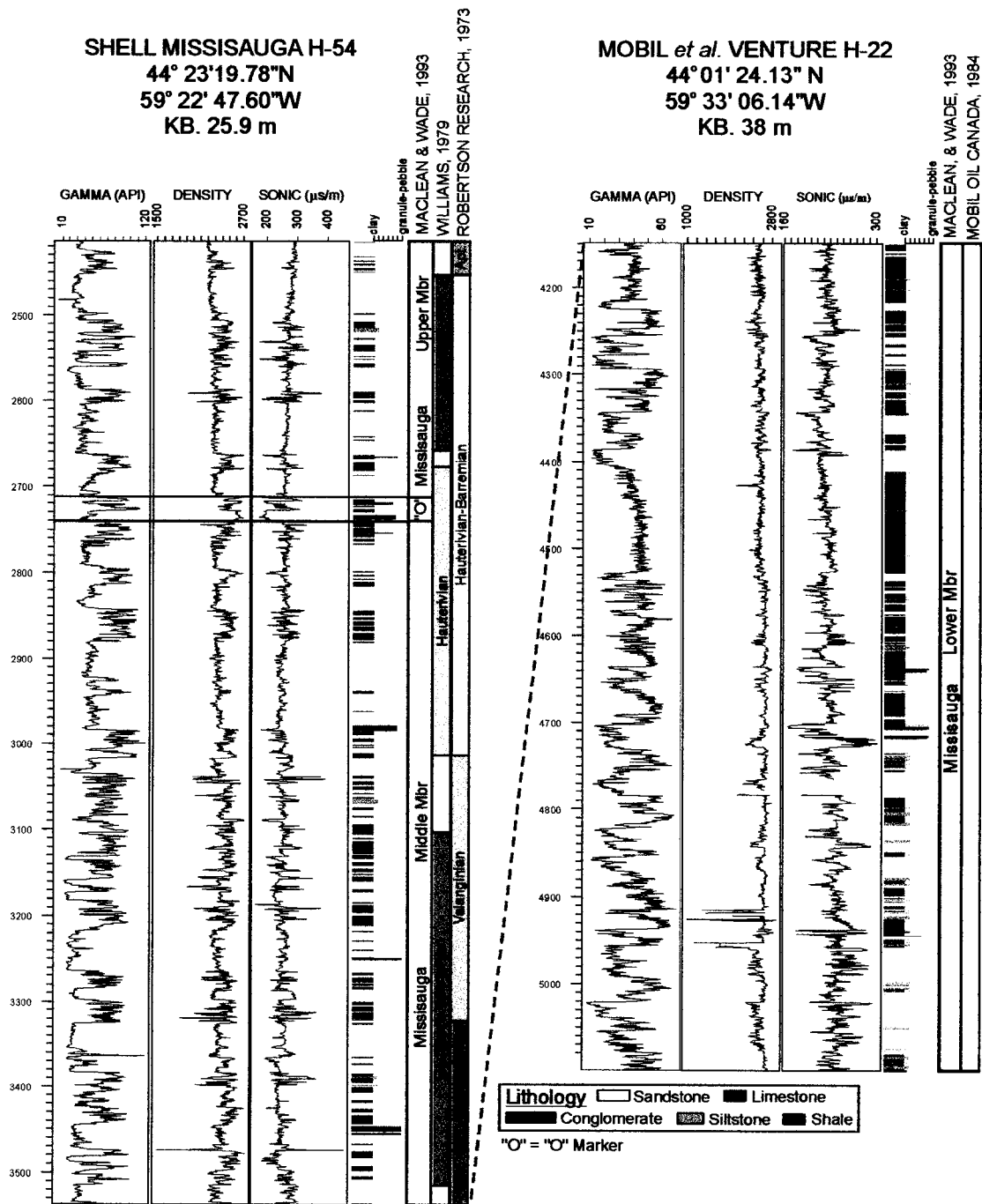


Figure 1.4. Type section of the Mississauga Formation and its members (modified from Wade and MacLean, 1990). Depths are measured depth (m) below the rotary table. Data sources: Lithology from cuttings - CANSTRAT; wireline logs – IHS AccuMap, biostratigraphic ages – published and unpublished sources represented in the BASIN database (<http://gsca.nrcan.gc.ca/BASIN/>). Stratigraphic sections were plotted with the “lithplot2.perl” program, written by A. MacRae. Access to the above mentioned data was possible due to collaboration with D.J.W. Piper at the GSC (Atlantic) for this project.

SHELL CREE E-35  
 43 44' 20.71" N  
 60 35' 55.90" W  
 KB 31.4 m

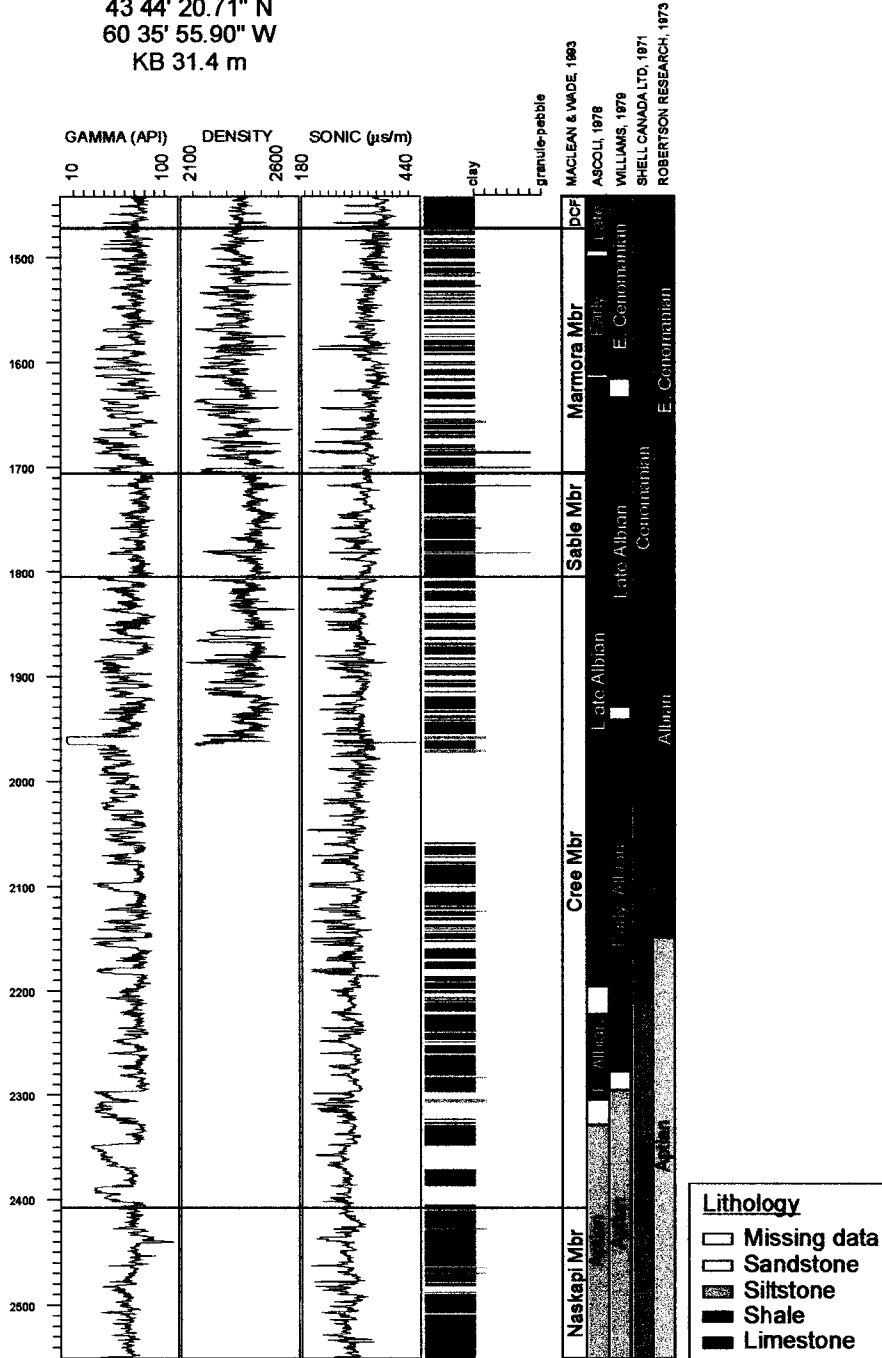


Figure 1.5. Type section of the Logan Canyon Formation and its members (modified from Wade and MacLean, 1990). Depths are measured depth (m) below the rotary table. Data sources: Lithology from cuttings - CANSTRAT; wireline logs – IHS AccuMap, biostratigraphic ages – published and unpublished sources represented in the BASIN database (<http://gsca.nrcan.gc.ca/BASIN/>). Stratigraphic sections were plotted with the “lithplot2.perl” program, written by A. MacRae. Access to the above mentioned data was possible due to collaboration with D.J.W. Piper at the GSC (Atlantic) for this project.

as a very thick succession (approximately 1 km) of alternating sandstone and shale. On the Canso Ridge, deposition of the Logan Canyon occurred in an alluvial plain environment from the Aptian to Cenomanian, with the exception of the mainly marine Upper Albian succession (Jansa and Wade 1975a). The type section (Figure 1.4) of this formation and its members are in the Shell Cree E-35 well between 4730 ft (1442 m) and 8370 ft (2551 m) (McIver,1972). McIver (1972) described two major shale (Naskapi and Sable members) units within this formation and Jansa and Wade (1975b) designate the basal member of this formation to be the Naskapi Member. The sand and shale sequence between the Naskapi and Sable members and between the Sable Member and Dawson Canyon Formation were named the Cree and Marmora members, respectively, by Wade and MacLean (1990). In the type area the basal Naskapi Member is a transgressive shale unit consisting of various colours (yellow-brown, green-grey, red-brown, light grey) of shale with interbedded silty and zones. Micropaleontological evidence and small scale multidirectional trough cross bedding indicate a marginal nearshore marine and tidal flat depositional environment (Magnusson, 1973). The Naskapi Member is mainly Aptian in age and grades upward into an alternating sandstone-shale succession (Jansa and Wade, 1975a).

In the type area the Cree Member is divided into a lower and upper section. The lower section of the Cree Member is composed of medium to coarse grained sandstone beds interbedded with shale, mudstone and silty mudstone. In the upper portion of the same member, the sandstones are very fine to medium grained and are interbedded with shale, mudstone and silty mudstone. The Cree Member is Upper Aptian to Upper Albian in age

and overlies the Naskapi Member. The overlying shale-dominated Sable Member is Upper Albian to Lower Cenomanian in age (Williams, 1975), and the type section is in Shell Cree E-35 between 5492 ft (1674 m) and 5735 ft (1748 m) (McIver, 1972). The Marmora Member overlies the Sable Member and is compositionally similar to the upper section of the Cree Member, with fine to very fine sandstone intervals interbedded with shale, mudstone, and silty mudstone beds. The contact with the overlying Dawson Canyon Formation is generally gradational.

The Dawson Canyon Formation was deposited during a continuing Upper Cretaceous transgression (Jansa and Wade, 1975a). The type section is in the Shell Missisauga H-54 well between 3335 ft (1017 m) and 4225 ft (1288 m) (McIver, 1972), and its age is Late Cenomanian to Early Campanian (Williams, 1975) or Coniacian to Campanian (Jenkins *et al.*, 1974) in the northeastern part of the basin. The Petrel Member of this formation is Turonian on the southern Scotian Shelf and Turonian to Coniacian beneath the northwest Grand Banks (Williams, 1975). The Petrel Member divides the formation into the informal lower and upper parts (Jansa and Wade, 1975a). The lower part is composed of interbedded siltstone, silty shale, and some sandstone beds, representing a transition between the Logan Canyon and the Dawson Canyon formations (Jansa and Wade, 1975a). The Petrel Member is composed of interbedded calcareous shale and foraminiferal wackestone or dense chalky limestone and represents a moderately deep shelf environment (Jansa and Wade, 1975a). The Turonian shales contain glauconite and phosphatic pellets, which grade into unconsolidated conglomeratic sandstones interbedded with calcareous sandstone and mudstone (Jansa and Wade, 1975a). The

upper part is mainly mudstone or shale with rare fine grained sandstone and siltstone beds and represents a marginal marine environment (Jansa and Wade, 1975a).

#### **1.3.4 Volcanic Rocks**

Volcanism in the Orpheus Graben and on the Grand Banks may be an expression of transtensional tectonics that occurred along the Cobequid – Chedabucto – SW Grand Banks fault system as a result of rejuvenated plate motion during continental spreading (Jansa and Pe-Piper, 1988). Minor basalt flows were extruded during this time as well as later in the Early Cretaceous in the form of volcanic cones and basalt flows along the southwest Grand Banks margin and the northern part of the Scotian Shelf (Jansa and Pe-Piper, 1988). Wade and MacLean (1990) pointed out that the seismic data do not confirm the presence of volcanic cones. Volcanic and other igneous rocks within the Orpheus Graben were interpreted by Wade and MacLean (1990) to be within the Naskapi Member in the Hercules J-15, Jason C-20, and Argo F-38 wells. The lower unit of the igneous rocks penetrated by the wells is composed of basalt, as possible sills and feeder dikes or flows, a few metres to a few tens of metres thick (14 m in Jason C-20 and 23 m in Hercules G-15). The upper unit consists of 10 m to 82 m of pyroclastic and volcanoclastic rocks in which volcanic tephra, including glass, is mixed with quartz rich sediments that are interbedded with thin lava flows (Jansa and Pe-Piper, 1988).

Lyngberg (1984) recognized a volcanic interval within the Missisauga Formation in Argo F-38 (1366 m to 1376 m, 4481 ft to 4514 ft) and states that the igneous units in all three wells are probably volcanic flows erupted onto the surface because above the igneous intervals the maturation profile is not deflected but there is notable darkening of spore colour immediately below the igneous units.

## **CHAPTER 2** **METHODS**

### **2.1 Petrographic study**

#### **2.1.1 Conventional cores**

No conventional cores were available from the Lower Cretaceous in the study area.

#### **2.1.2 Sidewall cores**

Sidewall cores stored at the Canada-Nova Scotia Offshore Petroleum Board (CNSOPB) Core Lab were described by noting the colour, grain size, induration (very poor, poor-moderate, moderate, moderate to well, and well) and the amount of coal or plant fragments (few, some, many, and abundant), if present. Laminations, shells, foraminifera, oxidization, and identifiable clasts and minerals (muscovite, feldspar) within the sidewall cores were also noted. The new sidewall core descriptions were then compared to the sidewall core descriptions in the well log reports (Shell, 1972, 1971a, 1971b, and 1971c; Union et al, 1974 and 1975; and Mobil, 1975) for any major discrepancies. Our sidewall core description for each well (Fox I-22, Crow F-52, and Argo F-38) can be found in the corresponding Appendices 1-3.

#### **2.1.3 Cutting sample preparation**

Representative sub-samples of archived cutting samples from the CNSOPB Core Lab were taken from the Logan Canyon and Missisauga formations of wells Fox I-22 (D23), Crow F-52 (D20), Argo F-38 (D17), and Jason C-20 (D131). These cutting samples were washed with warm tap water through a 63 µm sieve to remove any unwanted material (mud and oil from the drilling). Samples that were either too old or included excess

debris had to be soaked in soapy water for a short period of time to facilitate the washing procedure. Samples were then sieved at 2 mm, allowing the separation of the grains into two classes:  $> 63 \mu\text{m}$  to  $< 2 \text{ mm}$  and  $> 2 \text{ mm}$ . Heavy mineral separation was performed on all sub-samples for the  $> 63 \mu\text{m}$  to  $< 2 \text{ mm}$  fraction using the heavy liquid tetrabromomethane, which has a density of 2.95 g/mL. The heavy separates of this fraction were then used to make polished thin sections.

#### **2.1.4 Identification of cuttings $> 2 \text{ mm}$**

Cuttings larger than 2 mm were identified using a binocular microscope and were separated based on lithology/mineralogy, grain size, colour or apparent cement. Each group of cuttings was placed into separate vials and labeled with the corresponding well, depth and lithology. Representative unidentified cuttings were used to make polished thin section mounts and analysed under a polarized/reflected light petrographic microscope and an electron microprobe. A numerical summary of the cuttings and clasts  $> 2 \text{ mm}$  can be found in Appendices 1 to 4 (Table 4). These tables list the quantity of rock cuttings and clasts for each identified lithology found at each sampled depth.

#### **2.1.5 Identification of heavy fraction of cuttings $< 2 \text{ mm}$**

Polished thin section mounts (85 in total) of the heavy separates of the  $> 63 \mu\text{m}$  to  $< 2 \text{ mm}$  grains were made for all available samples. For samples with bimodal sizes and enough heavy separates from both size classes, two polished thin sections were made, one for the finer fraction (F) and one for the coarser fraction (C). The grain size and preliminary identification of mineralogy/lithology of cutting grains was done using a

polarized/reflected light petrographic microscope and subsequently refined with the use of an electron microprobe.

### **2.1.6 Microprobe analysis**

Polished thin sections and mounts were analysed at the Regional Electron Microprobe Centre located at Dalhousie University to find the chemical composition of both detrital and diagenetic minerals. The microprobe used is a JEOL-8200 electron microprobe with five wavelength spectrometers and a Noran 133 eV energy dispersion detector. The beam was operated at 15 kV and 20 nA, with an average beam diameter of 5  $\mu\text{m}$ .

Elements set up to be measured were Si, Al, Ti, Cr, Fe, Mn, Mg, Ca, Na, K, P, Zr, and Ba. The elements Sr, Cl, and F were also analyzed in phosphate minerals. The energy dispersive spectrometer (EDS) was used for fast and easy identification of minerals such as quartz, calcite, barite, rutile, and staurolite. It was also used to find elements not set up to be measured by the microprobe, such as S to identify pyrite, Zn and S to identify sphalerite, and Pb and S to identify galena. Cuttings and minerals (detrital or diagenetic) of interest were also viewed and photographed as back-scattered electron images.

### **2.1.7 Scanning electron microscopy**

The environmental scanning electron microscope (ESEM) at the Geological Survey of Canada (Atlantic) (GSCA) located in the Bedford Institute of Oceanography was used as a relatively fast and easy way to identify phosphatic cuttings, as they were optically difficult to distinguish from sideritic cuttings. This ESEM is an ElectroScan E3 equipped with a Noran Voyager X-ray energy dispersive spectrometer (EDS).

### **2.1.8 Carbonate analyses**

Samples were prepared by first crushing them into a very fine powder using a mortar and pestle. Samples to be analysed for their total carbon content were prepared by placing 0.25 g of sample into a crucible and adding distilled water. Once dry, a mixture of copper and lead accelerators were added to the crucible before it was analysed. The samples to be analysed for their organic carbon content were prepared by placing 0.25 g of sample into a crucible and treating them with 10% HCl to remove the inorganic carbon. Once dry, they were washed with distilled water to remove any residual HCl. When the sample was dry again, the same mixture of accelerants as that for the total carbon analysis was added. The samples were analysed using the LECO WR-112 carbon determinator located at the Bedford Institute of Oceanography. The amount of inorganic carbon was determined by subtracting the amount of organic carbon from the total carbon. A 1 g calibration standard containing a known carbon percent of 0.0496+/- 0.0018 was used and was run every 5-6 samples. The percent carbonate was determined by multiplying the weight percent of inorganic carbon by the molecular weight of CaCO<sub>3</sub> (Ca: 40.078, C: 12.011, O: 15.9994\*3 = 100.0872) and dividing by the atomic weight of carbon (12.011).

### **2.2 Lithostratigraphic Interpretations**

Lithostratigraphic formation boundaries were previously interpreted by MacLean and Wade (1993) for the wells in this area. Interpretations of electrical logs (gamma, density, sonic, deep induction, dip, and caliper), sidewall core and cutting descriptions, and the new petrographic data of this study led to significant revisions in this study (see Table 1.1). The Logan Canyon and Missisauga formations were divided into members, a

process only partially considered in previous work in the study area. The wireline logs were constructed using digital electrical log data obtained from IHS AccuMap and plotted along with the interpreted lithology using LogPlot 2001 software. Access to this digital data was possible due to the collaboration with D.J.W. Piper at the GSC (Atlantic). Lithology was based on the results of this study. Biostratigraphic information from many authors is summarized in the BASIN database (<http://gsca.nrcan.gc.ca/BASIN/>). Individual authors for biostratigraphy in these wells are cited for each well in Chapter 3. Depths are measured depth (ft/m) below Kelly Bushing (KB).

### **2.3 Seismic Reflection Data**

Publicly released microfiche copies of reflection seismic records acquired by industry in the 1970s and early 1980s were obtained from the CNSOPB. These records were used to describe the architecture and tectonics of the Cretaceous strata in the Orpheus Graben, in particular to identify seismic facies, faults, and evidence for periods of salt growth and withdrawal. Projects used in this study are listed in Table 2.1 and a list of the lines interpreted from each project can be found in Table 1 of Appendix 5 and their locations can be seen in Figures 2.1 and 2.2.

Project	Year	Company
8620-C004-002E	1971	Chevron
8624-C020-001E	1972	Canadian Superior
8624-P028-030E	1981	Petro-Canada
8624-B011-003E	1982	Bow Valley
8624-C055-003E	1982	Canterra Energy
8624-C055-003E	1982	Canterra Energy
8624-P028-068E	1983	Petro-Canada
8624-P028-072E	1985	Petro-Canada

Table 2.1 Company and year of acquisition of seismic projects used in this study.



### **2.3.1 Data preparation**

The microfiche copies of the lines from five projects in and around the Orpheus Graben were scanned at the GSC (Atlantic) and in the Geology Department at Saint Mary's University. As necessary, scanned images were inverted, rotated, cropped, resized, and spliced together or cut (using Adobe PhotoShop) in order to match navigation data from the BASIN database. Scanned images were converted into SEG-Y format using a program developed by Dr. Andrew MacRae of Saint Mary's University that relies on Seismic Unix (Cohen and Stockwell, 2003) and the netpbm tools (<http://netpbm.sourceforge.net/>). Images were merged with navigation data and loaded into The KINGDOM Suite 7.2 seismic interpretation software (SMT, 2003).

### **2.3.2 Data interpretation**

Interpretations were made using The KINGDOM Suite 7.2 software at the GSC (Atlantic) and in the Geology Department at Saint Mary's University. Zone 20N (66° W to 60° W) was used as the UTM projection coordinate system. WGS 1984 geodetic datum was used with WGS 1984 Ellipsoid. Navigation data was converted from NAD27 to WGS84 datum as necessary during import. Horizon grids were generated using the inverse distance to a power algorithm (Franke and Neilson, 1980) (see map captions for the grid spacing, maximum distance away from a point, and type of smoothing used to generate that map).

#### **2.3.4 Synthetic seismograms**

Synthetic seismographs were created for each well using The KINGDOM Suite. A synthetic seismogram is a simulated seismic response computed from well data, and is most commonly used to correlate geologic information from well logs with seismic data. Seismic data only provides time values, whereas synthetics provide a relationship between time and depth values that are used to verify the geological interpretation of reflection events. The SynPAK module of The KINGDOM Suite used the digital velocity and density data obtained from IHS AccuMap to calculate the Acoustic Impedance (AI) and the Reflection Coefficient (RC) for each sample interval (corresponding to a time spacing of about 0.3ms). SynPAK generates a synthetic seismogram using the RC series and a wavelet, which is extracted from the seismic data (if the data is digital) or from standard SynPAK theoretical wavelets (Ormsby, O'Brien, Klauder, Butterworth, Minimum Phase, Gaussian, or Ricker). Because of the limitations of working with scanned seismic images, wavelets extracted from the data do not match the seismic data as well as those generated using an Ormsby (positive phase) theoretical wavelet (2.0 ms sampling interval and no filtering). Once the synthetic is created the depth to the top of the formations and members (previously entered under the Wells menu: Edit-wells-> borehole -> Formation Tops) were converted to time and plotted at the location of the corresponding well, connecting known lithology to the seismic data. Strong seismic peaks and troughs commonly corresponded to significant velocity and density changes in the synthetic seismogram. An estimate of approximately 10 ms and 30 m is made for precision of the time to depth correlation within the Cretaceous interval, approximately to within one wavelet cycle.

As an example the lower unit of the Cree Member volcanic interval has a velocity of approximately 3000 m/s and is approximately 25 m thick. This unit is clearly imaged in the seismic data as a high amplitude, often continuous reflection, however, the thinner (10-15 m) upper volcanic unit is not clearly imaged suggesting the resolution limit is somewhere in this range of thickness for strong acoustic contrast. The velocities within the Cretaceous sedimentary interval range from 2000 m/s to 2500 m/s and an estimate of approximately 50 m of depth and 40 ms in time is made for the precision of the seismic data in this interval. Registration problems, scanned data, and redigitized wireline logs may also decrease the precision. This precision estimate probably also worsens with depth.

Lithostratigraphic plots (see Chapter 3) for each well were converted from depth to time using the depth to time relationship from the synthetic seismogram and a linear interpolation program written by Dr. A. MacRae. Once in the time domain, the well sections were overlain on the seismic section to correlate lithostratigraphy to the seismic markers of Chapter 4 more directly (Appendix 5 – Figures 1-7).

## **CHAPTER 3**

### **LITHOSTRATIGRAPHY**

#### **3.1 Introduction**

Nine lithotypes are distinguished from the cuttings, sidewall cores and wireline logs of the four wells that were studied in detail (Fox I-22, Crow F-52, Argo F-38 and Jason C-20). Each lithotype and the corresponding wireline log responses are described in Table 3.1. These lithotypes allow the stratigraphy for each of the wells to be inferred. The term lithotype is used when dealing with cuttings, instead of lithofacies, because of the limitations caused by the size and nature of the cuttings. Bioturbation, ripples and laminations, for example, are rarely if ever seen in cuttings, and the distinction between cuttings from subtly different depositional environments (e.g., a fluvial channel versus a tide-influenced fluvial channel) cannot be made reliably. More generalized facies assignment, such as marine sands versus channel sands are possible, but the limitations of such general environmental interpretations must be kept in mind. Cuttings provide a record biased towards the moderate to well lithified sediments within the well, because the poorly lithified lithologies break apart and are mostly lost in the drilling muds. Sidewall cores have been taken in these sandy, poorly indurated intervals and provide more reliable information about these lithologies, but they are in limited number. Information from the well log report, cuttings, sidewall cores and wireline logs are combined to produce a lithostratigraphy for each well that is much more detailed than previously published interpretations (e.g. MacLean and Wade, 1993). Lithostratigraphic boundaries were modified from MacLean and Wade (1993) who only identified boundaries at the formation level in this area. Member boundaries were determined,

where possible, based on the type sections outlined in Chapter 1. A correlation diagram for the wells of the Orpheus Graben is shown at the end of this chapter in Figure 3.8.

This chapter is divided into eight sections. Following this introduction, four sections outline the lithostratigraphy for the wells Fox I-22, Crow F-52, Argo F-38 and Jason C-20 that were petrographically studied in this thesis. For each of these wells, a lithostratigraphic plot is presented based on the petrographic studies, sidewall core descriptions, cuttings descriptions, and the wireline log response. A petrographic summary table (Appendices 1-4, Table 4) provides a quantitative description of the predominant cuttings, whereas Appendices 1-4, Table 5 describes the predominant cuttings and distinguishes between those interpreted as being in place (the most abundant cuttings in a sample, which have a matching wireline log response) and those interpreted as down-hole caving (a few cuttings of a lithotype previously seen higher in the well, or cuttings that do not match the wireline log response). Data obtained from the Fox I-22, Crow F-52, Argo F-38, and Jason C-20 wells were used to interpret the wireline logs from the remaining three wells in the Orpheus Graben (Eurydice P-36, Hercules G-15, and Adventure F-80), discussed in the last three sections of this chapter. Each of the seven sections will describe the lithostratigraphy of one well using the lithotypes outlined in Table 3.1. Each lithostratigraphic plot shows the interpreted lithology, sampled interval, sidewall core locations (if any), biostratigraphic, formation and member boundaries of this thesis as well as the formational interpretations of MacLean and Wade (1993).

<b>Lithotype</b>	<b>Character of cuttings</b>	<b>Well log response</b>
1 – Marl	White to light grey in colour; soft; reacts with diluted acid; contains silt-sized brown and black grains.	Low gamma; high density; high velocity.
2 – Mudstone/ Shale	Light to dark grey; may have laminations; well lithified.	Very high gamma; variable density from medium to high.
3 – Silty mudstone <sup>1</sup>	Red-brown; purple-brown, or grey-brown; well lithified.	High gamma; variable medium to high density may have high velocity.
4 – Carbonate-cemented very fine to fine grained sandstone.	Red-brown to brown or white to light yellow-brown in colour depending on cement type (siderite or calcite). Well lithified quartz arenites <sup>2</sup> and wackes <sup>3</sup> .	Medium-high gamma; variable medium to high velocity and density.
5 – Carbonate-cemented fine to medium grained sandstone.	Red-brown to brown or white to yellow-brown in colour depending on cement type (siderite or calcite); well lithified; may contain coal fragments; dominantly quartz wackes with lesser amounts of quartz arenites.	Medium-low gamma; mostly stable medium velocity and density.
6 – Carbonate-cemented medium to coarse grained sandstone.	White to light yellow-brown in colour; may have coal fragments; moderately to well lithified. Dominantly quartz arenites with lesser amounts of quartz wackes.	Low gamma; stable medium velocity and density.
7 – Coarse to very coarse grained sandstone.	Granules of quartz and feldspar are interpreted to come from a coarse to very coarse grained; poorly indurated quartz arenite.	Very low gamma; stable medium velocity and density.
8 – Coal and shaly coal	Black; friable; dull to glossy appearance; many have woody appearance; some are slightly pyritized.	Medium to high gamma; low density and velocity.
9 – Basalt/diabase	Black to dark grey flat and angular cuttings; elongated grey to white minerals; may be altered greenish-yellow.	Very distinct log reading of low to low-very low gamma; high density, very high velocity.

1. Mudstone with more than 15 % silt sized grains.
2. Sandstone with quartz content greater than 95 % (Pettijohn, 1987).
3. Sandstone with 15 % or more matrix content (Pettijohn, 1987).

Table 3.1. Descriptions of the nine lithotypes, the character of the cuttings and the well log response. Lithotypes are based on the sidewall cores, wireline logs and the dominant cuttings types found in the four wells studied in greatest detail (Fox I-22, Crow F-52, Argo F-38 and Jason C-20).

### **3.2 Fox I-22 (D23)**

The Fox I-22 well is located on the Canso Ridge (Figure 1.1) at 45° 21'33.6" N, 59° 33' 16.0" W and penetrates 2722 ft (829 m) of sediment. This well cuts through the Logan Canyon (Marmora, Sable, Cree and Naskapi members), Missisauga (Upper and Middle members) and Mic Mac formations before entering Meguma basement rocks (MacLean and Wade, 1993). Table 11 in Appendix 1 presents a lithological description of the sidewall cores taken from the Missisauga and Logan Canyon Formations.

The Missisauga Formation in the Fox I-22 well (Figure 3.1) is interpreted to be from 2282 ft (697 m) to 1940 ft (591 m). The dominant sandstone in this interval is divided into the Middle and Upper members, with the Middle Member comprising the section between 2282 ft to 2060 ft (628 m). The lower part of the Middle Member is composed of beds of lithotype 4 interbedded with beds lithotypes 2, 3, 5, 6 and 7. There is also one thin bed of lithotype 1 observed. The upper part of the Middle Member is a thick bed of lithotype 7 with granules of quartz and feldspar. The cuttings in this interval are siderite-cemented fine to medium grained quartz arenites and wackes. The upper Member spans from 2060 ft to 1940 ft and is composed of a thick bed of lithotype 6 with one thin bed of lithotype 1.

The Logan Canyon Formation overlies the Missisauga Formation from 1940 ft to 800 ft (244 m). The abrupt change at 1940 ft from coarse sandstone to thick shale of Aptian age was correlated by Jansa and Wade (1975b) and MacLean and Wade (1993) with the base of the Naskapi Member (type section in the Cree E-35 well) of the Logan Canyon

Formation. The basal Naskapi Member is composed of alternating beds of lithotypes 2 and 4.

The Cree Member is interpreted to overlie the Naskapi Member from 1800 ft to 1300 ft (396 m) with the lower part of this member from 1800 ft to 1575 ft (481 m) consisting of alternating beds of lithotypes 6, 3, 8 and 1. Cuttings in this member are siderite- and calcite-cemented fine to medium grained quartz arenites and wackes. The upper part of the Cree member spans from 1575 ft to 1300 ft and is characterised by thick beds lithotype 6 with many thin beds of lithotype 1 and the upper most part fines to beds of lithotype 5. Some fine grained quartz wacke of this member contain glauconite grains (1760-1790 ft) or coal fragments (1490-1520 ft).

The Sable Member is interpreted to overlie the Cree Member from 1300 ft to 1160 ft (353 m) and consists of three distinctive fining upward sequences, based on wireline logs, from sandstones of lithotype 5 to lithotype 3. The cuttings within this member are dominantly siderite- and calcite-cemented very fine to medium grained quartz wackes with lesser amounts of quartz arenites observed.

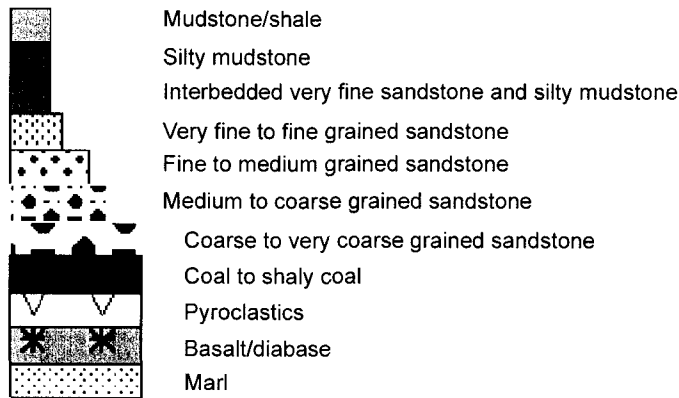
The Marmora Member is interpreted to overlie the Sable Member from 1160 ft to 500 ft (168 m) and is composed mostly of lithotypes 5 and 4 that are interbedded with a few beds of lithotypes 2 and 3. Cuttings within this member are dominantly siderite- and calcite-cemented very fine to medium grained quartz wackes that are well to moderately indurated and silty mudstone. A bed of lithotype 1 (Table 3.2) is interpreted from 828 ft

(252 m) to 800 ft (244 m): the wireline logs from this interval show a decrease in the density log, but this is probably an artifact of the start of the logging run.

		Wt (%)	Wt (%)	Wt (%)	%
Well	Depth (ft)	Total Carbon	C-org	C-inorg	Carbonate
Fox I-22	830-860	7.25	0.23	7.02	58.50
Fox I-22	890-920	8.01	0.01	8.00	66.67
Fox I-22	1040-1070	6.88	0.11	6.77	56.42
Fox I-22	1100-1130	7.12	0.10	7.02	58.50
Fox I-22	1220-1250B	7.39	0.11	7.28	60.67

Table 3.2. Analyses of percent carbonate in samples from the Fox I-22 well. Samples were identified as marl because the percent of carbonate was found to be less than 75% (a cut off of 75% was used to distinguish between chalks and marls).

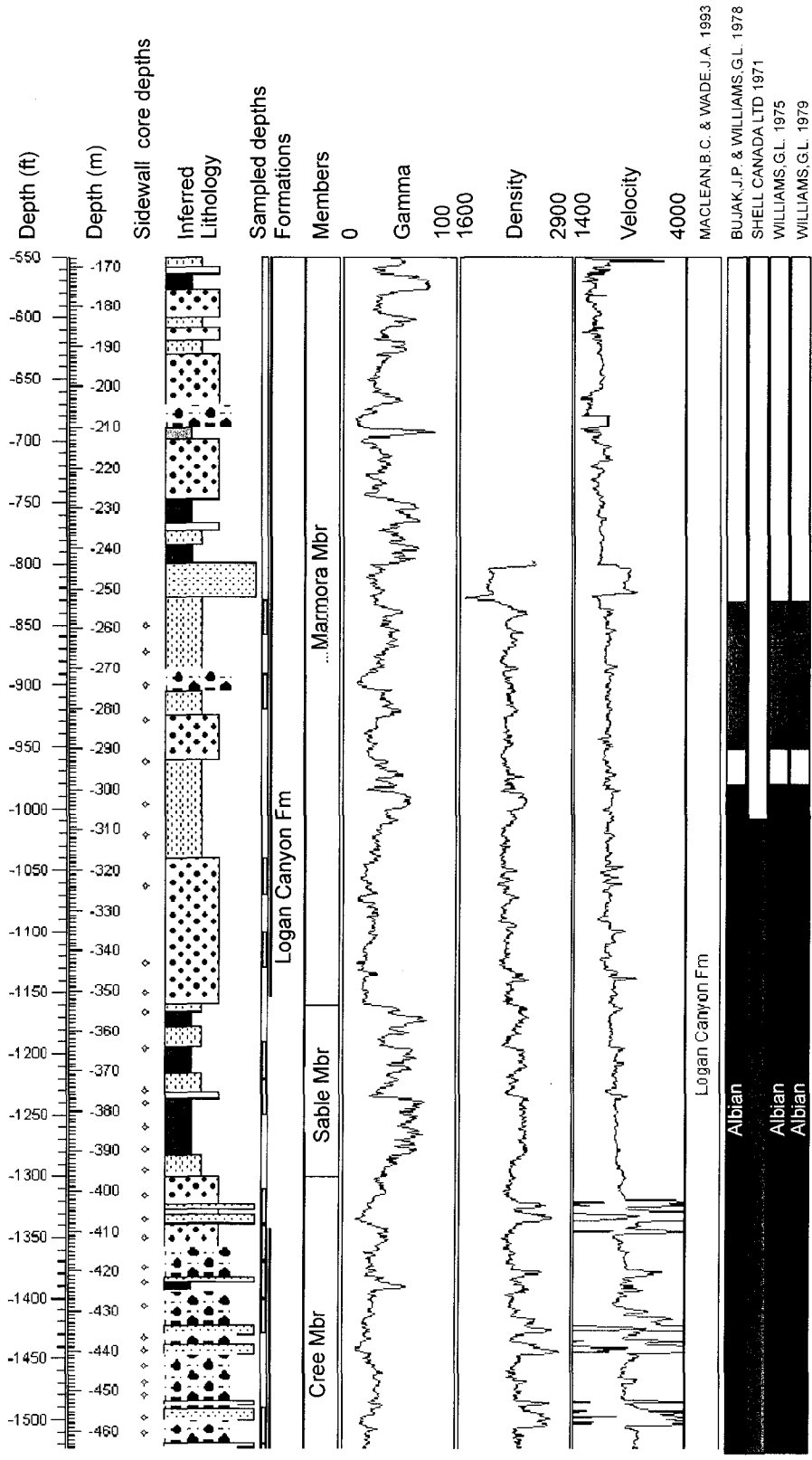
**Lithotypes**



**Biostratigraphy**



Figure 3.0. General legend for lithostratigraphic plots.



MACLEAN B.C. & WADE, J.A. 1993  
 BUJAK, J.P. & WILLIAMS, G.L. 1978  
 SHELL CANADA LTD 1971  
 WILLIAMS, G.L. 1975  
 WILLIAMS, G.L. 1979

Figure 3.1. Lithostratigraphic plot for Fox I-22 showing formation, member and age boundaries and gamma, velocity and density wireline logs.

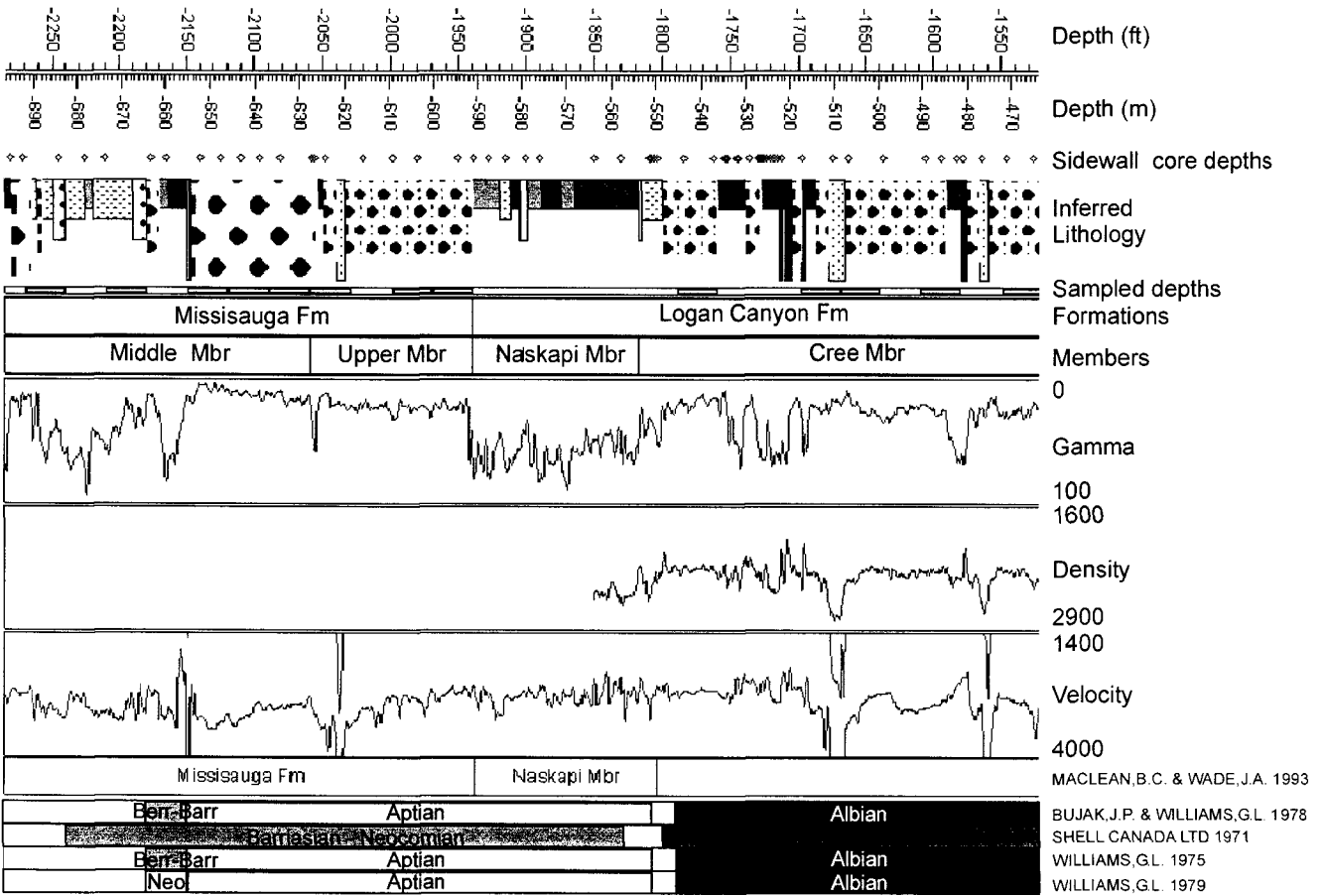


Figure 3.1. Lithostratigraphic plot for Fox I-22 showing formation, member and age boundaries and gamma, velocity and density wireline logs (continued).

### **3.3 Crow F-52 (D20)**

The Crow F-52 well is also located on the Canso ridge (Figure 1.1) at 42° 21'24.2" N, 59° 08'22.8" W, 32.6 km east of the Fox I-22 well. This well penetrated 4943 ft (1506 m) of rocks from the Logan Canyon Formation (Marmora, Sable, Cree and Naskapi members), Missisauga Formation (Middle and Upper members), Mic Mac, and Meguma basement. Table 11 in Appendix 2 presents a lithological description of the sidewall cores within the Missisauga and Logan Canyon Formations.

The Missisauga Formation (Figure 3.2) overlies the Mic Mac Formation from 3275 ft (998 m) to 2550 ft (776 m). The Middle Member is interpreted to span from 3275 ft to 2700 ft (823 m) and is composed of thick beds of lithotype 7 interbedded with thin beds of lithotypes 2, 3, 4, 5 and 1. Cuttings are dominantly siderite-cemented quartz wackes and arenite but pyrite, barite and limonite cements are also observed. Cuttings of very fine to fine grained quartz wackes from 2766 ft are siderite-cemented and can not be distinguished in the wireline logs from the surrounding coarse to very coarse quartz arenite beds. This is also true for the coal and shaly coal cuttings from 2630 ft (802 m). The Upper Member of the Missisauga Formation is interpreted to be from 2700 ft to 2550 ft and is composed of beds of lithotype 6 interbedded with lithotypes 3, 4 and 5.

The Logan Canyon Formation overlies the Missisauga Formation from 2550 ft to 1140 ft (348 m). Although very thin, the Naskapi Member in the Crow F-52 well is interpreted to be present from 2550 ft to 2500 ft (762 m) and the base of the Naskapi Member can be seismically correlated with the same horizon in the Fox I-22 well. It is composed of

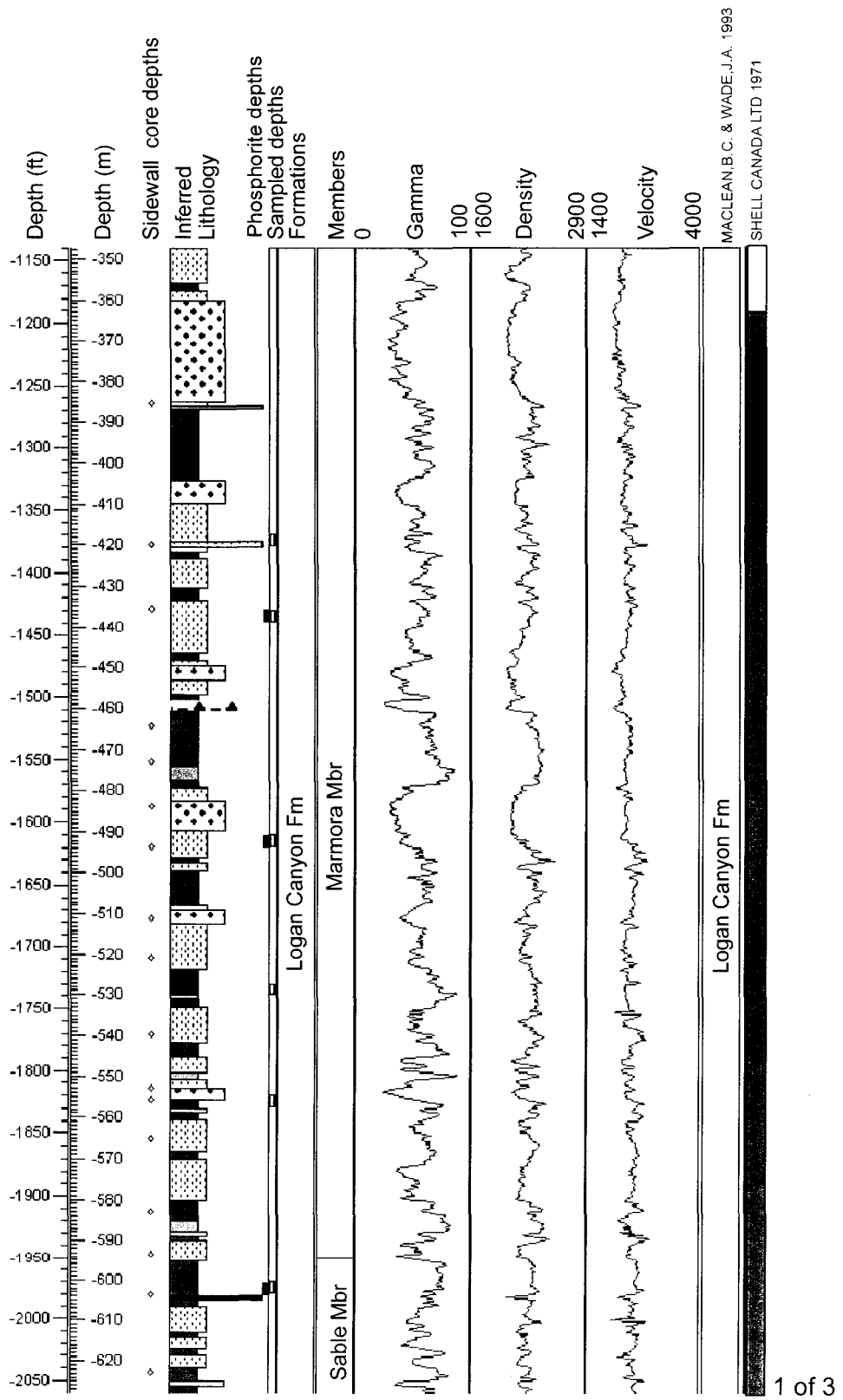
alternating silty mudstone and very fine to fine grained quartz wacke of lithotypes 3 and 4 respectively.

The Cree Member overlies the Naskapi Member from 2500 ft to 2150 ft (655 m) with the lower part of the member represented from 2500 ft to 2250 ft (686 m) by thick beds of lithotype 6 interbedded with thin beds of lithotypes 4 and 1. Cuttings within this part are dominated by very fine to fine siderite-cemented quartz wackes, siderite-cemented mudstone and silty mudstone, quartz and feldspar granules, and medium calcite-cemented quartz arenites. The upper part of the Cree Member, from 2250 ft to 2150 ft, is much finer grained than the lower section with beds of lithotype 4 interbedded with thin beds of lithotypes 5, 3 and 1.

The Sable Member of the Logan Canyon Formation is interpreted to be present from 2150 ft to 1950 (593 m) and is composed of alternating lithotypes 2, 3 and 4. One thin bed of lithotype 8 is also observed in this member. The wireline logs also show three fining upward sequences within this interval that are similar to those found in the Fox I-22 well.

The Marmora Member of the Logan Canyon Formation overlies the Sable Member from 1950 ft to 1140 ft (347 m) and consists of beds dominantly of lithotype 4 interbedded with beds lithotypes 2, 3, and 5. Cuttings within this member are dominantly of siderite-cemented very fine to fine grained quartz wackes and siderite-cemented mudstone and silty mudstones with lesser amounts of calcite-cemented medium to coarse grained quartz

arenites. Other cements observed are calcite, pyrite, and limonite. The cuttings at 1610 ft (491 m) and 1430 ft (436 m) contain phosphate nodules and phosphate-cemented silty mudstones. The cuttings at 1370 ft (419 m) are dominantly marl and siderite-cemented very fine to fine grained quartz wackes but the wireline logs do not show a response typical of a marl bed and therefore it is interpreted that the bed is too thin to be detected in the logs.



MACLEAN, B.C. & WADE, J.A. 1993  
SHELL CANADA LTD 1971

Figure 3.2. Lithostratigraphic plot for Crow F-52 showing formation, member and age boundaries and gamma, velocity and density wireline logs.

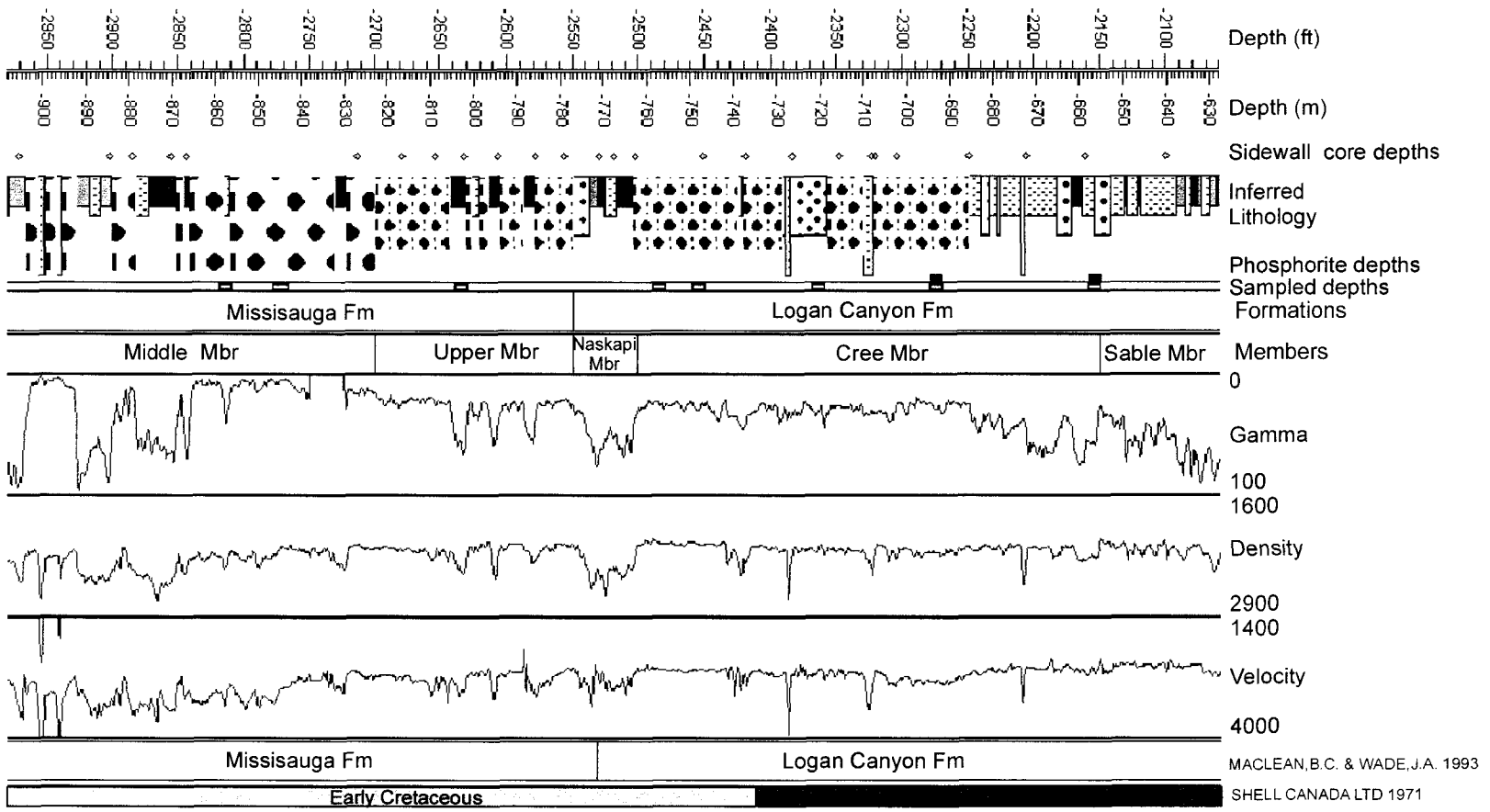


Figure 3.2. Lithostratigraphic plot for Crow F-52 showing formation, member and age boundaries and gamma, velocity and density wireline logs (continued).

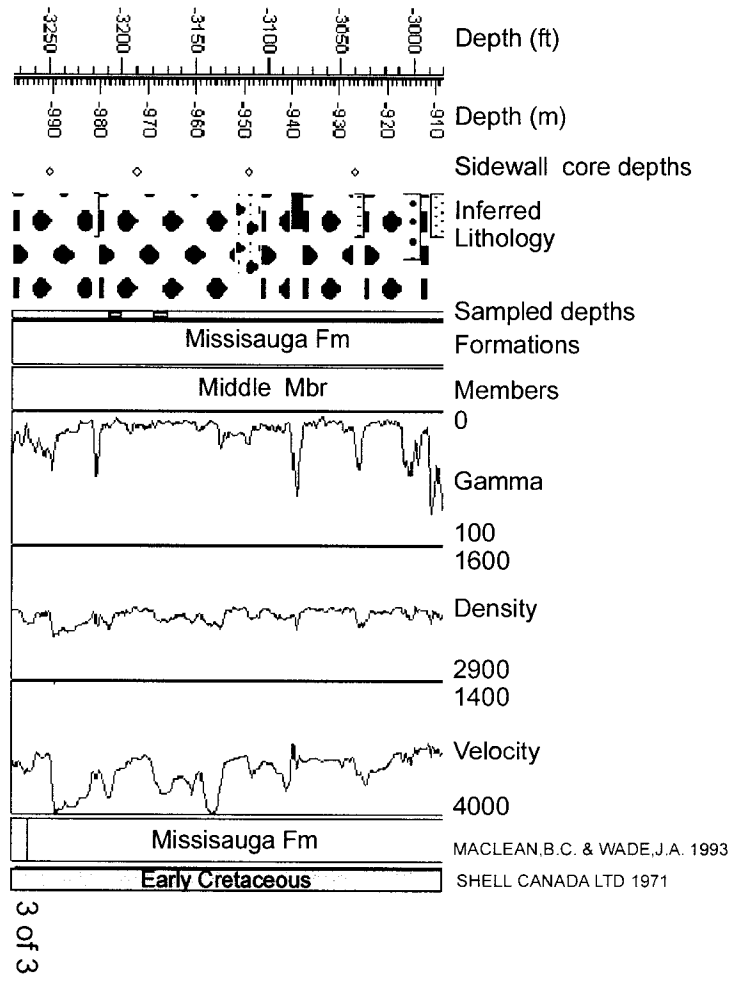


Figure 3.2. Lithostratigraphic plot for Crow F-52 showing formation, member and age boundaries and gamma, velocity and density wireline logs (continued).

### **3.4 Argo F-38 (D17)**

The Argo well is located 21.6 km northeast of the Crow F-52 well (Figure 1.1) at 45° 27'23.2"N, 58° 50'24.4" W. It is 11,110 ft (3386 m) in depth and penetrates the Dawson Canyon, Logan Canyon (Naskapi, Cree, Sable and Marmora members), Missisauga (Middle and Upper members), Mic Mac, Mohican, Argo, Iroquois, and Eurydice formations and Meguma Group basement rocks. This well also encountered two distinct igneous intervals, one near the base of the Cree Member and the other in the Middle Member of the Missisauga Formation. A lithological description of the sidewall cores within the Missisauga and Logan Canyon formations is provided in Table 11 in Appendix 3.

The Missisauga Formation (Figure 3.4) overlies the Mic Mac Formation from 5019 ft (1529 m) to 3685 ft (1124 m). The Middle Member of the Missisauga Formation is interpreted to be present from 5019 ft to 3880 ft (1183 m). The lower part of this member from 5019 ft to 4730 ft (1442 m) consists of beds of lithotype 6 interbedded with beds of lithotypes 5, 4 and 3. A thin bed of lithotype 8 is interpreted to also be present in this part of the member. Cuttings in this member are dominantly that of coal and shaly coal, fine to medium grained pyrite-cemented quartz arenites, and fine to medium grained quartz arenites and wackes with coal fragments. The upper part of the Middle Member extends from 4730 ft to 3880 ft (1182 m) and is mostly composed of thick beds of lithotype 7 interbedded with thinner beds of lithotypes 4 and 3. The wireline logs from 4588 ft (1398 m) to 4567 ft (1392 m) and 4430 ft (1350 m) to 4410 ft (1344 m) show peaks in density with matching spikes in velocity which are interpreted as possible thin

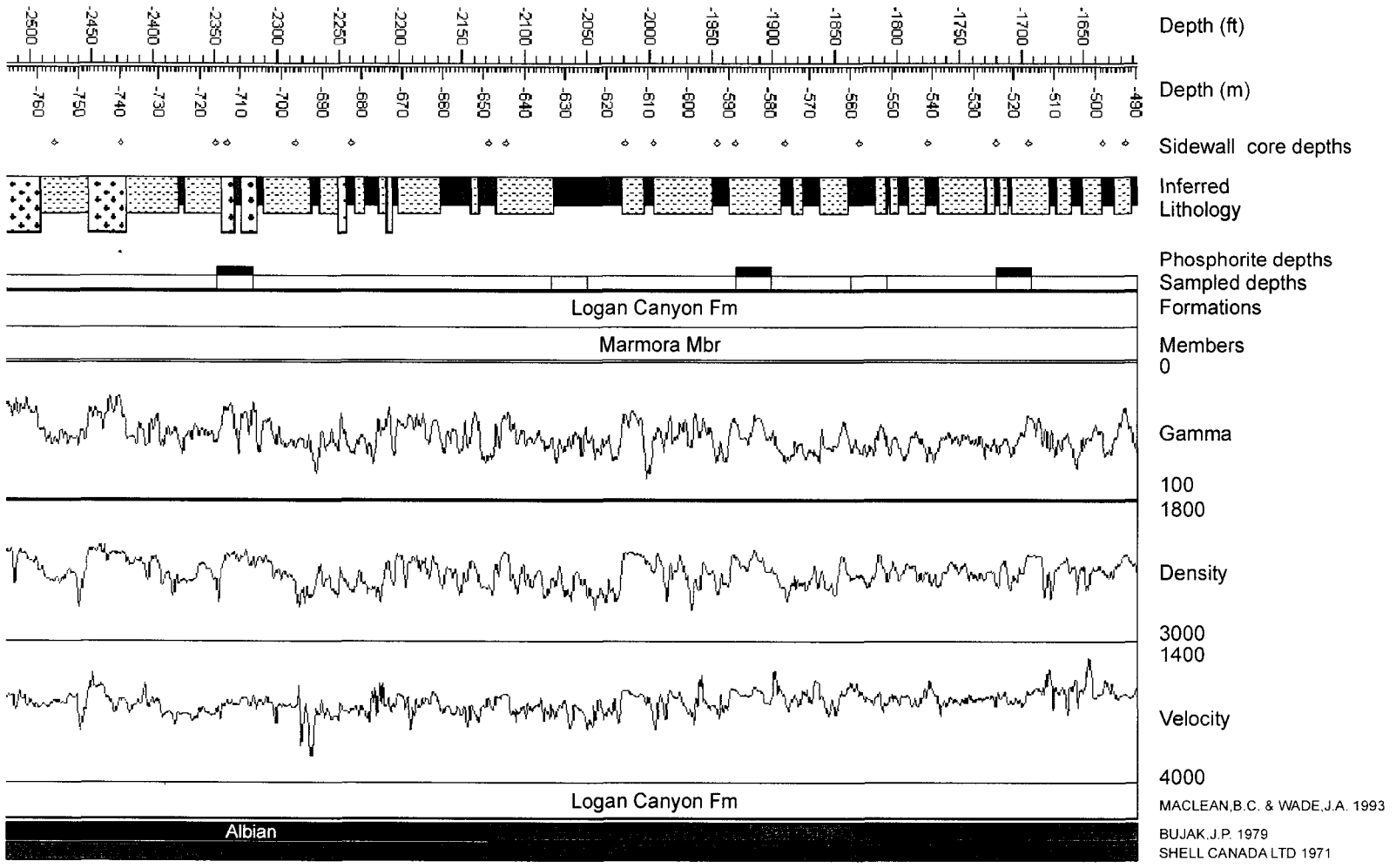
igneous beds or sills. Below the volcanic interval the spores are notably darker in colour, but not darkened above (Lyngberg, 1984) suggesting that these igneous units are volcanic rather than sills. The cuttings from below this interval at 4680 to 4700 ft have many basalt/diabase cuttings which strengthens the interpretation of thin basalt flows or sills at these depths. The Upper Member of the Missisauga Formation is interpreted to span from 3878 ft to 3685 ft and consists of beds of lithotype 7, between 10 and 20 feet thick interbedded with thinner beds of lithotypes 6, 5, 4 and 2.

The Logan Canyon Formation is 2191 ft (668 m) in thickness, overlying the Upper Member of the Missisauga Formation at 3685 ft and ending just below the Petrel Member of the Dawson Canyon Formation at 1495 ft (456 m). The Naskapi Member at the base of the formation is interpreted to be present in the well from 3685 ft to 3582 ft (1091 m) and consists of beds lithotype 2 interbedded with lithotype 3 and 4.

The Cree Member overlies the Naskapi Member from 3582 ft to 3021 ft (925 m). The lower part of this formation is characterized by lithotype 6 interbedded with lithotypes 5 and 4, with the occasional bed of lithotypes 3 and 1. Cuttings in this interval from medium sandstone beds include many quartz and feldspar granules and cuttings from silty mudstone to fine to medium grained sandstone beds are predominantly cemented with siderite. Two volcanic intervals are easily recognizable in the wireline logs from 3419 ft (1042 m) to 3360 ft (1024 m) and 3280 ft (1000 m) to 3210 ft (998 m) from their distinct high density and velocity responses. Abundant basalt/diabase cuttings are found in the interval from 3400 ft (1036 m) to 3410 ft (1039 m). Cuttings from both 3030 ft

(923 m) to 3060 ft (936 m) and 3060 ft to 3090 ft (942 m) have abundant cuttings of lithotype 1 but there is no corresponding response in the logs at or above these depths, which indicates that the bed may be too thin to be detected. The upper part of the Cree Member from 3210 ft to 3021 ft is dominantly lithotype 5, interbedded with lithotypes 4 and 3. The sandstone cuttings examined within this part are dominantly of quartz wackes cemented with siderite.

The Sable Member in the Argo F-38 well is thought to be present from 3021 ft to 2894 ft (882 m) and is composed of alternating beds of lithotypes 2, 3 and 4. Cuttings from this member are dominantly cemented with siderite. Above the Sable Member is the Marmora Member from 2894 ft to 1605 ft and it contains a thick bed of lithotype 5 at the base. Above this there are beds of dominantly lithotype 4 interbedded with lithotypes 5 and 3. This member fines upwards into beds dominantly of lithotype 4 interbedded with beds of lithotype 3. Cuttings from this member are very fine to medium grained siderite-cemented quartz wackes, coaly quartz wackes and phosphate-cemented very fine grained quartz wackes.



1 of 4

Figure 3.3. Lithostratigraphic plot for Argo F-38 showing formation, member and age boundaries and gamma, velocity and density wireline logs.

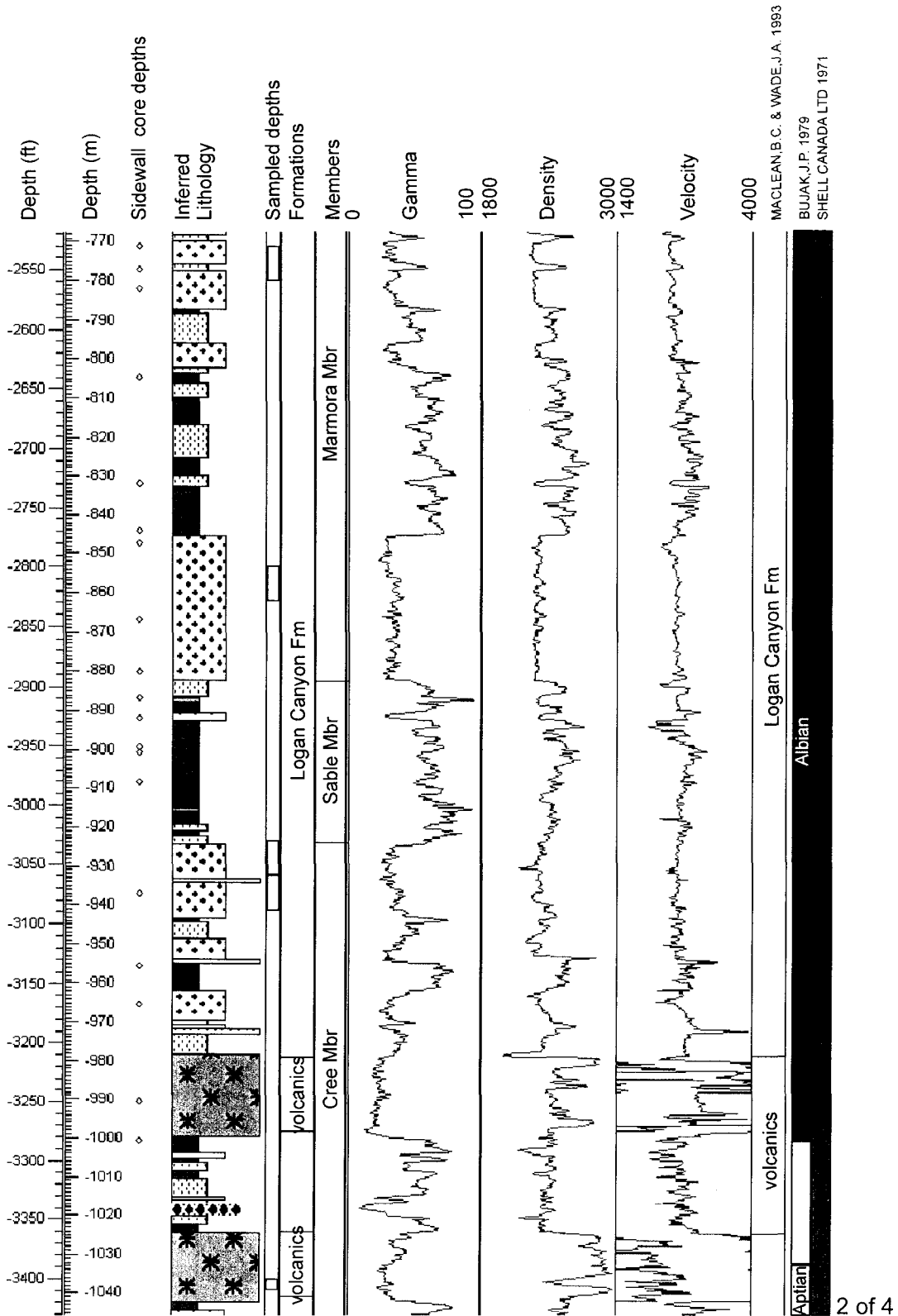
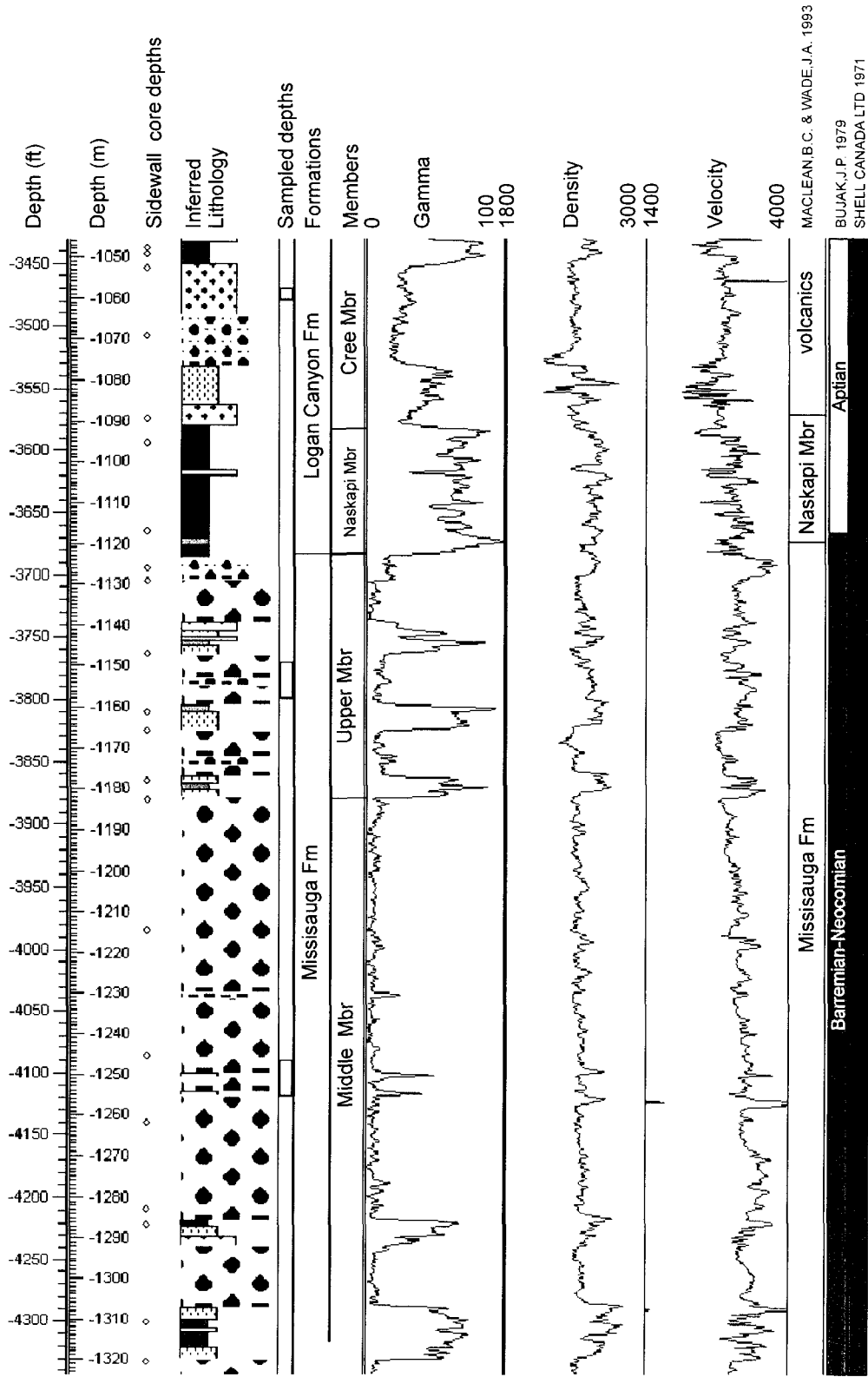
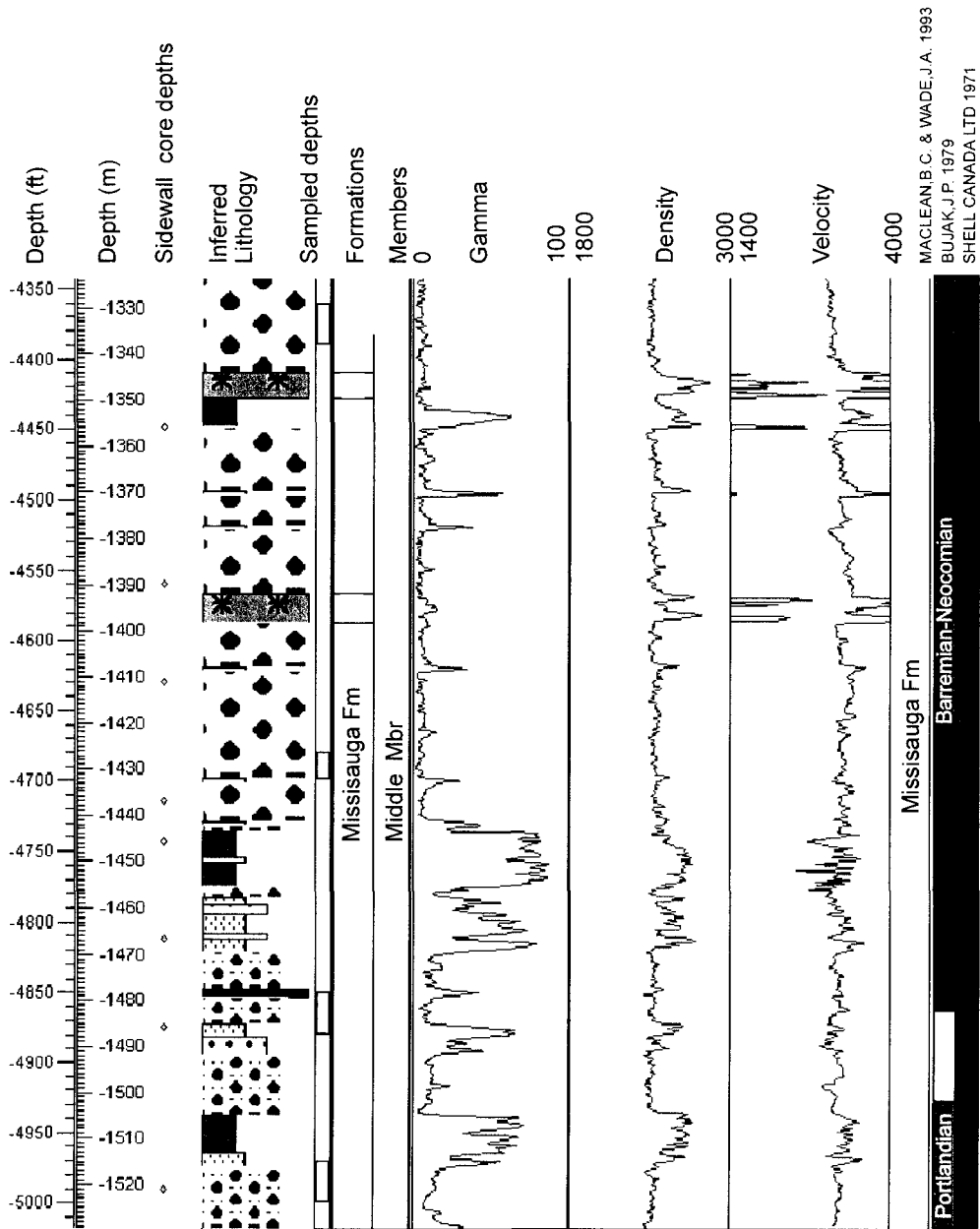


Figure 3.3. Lithostratigraphic plot for Argo F-38 showing formation, member and age boundaries and gamma, velocity and density wireline logs (continued).



3 of 4

Figure 3.3. Lithostratigraphic plot for Argo F-38 showing formation, member and age boundaries and gamma, velocity and density wireline logs (continued).



4 of 4

Figure 3.3. Lithostratigraphic plot for Argo F-38 showing formation, member and age boundaries and gamma, velocity and density wireline logs (continued).

### **3.5 Jason C-20 (D131)**

The Jason C-20 well is located 35.6 km east of the Argo F-38 well (Figure 1.1) at 45° 29' 05.5" N, 58° 32' 28.3" W. This well penetrates 8146 ft (2483 m) and encountered sediment from the Dawson Canyon (Petrel Member), Logan Canyon (Marmora, Sable, and Cree members), Missisauga (Middle Member), Mic Mac, Mohican, Iroquois, and Argo formations. There are no sidewall cores for this well.

The Missisauga Formation (Figure 3.5) extends from 5958 ft (1816 m) below KB to 4512 ft (1376 m), all of which is interpreted to be the Middle Member. The Upper Member is interpreted to have been eroded by the Top Missisauga unconformity at this well. The lower part of the Middle Member from 5958 ft to 5300 ft (1616 m) consists of thick beds of lithotype 7 interbedded with lithotypes 2, 3, 4 and 5. The cuttings from the lower part of the Middle Member are very fine to fine grained carbonate-cemented quartz wackes. The upper part of the Middle Member from 5300 ft to 4512 ft consists of thick beds of lithotype 7 interbedded with thinner beds of lithotypes 6, 5, 4, 2 and 3. Two thin beds of lithotype 1 are also observed in this member. No cuttings were recovered from 4910 ft suggesting that the sandstones are very poorly indurated.

The Logan Canyon Formation overlies the Missisauga Formation from 4512 ft to 2135 ft (651 m). There is no thick shale unit similar to the Naskapi Member of the Logan Canyon Formation present in this well. Two volcanic units, separated by a thin bed of lithotype 5, are present at the base of this formation from 4512 ft to 4483 ft (1367 m) and 4471 ft (1363 m) to 4462 ft (1359 m). A pyroclastic unit from 4325 ft (1318 m) to 4088 ft (1246

m) was interpreted by Jansa and Pe-Piper (1985). No cuttings > 2 mm were recovered from 4220 ft to confirm this but cuttings interpreted to be from the pyroclastic unit were found in the heavy fraction at and below 4220 ft. The sedimentary rocks overlying the pyroclastic unit from 4088 ft to 3169 ft (965 m) are interpreted as the Cree Member. The lower part of the Cree Member is thought to extend from 4088 ft to 3673 ft (1120 m) and consists of lithotype 6 interbedded with lithotypes 5, 4, and 3. The cuttings within this part of the member are coarse to very coarse grained carbonate-cemented sandstones, coal and shaly coal and fine to medium grained carbonate-cemented quartz wackes. The upper section of the Cree Member is interpreted from 3673 ft to 3169 ft and is characterised by beds lithotype 4 interbedded with lithotypes 6 and 3 with a few thin beds of lithotype 1.

The Sable Member is thought to be present from 3169 ft to 3000 ft (914 m) and is an interval of alternating beds of lithotypes 3 and 4. The location of this member in this well was based principally on seismic correlation. The wireline logs in this interval show a decrease in velocity from 3018 ft (920 m) to 3014 ft (919 m) and are interpreted to be a coal bed of lithotype 8, although no cuttings were sampled in this member to verify this. The Marmora Member of the Logan Canyon Formation overlies the Sable Member from 3000 ft (914 m) to 2135 ft (651 m) and is composed of thick beds of lithotype 4 interbedded with thinner beds of lithotypes 5 and 3 with a few very thin beds of lithotypes 8 and 1. There were no cuttings sampled from this member.

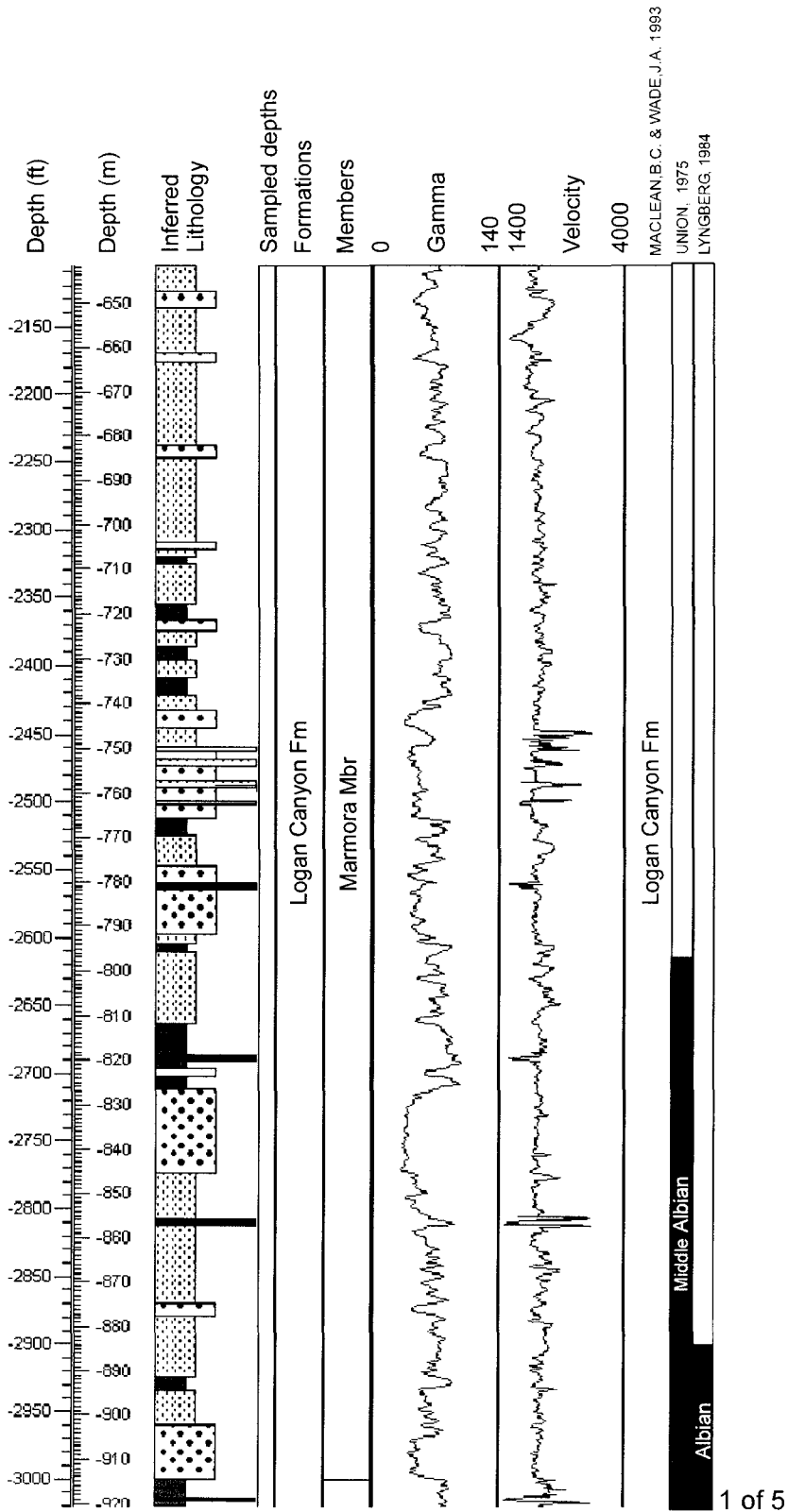
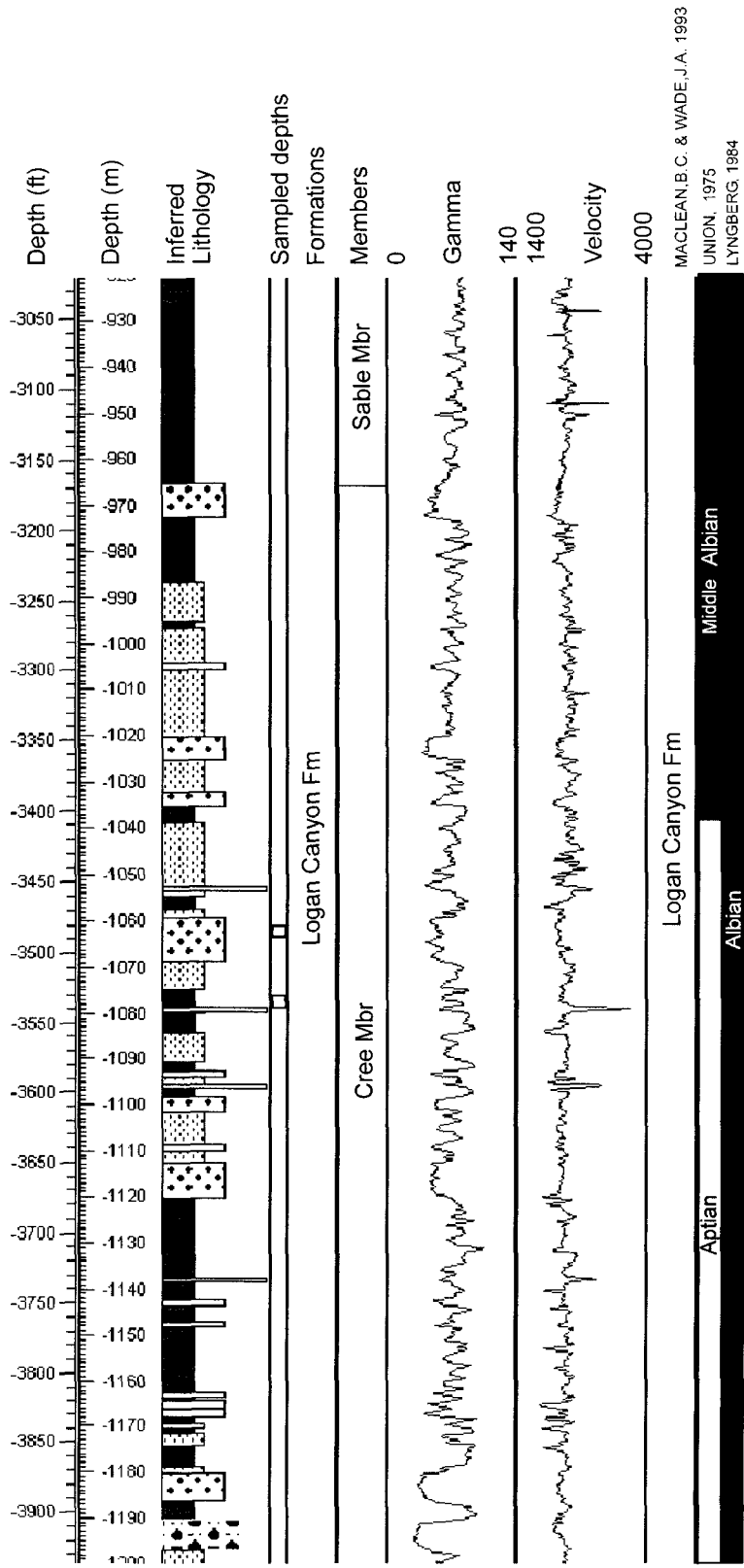


Figure 3.4. Lithostratigraphic plot for Jason C-20 showing formation, member and age boundaries and gamma, velocity and density wireline logs.



2 of 5

Figure 3.4. Lithostratigraphic plot for Jason C-20 showing formation, member and age boundaries and gamma, velocity and density wireline logs (continued).

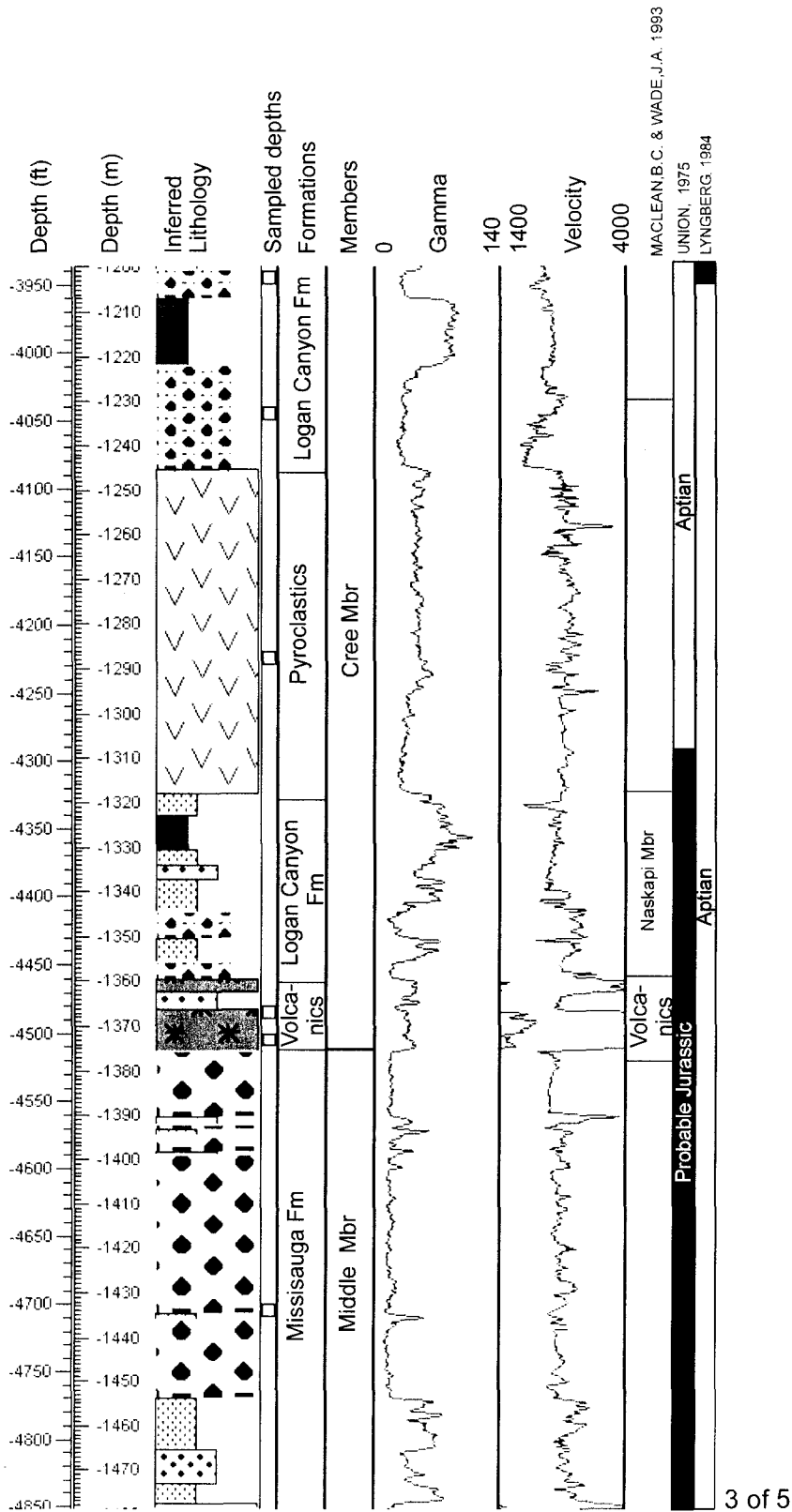


Figure 3.4. Lithostratigraphic plot for Jason C-20 showing formation, member and age boundaries and gamma, velocity and density wireline logs (continued).

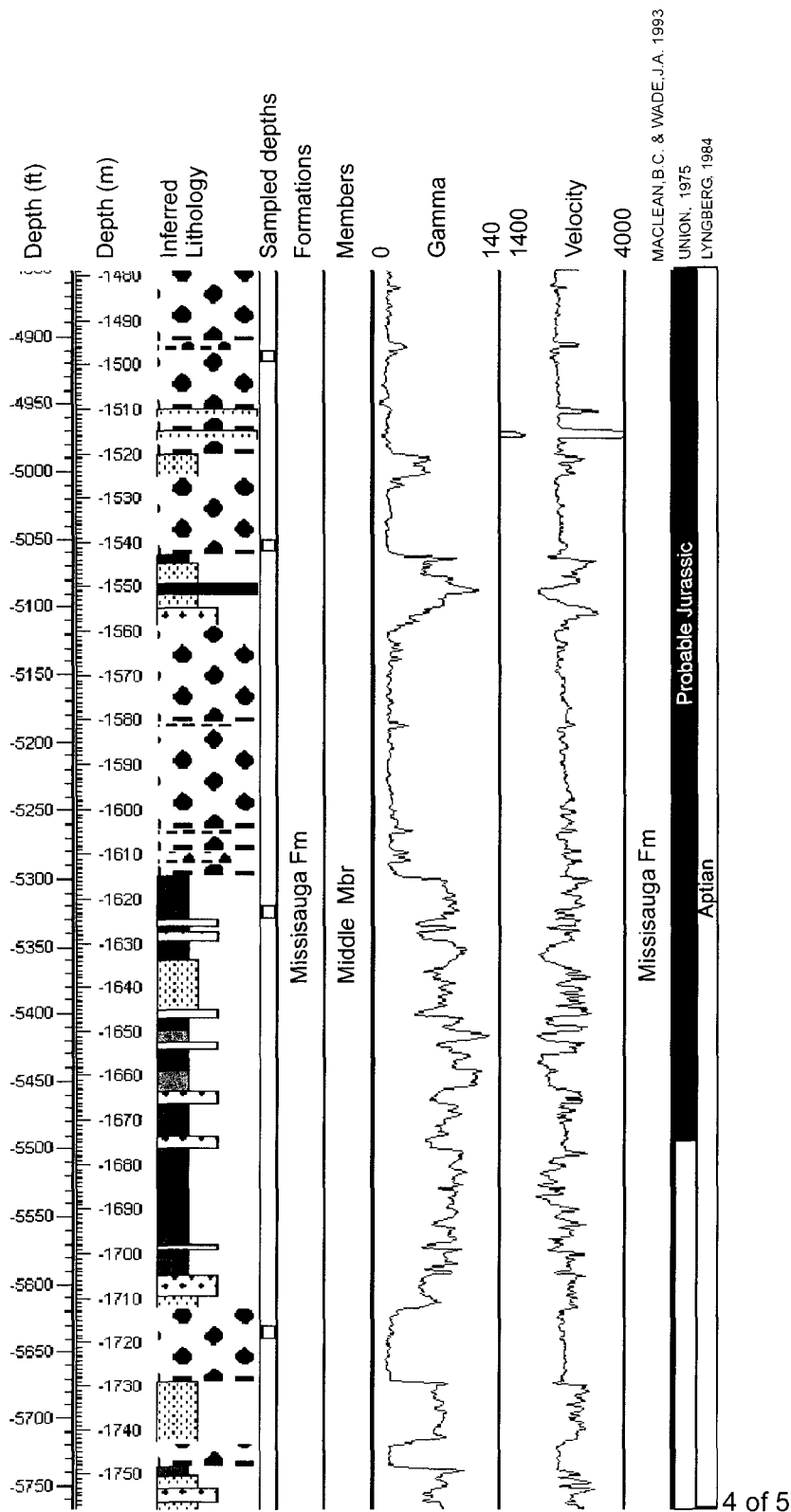


Figure 3.4. Lithostratigraphic plot for Jason C-20 showing formation, member and age boundaries and gamma, velocity and density wireline logs (continued).

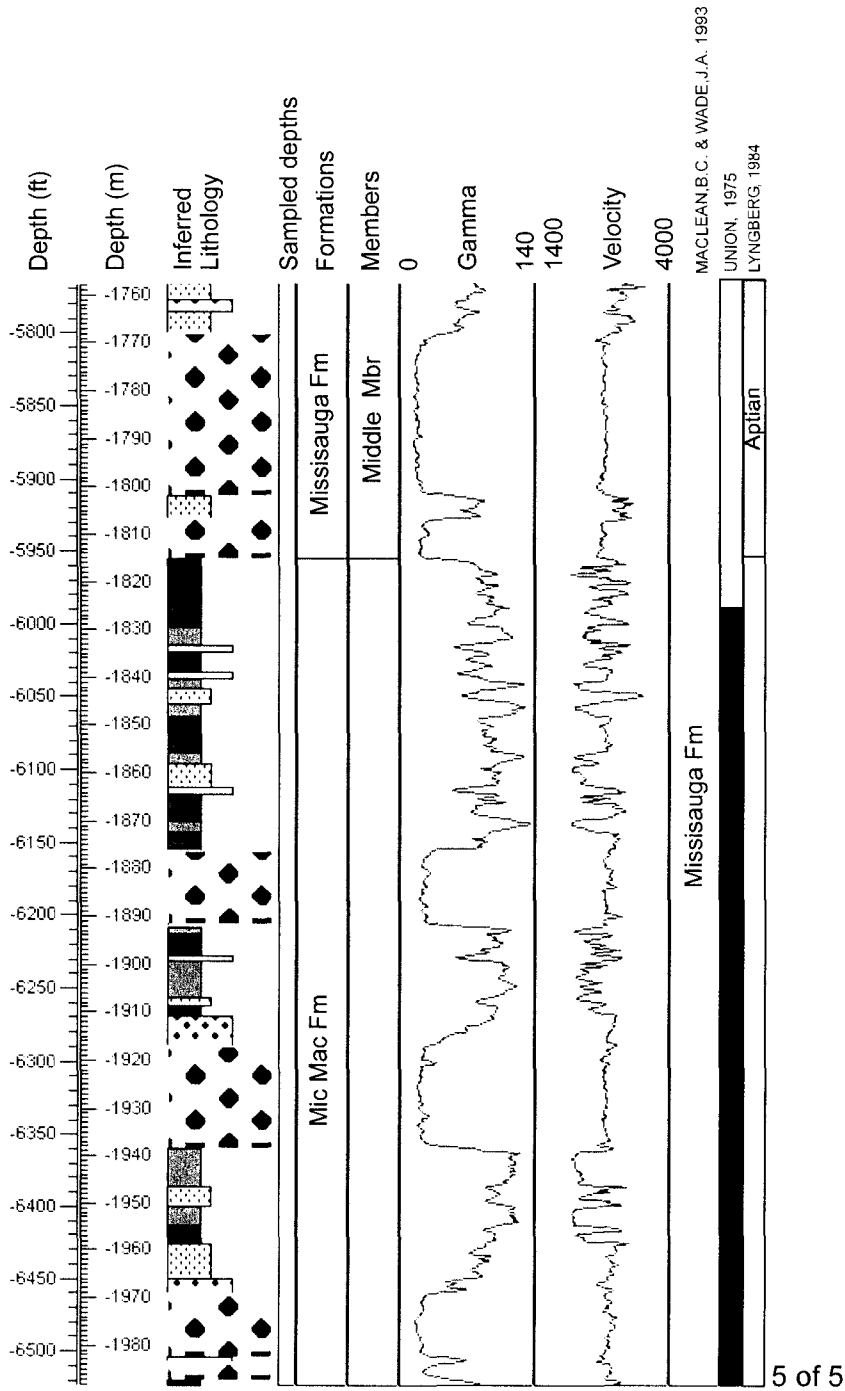


Figure 3.4. Lithostratigraphic plot for Jason C-20 showing formation, member and age boundaries and gamma, velocity and density wireline logs (continued).

### **3.6 Eurydice P-36 (D034)**

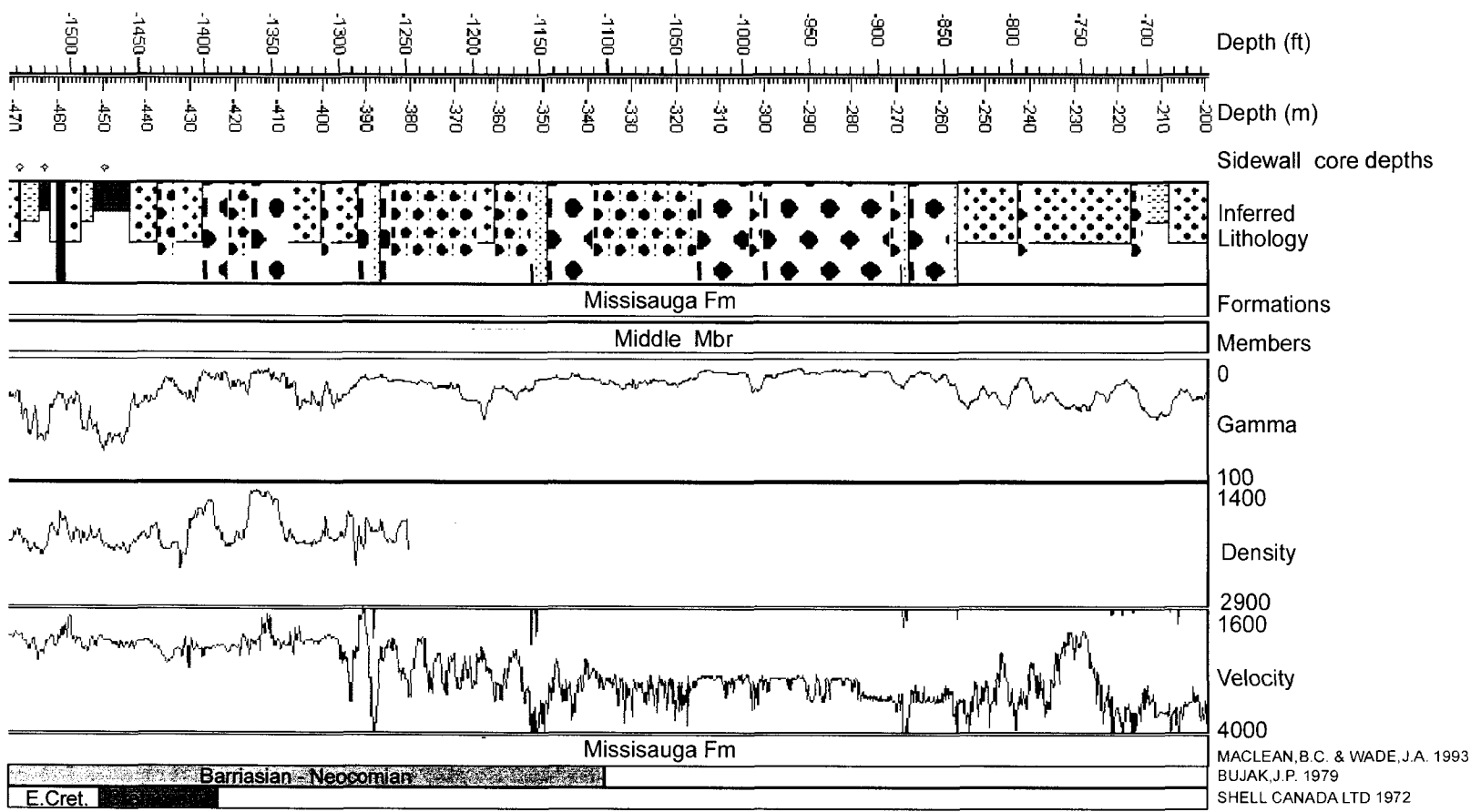
The Eurydice P-36 well is located 41.5 km west of the Fox I-22 well (Figure 1.1) at 45° 25' 47.3" N, 60° 04' 47.0" W. This well penetrates 9723 ft (2965 m) and encountered sediment from the Missisauga, Iroquois, Argo, and Eurydice formations. Sidewall core descriptions for the Missisauga Formation are shown in Table 3.3. There are no sidewall cores within the Logan Canyon Formation for this well.

<b>Depth (ft)</b>	<b>Description</b>
1475	Brown and white very fine grained to fine grained sandstone, well indurated. White grains look like milky quartz (solid white) few coal fragments.
1520	Light grey mostly silt to mud sized with a few fine to medium grained grains of quartz (rounded) also abundant orange (?) and black (coal?) fragments.
1538	Tan colored medium grained quartz arenite oxidizing darker brown-orange in places, poorly indurated
1575	Light grey very fine grained sandstone with very fine laminations, moderate to well indurated
1605	Light grey medium grained quartz arenite, poor to moderate induration oxidizing orange-brown
1625	Tan-brown medium grained quartz arenite with coal and mica grains, moderate to poor induration
1657	Grey-brown fine to medium grained sandstone, well indurated
1666	Tan-brown medium grained quartz arenite with coal and mica grains, moderate to poor induration
1673	Medium grey mudstone- very fine grained sandstone, well indurated
1700	Medium grey mudstone- very fine grained sandstone, well indurated

Table 3.3. Sidewall core descriptions for the Missisauga Formation from Eurydice P-36.

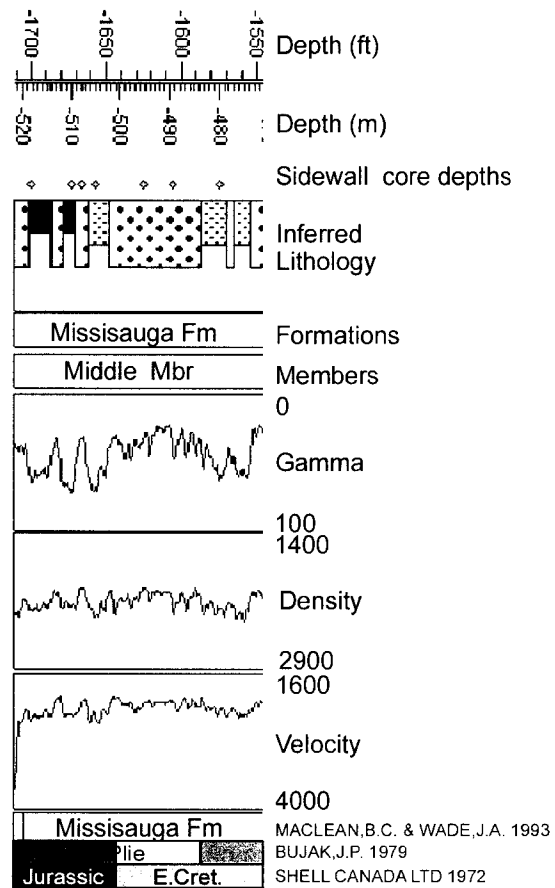
The Missisauga Formation is the first formation encountered by the Eurydice P-36 well and is interpreted to be present from the top of the logged and sampled interval of the well at 653 ft (199 m) to 1709 ft (521 m). The Middle Member of the Missisauga Formation is interpreted to span this entire section and is divided into a lower and upper part. The lower part, from 1709 ft to 1432 ft (436 m), consists of thick beds of lithotype

5 interbedded with lithotypes 4 and 3. Sidewall core recovered from this interval were medium grey mudstones, some contained laminations, minor plant remains or burrows and fine and medium grained yellowish-brown sandstone. The well history report describes the cuttings as loose sands, mainly coarse grains of quartz, feldspar, chert, ironstone and igneous grains. Coal, medium grey silty mudstone, fine grained quartzose sandstone and medium grained quartzose sandstones, and grey-brown carbonaceous, slightly micaceous and pyritic mudstones. The upper part of the Middle Member is more coarser grained than the lower part and is composed dominantly of thick beds of lithotypes 6 and 7 interbedded with thin beds of lithotypes 4 and 1. The density log starts at 1206 ft (379 m), so above this marl beds are picked on gamma and velocity logs only, with much less confidence. There are no sidewall cores from this part of the Middle Member.



1 of 2

Figure 3.5. Lithostratigraphic plot for Eurydice P-36 showing formation, member and age boundaries and gamma, velocity and density wireline logs.



2 of 2

Figure 3.5. Lithostratigraphic plot for Eurydice P-36 showing formation, member and age boundaries and gamma, velocity and density wireline logs (continued).

### **3.7 Hercules G-15 (D130)**

The Hercules G-15 (D130) well is located 13.7 km east of the Argo F-38 well (Figure 1.1) at 45° 34' 20.6" N, 58° 47' 13.1" W. This well penetrates 3546 ft (1081 m) and encountered sediment from the Logan Canyon (Cree, Sable and Marmora members), Missisauga, Mic Mac, Mohican, Iroquois, and Argo formations. Two volcanic beds and one pyroclastic bed were also encountered. There are no sidewall cores taken in this well.

The Upper Member of the Missisauga Formation is interpreted to be present from 2714 ft (827 m) to 2539 ft (774 m) and consists of beds of lithotype 4 interbedded with thinner beds of lithotypes 5, 6 and 7. The Logan Canyon Formation overlies the Missisauga Formation from 2539 ft to top of the well at 1059 ft (323 m). The Cree Member extends from 2539 ft to 2058 ft (627 m) with two volcanic beds of lithotype 9, separated by a bed of lithotype 5 are at the base of the member from 2539 ft to 2465 ft (752 m). A pyroclastic unit is found within this member from 2333 ft (711 m) to 2085 ft (636 m). The remainder of the Cree Member consists of beds of lithotype 6 interbedded with lithotypes 5 and 4.

The Sable Member is interpreted to be from 2058 ft to 1884 ft (575 m) and is composed of thin alternating beds of lithotypes 4, 5, 3 and 2. The location of this member is strengthened by seismic correlation with the Argo F-38 well described in Chapter 5. The Marmora Member is thought to span from 1884 ft to the top of the sampled and logged interval of the well at 1059 ft. This member is dominantly composed of thick beds of lithotypes 5 and 4 interbedded with lithotypes 3, 2, 1 and 8. This member is different

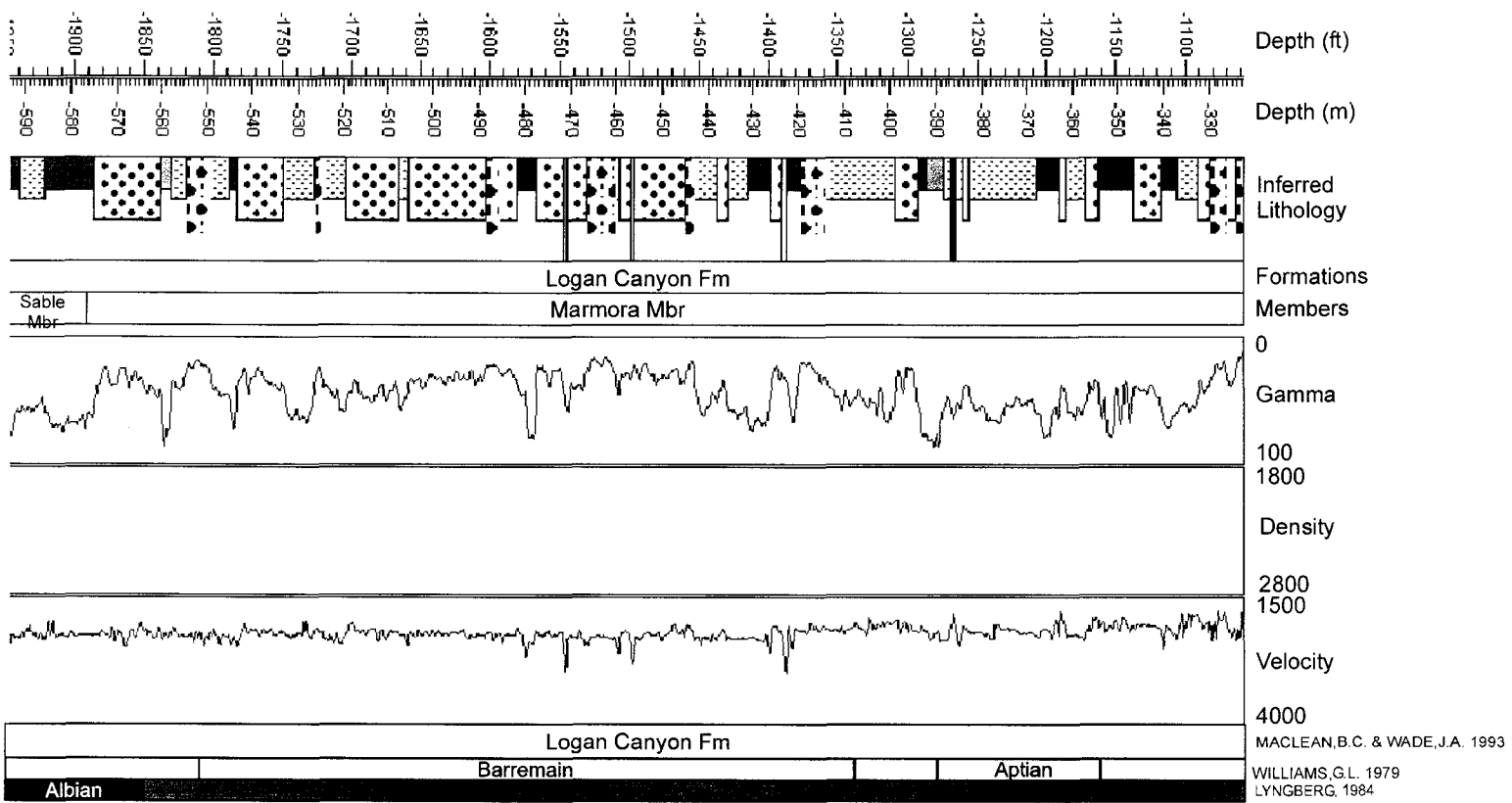
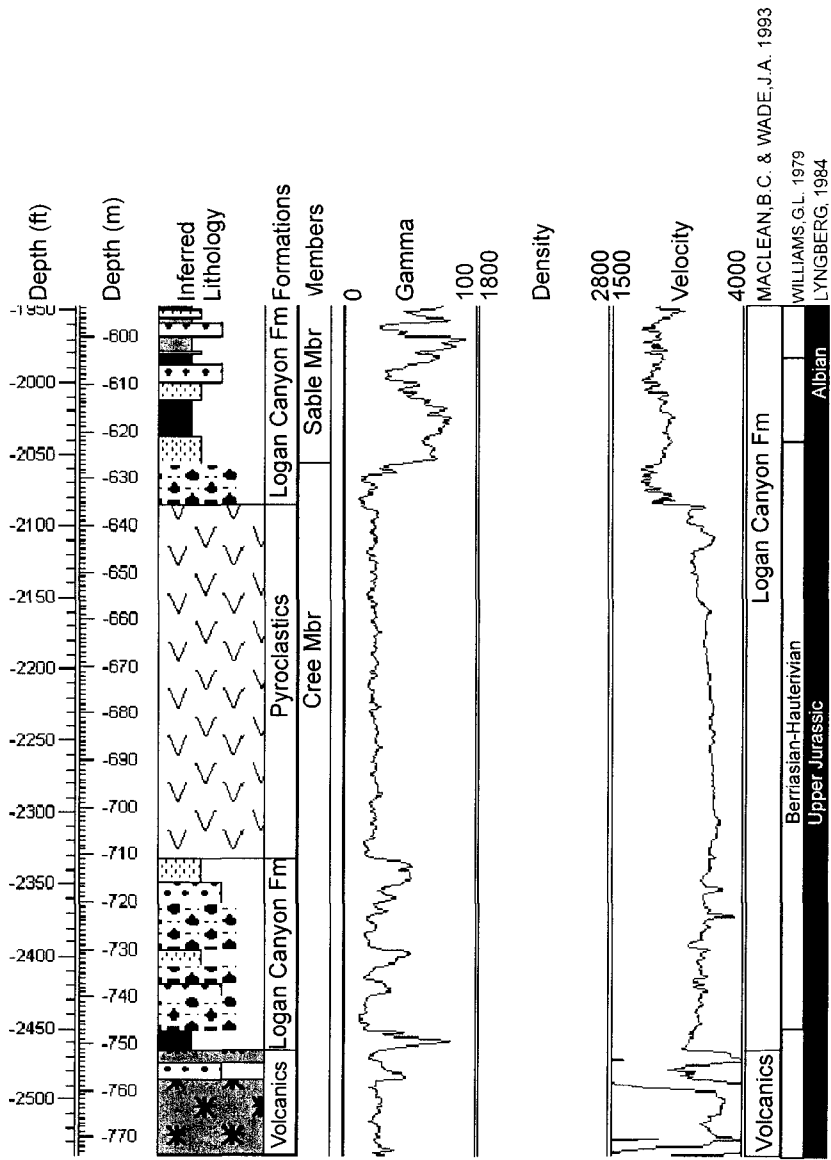


Figure 3.6. Lithostratigraphic plot for Hercules G-15 showing formation, member and age boundaries and gamma, velocity and density wireline logs.



2 of 2

Figure 3.6. Lithostratigraphic plot for Hercules G-15 showing formation, member and age boundaries and gamma, velocity and density wireline logs (continued).

from all the previously described Marmora Members in other wells because in addition to the above mentioned lithotypes there are also many beds of lithotype 6.

### **3.8 Adventure F-80 (D144)**

The Adventure F-80 well is located 50.2 km east of the Jason C-20 well (Figure 1.1) at 45° 19' 27.6" N, 57° 56' 22.8" W. This well penetrates 6557 ft (1999 m) and encountered sediment from the Wyandot, Dawson Canyon (Petrel Member), Logan Canyon (Marmora Member), Iroquois, and Argo formations. The Missisauga Formation is absent for this well because this well is drilled on the side of a salt diapir. There are no sidewall cores within the Logan Canyon Formation for this well.

The Logan Canyon Formation (Figure 3.8) in this well extends from 2719 ft (829 m) to 3149 ft (960 m) and is interpreted to be only the Marmora Member. This member is composed of thin alternating beds of lithotypes 4, 3 and 2 with a few thin beds of lithotype 5.



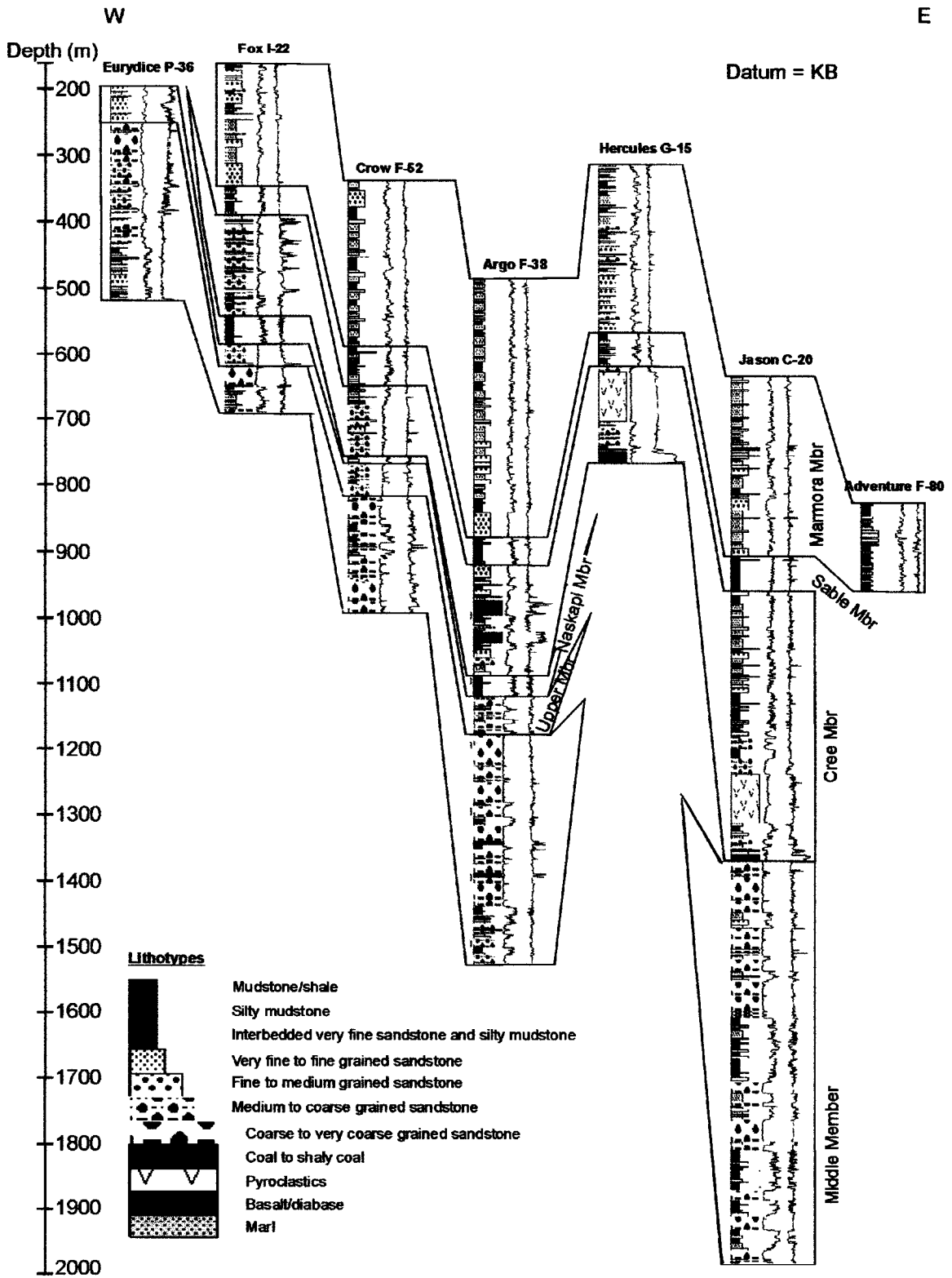


Figure 3.8. Correlation diagram showing the members of the Logan Canyon (Marmora, Sable, Cree, and Naskapi) and Missisauga (Middle and Upper) formations.

## **CHAPTER 4**

### **SEISMIC MARKERS AND CORRELATION WITH THE LITHOSTRATIGRAPHY**

#### **4.1 Introduction**

This chapter describes the key reflections that were used to determine the distribution of the Logan Canyon and Missisauga formations. Synthetic seismograms were used to correlate the lithostratigraphic plots to the seismic lines (as described in the Methods section of Chapter 2). Lithostratigraphic columns were converted from depth to time and matched with seismic lines at the well locations (Appendix 5 - Figures 1-7). Reflections were mapped away from wells only where they could be traced with confidence.

Lithologies that correspond to key reflections at the wells may vary laterally. Therefore, a lithologic interpretation of a reflection cannot be assumed away from the wells. The first part of this chapter will outline each seismic marker used for mapping and describes its attributes and the attributes of the overlying and underlying reflections (Table 4.1).

Unconformities identified in the seismic profiles were abbreviated U and given a number to signify the order from youngest to oldest. For example, U1 is therefore the youngest unconformity identified in the seismic profiles. The second part of this chapter will discuss the regional distribution of the lithostratigraphy based on the distribution of the seismic markers.

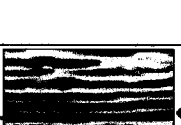
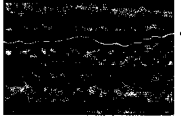
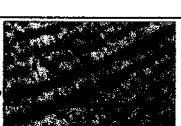
Horizons	Marker	Typical attributes	Reflections above marker	Reflections below marker
	U1	Positive, high amplitude, continuous, straight reflection	Reflection-free, low amplitude	Reflection-free or discontinuous with low frequency and low amplitude
	U2	Negative, high to medium amplitude, wavy to straight reflection	Parallel to subparallel, continuous to discontinuous and high amplitude	Truncated, medium to low amplitude, medium to low frequency, and discontinuous
	Petrel	1 to 3 positive, continuous, straight reflections with medium to high amplitude. Picked on bottom reflection when 2 reflections are present and middle when 3 are present	Subparallel to parallel, continuous reflections with high frequency and medium amplitude	Subparallel, continuous to discontinuous reflections with medium to low amplitude and medium frequency
	Green	1 positive, continuous straight to wavy reflection with medium to low amplitude	Subparallel, continuous to discontinuous reflections with medium to low amplitude and medium frequency	Subparallel to sigmoid, discontinuous, wavy reflections with medium to low amplitude and medium frequency
	U3	Positive, medium to high amplitude, continuous to discontinuous, wavy reflection	Subparallel to sigmoid, discontinuous, wavy, medium to low amplitude, and medium frequency	Truncated or subparallel, wavy, sigmoid to subparallel, semi-continuous to discontinuous, medium to low amplitude, medium to high frequency
	Volcanic	1 or 2 positive, continuous, straight reflection with high amplitude. Picked on bottom reflection	Subparallel, wavy, discontinuous reflection with medium to low amplitude and medium to high frequency	U3 underlies the volcanic marker
	U4	Positive or negative, medium to high amplitude, continuous, wavy or planar reflection	Subparallel, high to medium amplitude, and medium frequency. The volcanic marker overlies U2 in the eastern part of the graben.	Truncated to subparallel, medium to low amplitude, and medium frequency
	Top Mic Mac	Positive, straight to wavy, continuous reflection with high to medium amplitude	Subparallel, wavy, continuous to discontinuous reflections with low amplitude and frequency	subparallel, wavy, and continuous to discontinuous reflections with low amplitude and frequency
	U5	Negative, medium to high amplitude, wavy, continuous reflection	Subparallel, high to medium amplitude, and medium frequency	Truncated, low to medium amplitude, and medium frequency

Table 4.1. Key seismic markers, their attributes and the attributes of the reflections above and below.

#### **4.1.1 The U1 Marker**

The U1 marker is a positive, high amplitude, continuous reflection just below the seafloor (Figure 4.1). Reflections above and below are typically transparent, discontinuous and have a low amplitude. This unconformity appears to be present throughout the entire graben and is interpreted to be the result of Quaternary erosion.

#### **4.1.2 The U2 Marker**

The U2 marker is a negative, wavy to straight reflection with a high to medium amplitude. It occurs from several hundred milliseconds above the Petrel marker to just above the Volcanic marker. The reflections above are parallel to subparallel, continuous to discontinuous and with a high amplitude. The reflections below are truncated and discontinuous with a medium to low amplitude and a medium (between 60 Hz and 40 Hz) to low frequency (> 40 Hz). This reflection is only seen in the north eastern part of the graben (Figure 4.2) and may correlate to Early Eocene, mid-Oligocene or Mid-Miocene unconformities found, for example, in the Dauntless D-35 well to the southeast in the eastern extremity of the Abenaki and Sable Subbasins (Wade *et al.*, 1995). There are no wells that penetrate this unconformity to constrain the age and therefore it will be referred to as the Tertiary unconformity in subsequent chapters.

#### **4.1.3 The Petrel Marker**

The Petrel marker is characterized by one to three positive, continuous, high amplitude reflections, typically found between 0.3 s and 0.8 s (Two-way Travel-Time (TWTT)) in the seismic lines. The reflections above the Petrel marker are subparallel to parallel with high frequency (< 0.015 seconds) and a medium amplitude. The reflections below are

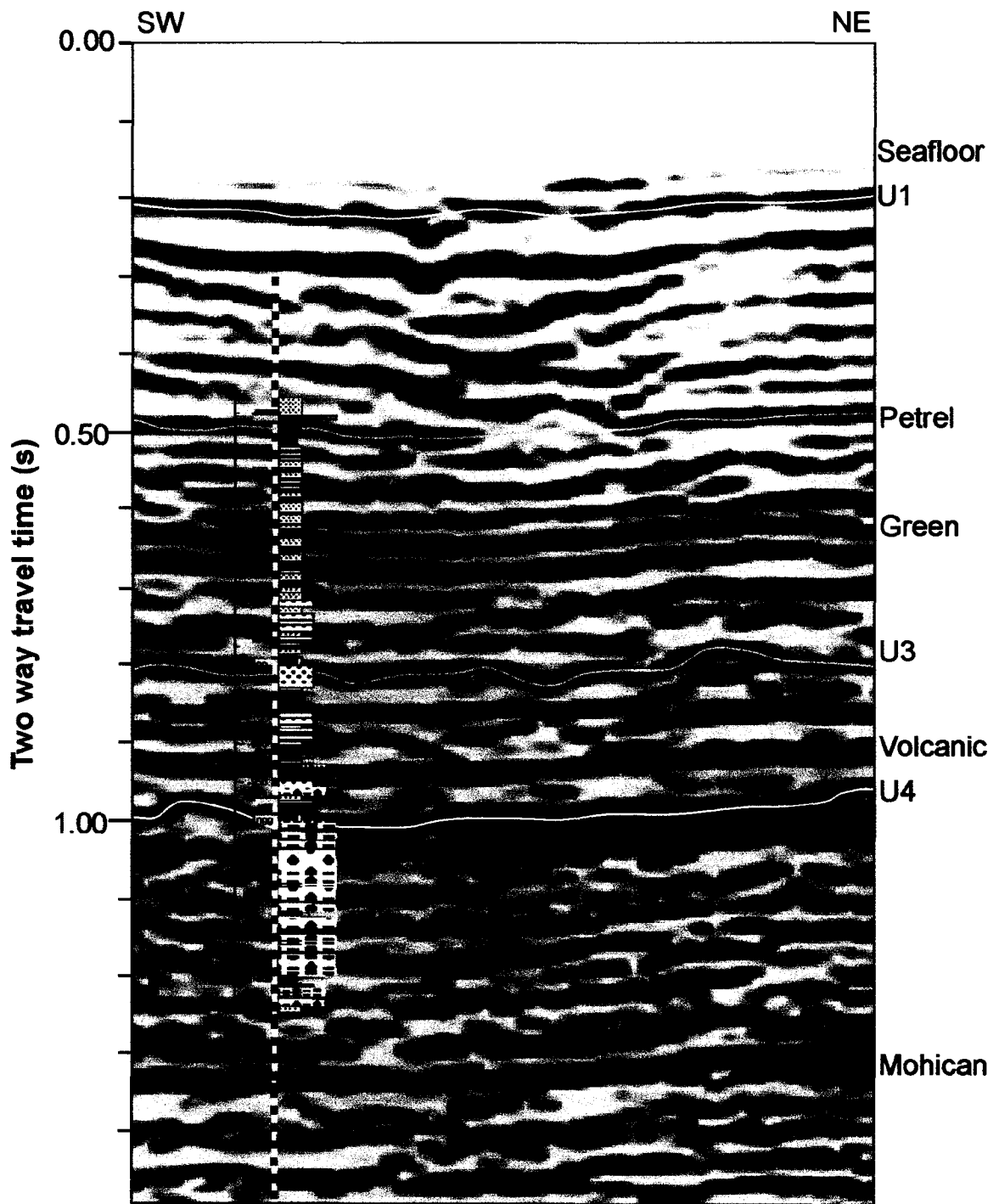


Figure 4.1. Line 390-B showing the correlation between the inferred lithostratigraphy at the Argo F-38 well and the corresponding seismic response. U2 marker and U5 marker are not imaged in this line (refer to Figure 2.1 for well and line location).

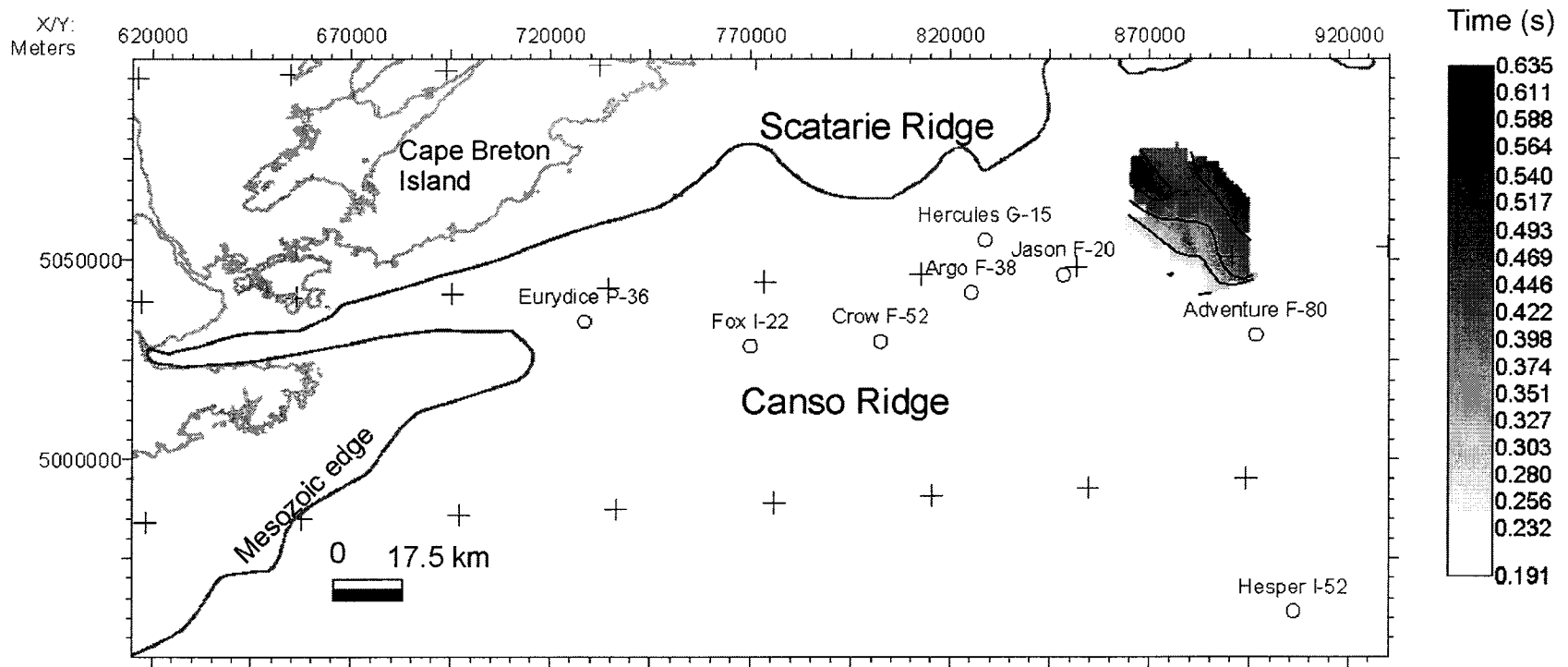


Figure 4.2. Map showing the extent of the U2 marker. Contours were generated using the inverse distance to a power algorithm with a grid spacing of 1 km, maximum distance of 30 km, weight of 2 and low smoothing. Bathymetry and Mesozoic edge are from MacLean (1991). Map plotted using The KINGDOM Suite with the UTM Zone 20N (66° W to 60° W) and WGS 1984 datum.

subparallel, continuous to discontinuous, with a medium to low amplitude and a medium frequency. The Petrel marker maintains an almost constant TWTT of 0.4 to 0.5 seconds above the Volcanic marker (Figure 4.1). At Adventure F-80, Argo F-38 and Jason C-20 this marker corresponds to the limestone and marl of the Petrel Member. This marker has been erosionally removed from the central, western and northeastern parts of the graben (Figure 4.3). Where two reflections are present for this marker, the bottom reflection correlates to the places with only one reflection, but where there are three reflections, the middle reflection correlates. The most laterally continuous reflection was chosen for regional mapping.

#### **4.1.4 The Green Marker**

The Green marker is a positive, medium to low amplitude, continuous, straight to slightly wavy reflection. The reflections above the Green marker are subparallel, continuous to discontinuous, with a medium to low amplitude and a medium frequency. The reflections below are subparallel to sigmoidal, discontinuous, wavy, with a medium to low amplitude and a medium frequency. The Green reflection correlates to a shale unit within the Marmora Member of the Logan Canyon Formation in the Argo F-38 (Figure 4.1) and Jason C-20 wells.

#### **4.1.5 The U3 Marker**

The U3 marker is a positive, continuous to discontinuous, wavy reflection with a medium to high amplitude. It occurs between the Green and Volcanic markers. The reflections above are subparallel to sigmoidal, discontinuous, wavy, with a medium to low amplitude, and a medium frequency. The reflections below are truncated or subparallel,

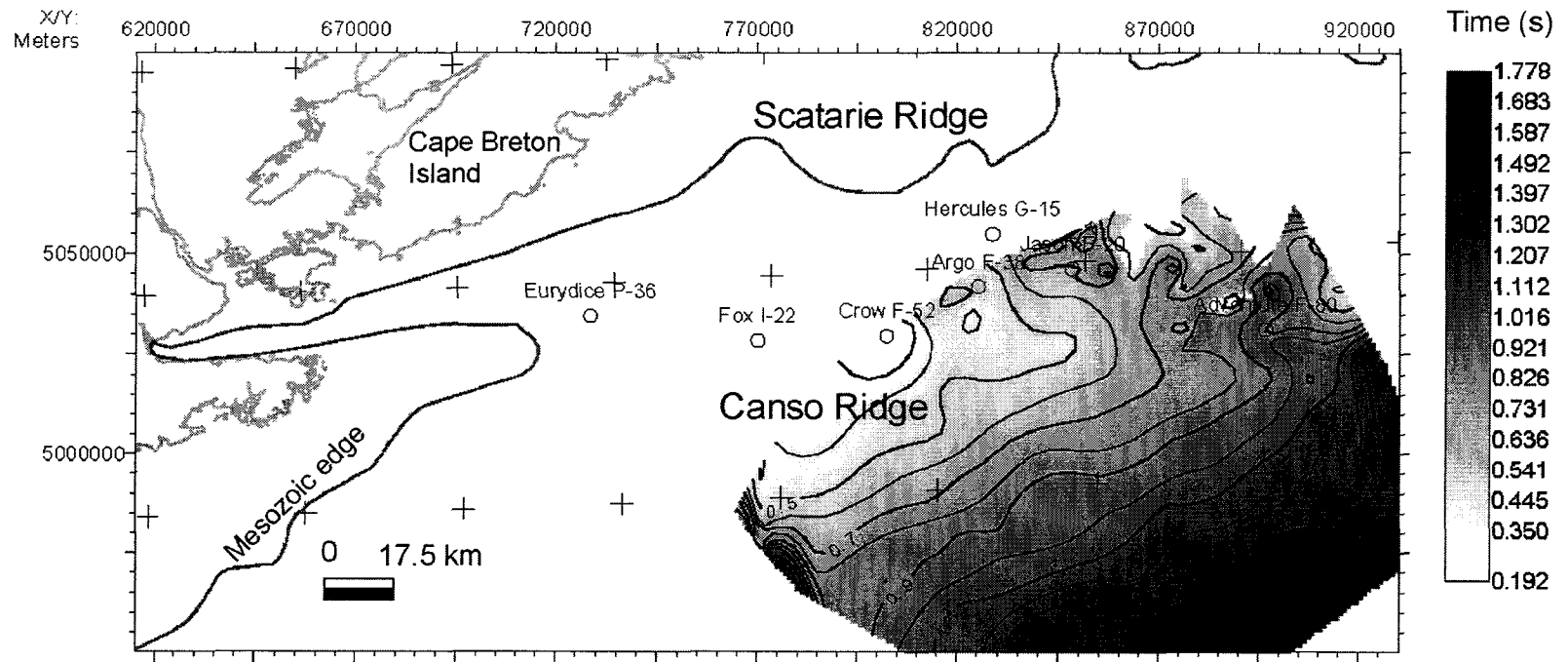


Figure 4.3. Map showing the extent of the Petrel marker. Contours were generated using the inverse distance to a power algorithm with a grid spacing of 1 km, maximum distance of 30 km, weight of 2 and low smoothing. Bathymetry and Mesozoic edge are from MacLean (1991). Map plotted using The KINGDOM Suite with the UTM Zone 20N (66° W to 60° W) and WGS 1984 datum.

wavy, sigmoid to subparallel, semi-continuous to discontinuous, with a medium to low amplitude, and a medium to high frequency. This unconformity is interpreted to be Barremian to Albian in age from its correlation to wells but its span is uncertain. At the Crow F-52, Argo F-38 (Figure 4.1) and Hercules G-15 wells, this unconformity correlates to the contact of the Cree Member with the Sable Member.

#### **4.1.6 The Volcanic Marker**

The Volcanic marker is one or two positive, high to medium amplitude, continuous to discontinuous, wavy to straight reflections which are typically found between 0.5 and 1.5 seconds (TWTT) in the seismic profiles. The reflections above this marker are discontinuous, subparallel to chaotic with, low to medium amplitude and frequency. Generally, in the N-S lines of the eastern part of the graben the reflections above the Volcanic marker are disrupted and transparent, whereas they are generally more continuous and of higher amplitude in the E-W sections (discussed in Chapter 5). The Volcanic marker is thought to be found only in the eastern to central part of the graben, but it is at the same stratigraphic level as a prominent reflection corresponding to the Naskapi Member in other parts of the graben and south of the Canso Ridge, making mapping the westerly extent of this Volcanic marker difficult with so few well ties. The Volcanic marker is also observed at the Hesper P-52 and I-52 wells to the south of the Orpheus Graben (Figure 4.4). The Volcanic marker correlates to the volcanic units in the Argo F-38 (Figure 4.1), Hercules G-15, and Jason C-20 wells near the base of the Cree Member. Where there are two reflections the bottom reflection is picked because it is more continuous. The reflection does not crosscut other reflections, suggesting it is more likely to be related to a flow and not a sill.

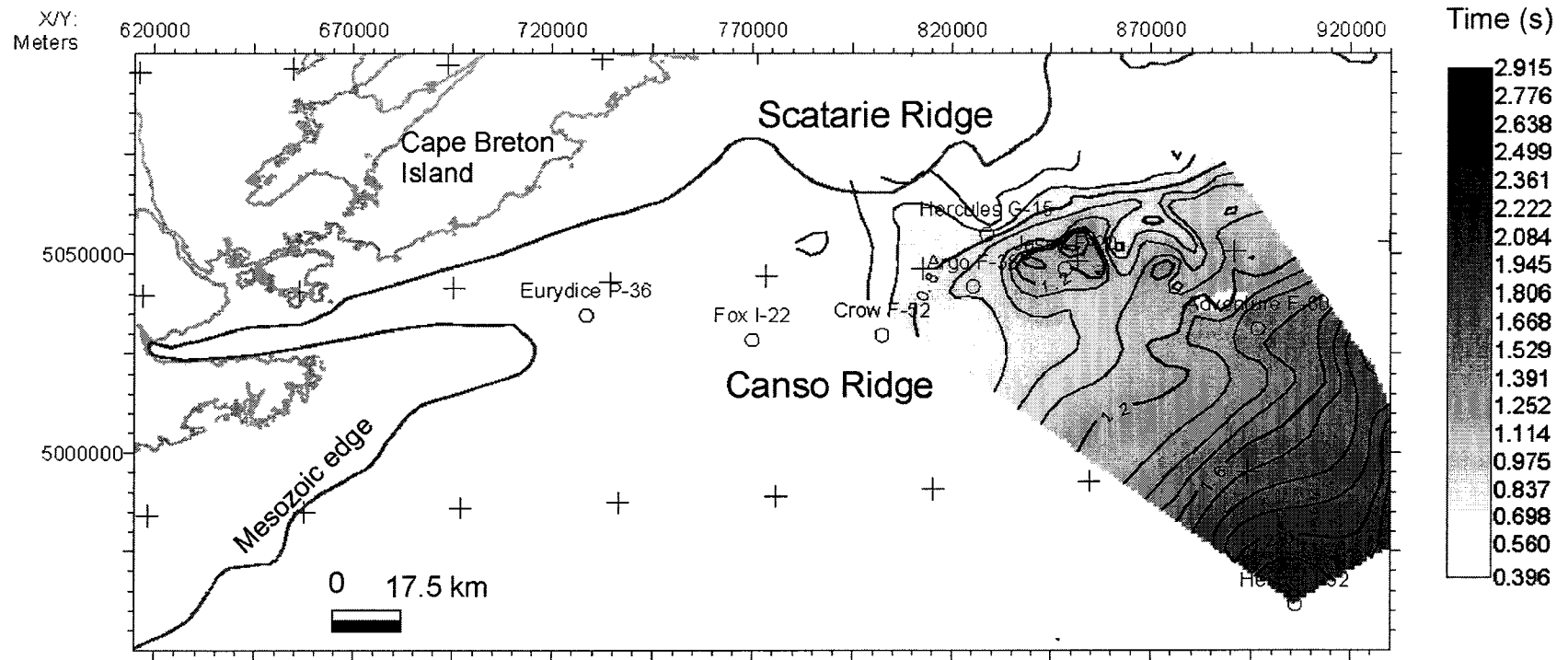


Figure 4.4 Map showing the possible extent of the Volcanic marker. Contours were generated using the inverse distance to a power algorithm with a grid spacing of 1 km, maximum distance of 30 km, weight of 2 and low smoothing. Bathymetry and Mesozoic edge are from MacLean (1991). Map plotted using The KINGDOM Suite with the UTM Zone 20N (66° W to 60° W) and WGS 1984 datum .

#### **4.1.7 The U4 Marker**

The U4 marker is typically a positive, continuous, wavy reflection with a medium to high amplitude. The reflections above are typically subparallel, with a high to medium amplitude, and a medium frequency. The volcanic marker overlies U4 in the eastern part of the graben. The reflections below the U4 marker are truncated or subparallel, with a medium to low amplitude, and a medium frequency. The U4 marker is mappable throughout the central and eastern parts of the graben, and typically corresponds to the top of the Missisauga Formation (Figure 4.5). In the Hercules G-15 and Jason C-20 wells this marker correlates to the base of the Cree Member (base of the Cree volcanic interval) and the top of the Mic Mac (Hercules G-15) and Missisauga (Jason C-20) formations. At the Fox I-22, Crow F-52 and Argo F-38 wells (Figure 4.1), the U4 marker corresponds to the Missisauga Formation/Naskapi Member contact.

#### **4.1.8 The Mic Mac Marker**

The Mic Mac marker is a positive, continuous to discontinuous reflection with a high to medium amplitude. It is generally found around 2.0 s (TWTT) but can be between 1.0 and 3.0 s (TWTT) depending on local salt growth or withdrawal. The reflections above this marker are generally discontinuous, subparallel to chaotic with a medium to low amplitude and a medium to high frequency. The reflections below this marker are parallel to subparallel with a medium to high amplitude and low frequency. The Mic Mac marker at Fox I-22, Crow F-52, Argo F-38, Hercules G-15, and Jason C-20 corresponds to a shale unit near the top of the Mic Mac Formation.

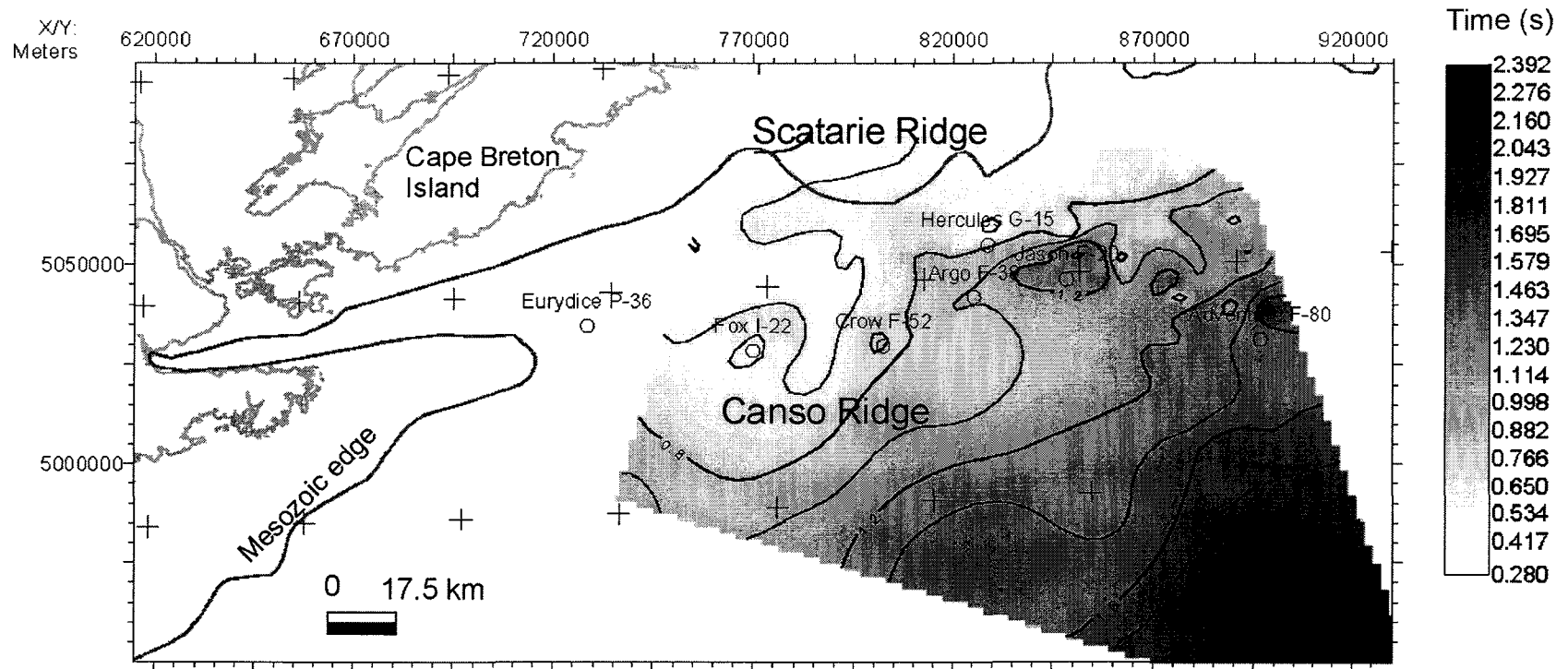


Figure 4.5 Map showing the extent of the U4 marker. Contours were generated using the inverse distance to a power algorithm with a grid spacing of 2 km, maximum distance of 30 km, weight of 2 and low smoothing. Bathymetry and Mesozoic edge are from MacLean (1991). Map plotted using The KINGDOM Suite with the UTM Zone 20N (66° W to 60° W) and the WGS 1984 datum.

#### **4.1.9 The U5 Marker**

The U5 marker is a negative, continuous, wavy reflection with a medium to high amplitude. This unconformity at the Eurydice P-36 well truncates the Mic Mac, Mohican and Iroquois formations and correlates to the Avalon unconformity produced during the rifting of Grand Banks and Iberia. In the western part of the graben the unconformity is shallow and only the sediments of the Missisauga Formation overlie it. It is inferred that eastward in the deeper parts of the graben it either becomes conformable, is too deep or has been disrupted by salt movement, as it is not imaged (Figure 4.6).

#### **4.1.10 Other Markers**

Other markers such as the Naskapi, Mohican, Iroquois, Argo, and Eurydice were picked where possible, but were not traceable over the entire study area. The Naskapi marker is a low to high amplitude wavy to straight, semi continuous to discontinuous reflection that can only be traced short distances from well ties. The Naskapi marker corresponds to the top of the Naskapi shale member. The Mohican marker, corresponding to the top of the Mohican Formation, is a high amplitude, continuous to discontinuous, straight to wavy reflection. Reflections above are medium to high amplitude, continuous to discontinuous, medium frequency reflections. Reflections below are low frequency, chaotic to discontinuous low amplitude reflections. Near the Canso Ridge, the positive reflection immediately above the Mohican marker is the Mic Mac marker. The Iroquois marker corresponds to the top of the Iroquois Formation. This reflection was only sparsely mapped in the western part of the graben, as it is difficult to distinguish between this reflection and that of the Argo marker.

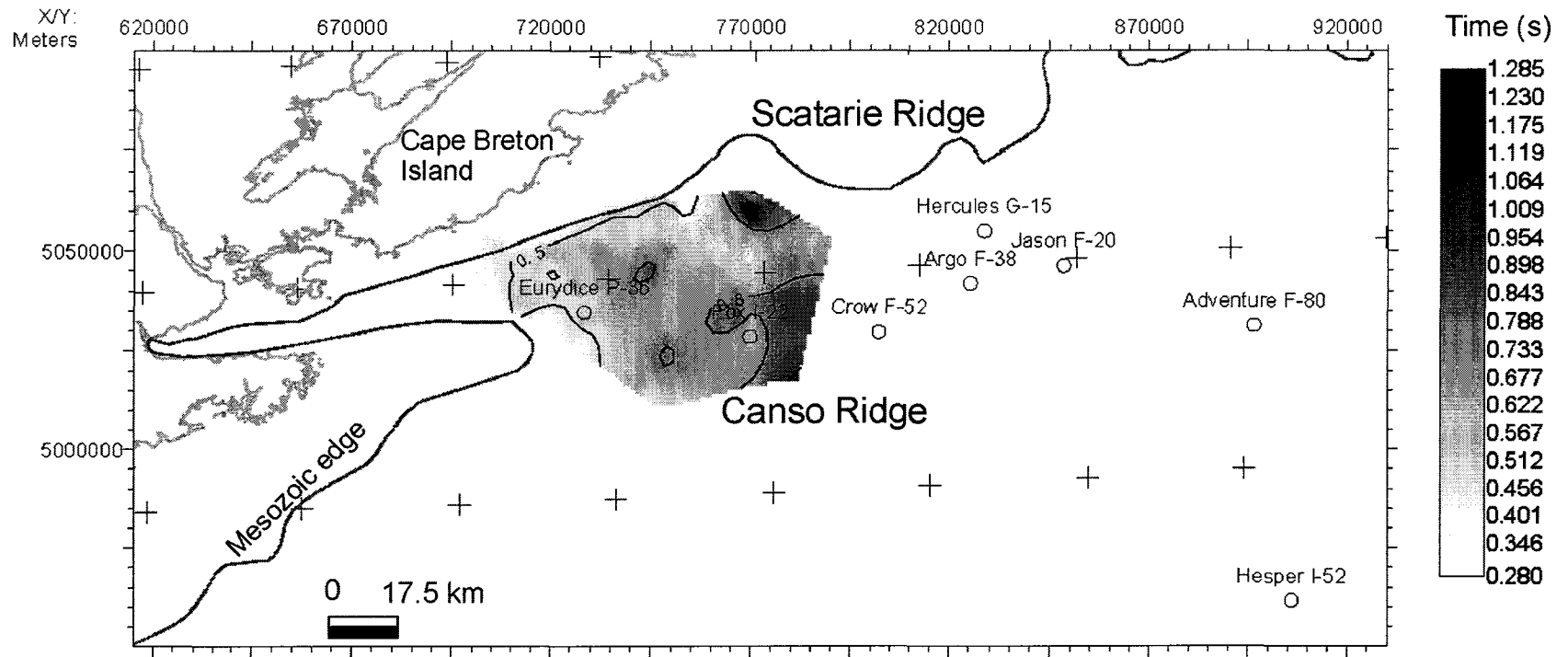


Figure 4.6. Map showing the extent of the U5 marker. Contours were generated using the inverse distance to a power algorithm with a grid spacing of 1 km, maximum distance of 30 km, weight of 2 and low smoothing. Bathymetry and Mesozoic edge are from MacLean (1991). Map plotted using The KINGDOM Suite with the UTM Zone 20N (66° W to 60° W) and WGS 1984 datum.

The Argo Formation in the Orpheus Graben is characterised by two different packages of reflections in the western part of the graben. One is dominantly parallel to subparallel, straight to wavy reflections with a medium to high amplitude and correlates to dominantly shale interbedded with anhydrite and dolomite with salt making up only the bottom of the formation. The second package of reflections are chaotic and correspond to salt that has become mobile. In the western part of the graben two reflections were traced with Eurydice P-36 as the starting point. One corresponds to the top of the Argo Formation and the other to the top of the Argo salt. In the central and western parts of the graben there is a higher salt-shale ratio and only the top of the Argo salt marker is picked. The reflections above may be subparallel, straight to wavy or broken, chaotic and discontinuous due to faulting and deformation associated with salt growth and withdrawal. The Argo marker was mapped throughout the Orpheus Graben, defining dominantly diapiric structures. Where obvious diapiric structures were not observed the position of the salt was very difficult to interpret. It is unclear why some withdrawal minibasins produce strong reflections whereas others are more chaotic making the thickness of salt appear much greater than it may actually be. The presence of salt was interpreted conservatively when mapping where there were greater uncertainties as to the thickness of the salt present. The interpretations in the eastern part of the graben are much less confident than in the central and western part of the graben.

The Eurydice marker was only mapped in the western part of the graben because it is too deep to be imaged in other parts of the graben. Where it was mapped, the marker is a high amplitude, discontinuous reflection. Reflections above this marker in the eastern

and central parts of the graben are chaotic, with a low to medium amplitude. They appear as subparallel to parallel, continuous reflections in the western part of the graben with a medium to high amplitude and a medium frequency.

#### **4.2 Regional distribution of the lithostratigraphic units from seismic data**

Figure 4.7 summarizes the chronological order of the seismic markers and how they correlate to the lithostratigraphy. In general, in the central part of the graben the basement is very shallow. At the Canso Ridge it is 1.0 s deep but to the north it slopes down into the graben to a depth of 3.0 s. Late Triassic –Jurassic sediments of the Eurydice, Argo and Iroquois formations onlap the basement and were not deposited on the Canso Ridge. Upper Jurassic to Lower Cretaceous sediments of the Mohican, Mic Mac and Missisauga formations thin as they approach the Canso Ridge and thicken to both the south (into the Abenaki and Sable Subbasins) and north into the graben. In the eastern part of the graben, large withdrawal minibasins (10-15 km wide by 1.5-3.0 second deep) are seen in which sediments of the Mohican, Mic Mac and Missisauga formations are much thicker (between 1.5 and 3.0 seconds thick) than in other parts of the graben. No wells penetrate these deep areas. These same formations are much shallower (between 0.3 s and 1.0 s) and thinner (0.2 to 0.4 seconds thick) in the western part of the graben and in places the Mohican, Mic Mac and Iroquois formations have been eroded by the base Cretaceous unconformity (U5). Younger sediments of the Logan Canyon Formation have a more uniform thickness, where it has not been eroded. The upper part of the Logan Canyon Formation has been eroded in the north eastern part of the graben

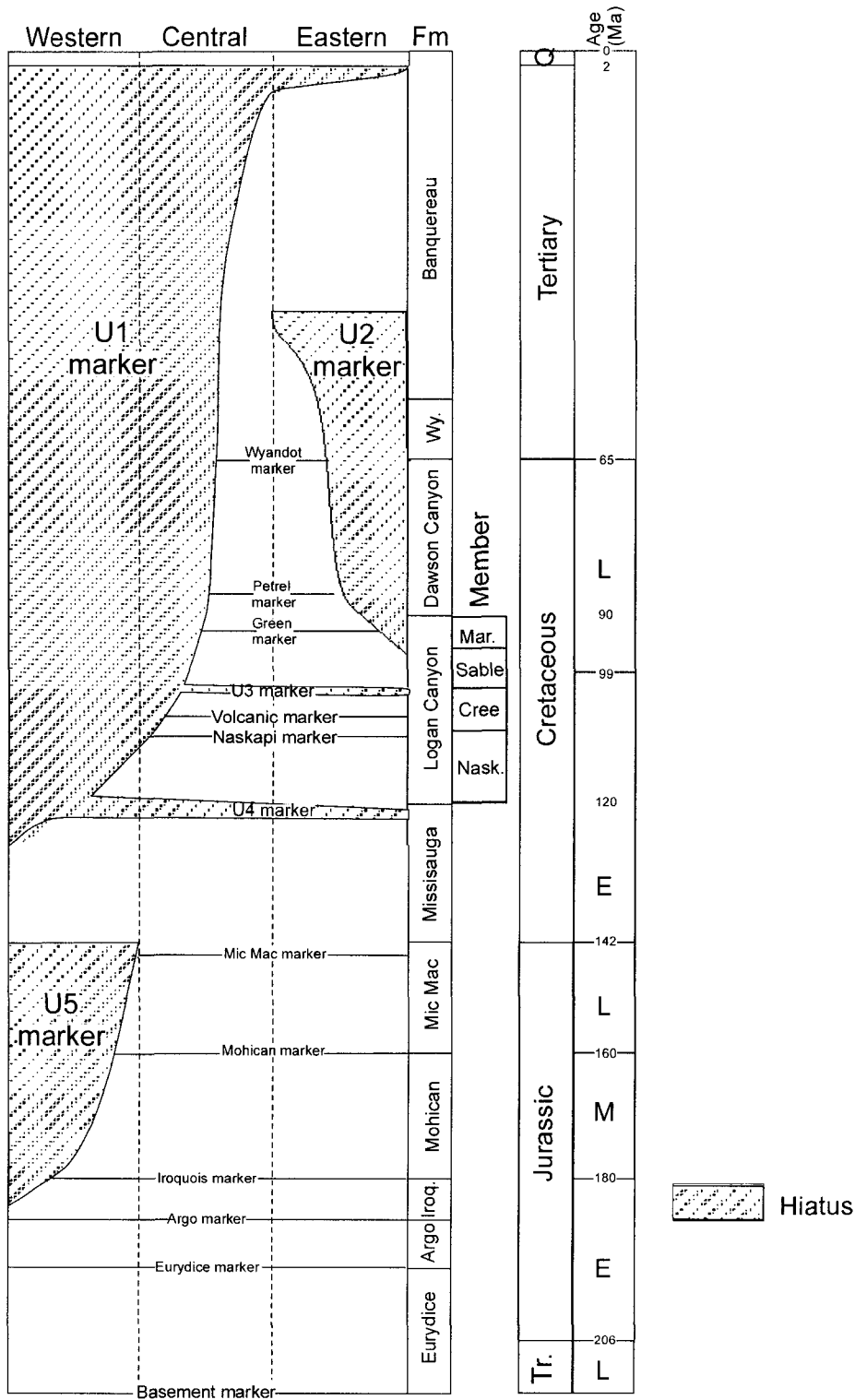


Figure 4.7. Illustration of the typical chronological order of the key reflection markers in the seismic profiles. This figure also depicts the general regional (east-west) distribution of the lithostratigraphic units within the Orpheus Graben (time scale from Gradstein and Ogg, 1996).

by the Tertiary unconformity (U2) and by the Quaternary unconformity (U1) in part of the central graben. All of this formation has been eroded away in the western part of the graben by the U1 unconformity. The Dawson Canyon Formation and younger formations are present only in the south eastern part of the graben and have been eroded by the U2 and U1 unconformities in the northeastern, central and western parts of the graben.

## **CHAPTER 5** **SEISMIC INTERPRETATIONS AND STRUCTURE**

### **5.1 Introduction**

This chapter summarizes my interpretation of the seismic reflection profiles. Six acoustic facies are seen in the seismic profiles of project 8624-P028-068E, in the eastern part of the graben. All other projects (Table 2.1 of Chapter 2) are of poorer quality and most seismic facies cannot be confidently delineated from the data. The acoustic facies are presented in Table 5.1, which describes the attributes of each facies, bounding markers above and below, and other interpretations and comments. The second part of this chapter deals with salt and fault tectonics in the graben.

### **5.2 Acoustic Facies**

#### **5.2.1 Facies A**

Facies A is characterized by low to medium amplitude, even, parallel to subparallel, continuous to semi-continuous reflections that give an overall transparent appearance. Its attributes show little variability. This facies makes up most of the section from the Quaternary unconformity (U1) or mid Tertiary unconformity (U2) down to the Green marker of the upper Marmora Member. It is interrupted by developments of acoustic facies B, discussed below. The seismic character suggests deposition in a low energy environment and a lack of strong impedance contrasts. Major limestone or marl units, such as the Petrel Member and the Wyandot formation, are represented by high amplitude reflections of facies B. Facies A is interpreted to be from a deep marine environment and corresponds to the Banquereau and Dawson Canyon formations and the Marmora

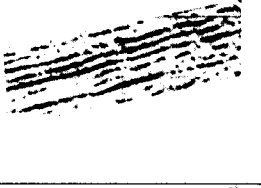
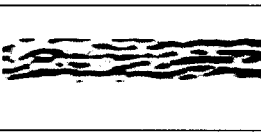
Example	Facies	Attributes	Occurrence	Interpretations/ comments
	A	Low to medium amplitude, transparent, even, parallel to subparallel, continuous to semi-continuous reflections	Banquereau Fm., parts of Dawson Canyon Fm., upper Marmora Member	-Deep marine shelf
	B	High amplitude, even, parallel, continuous reflections	Wyandot Fm., Petrel Member	-Offshore shelf chalk and interbedded facies
	C	Low to medium amplitude, transparent, even, parallel to wavy, continuous to discontinuous reflections	Lower Marmora Member and Sable Member	- Nearshore facies, delta front
	D	Low to high amplitude, transparent, discontinuous, hummocky reflections	Cree Member	-Shoreface sand deposits to lower alluvial plain
	E	Low to medium amplitude, transparent, semi-continuous to discontinuous, subparallel to hummocky reflections	Missisauga Formation	- Braided channel deposits of the upper part of an alluvial plain

Table 5.1 Acoustic facies of the Cretaceous seen in the seismic profiles of the Orpheus Graben. Interpretations are based on the well ties to lithostratigraphy (see Chapter 4, section 4.1).

Member of the Logan Canyon Formation. This acoustic facies has been eroded in parts of the central and all of the western part of the graben.

### 5.2.2 Facies B

Facies B consists of high amplitude, even, parallel, continuous reflections. As with Facies A, the regular character of the reflections suggests deposition in a uniform, low energy environment. This acoustic facies sometimes interbeds within facies A and is presented only in the eastern part of the graben, where it corresponds to the chalk,

limestone and marl deposits of the Dawson Canyon and Wyandot formations. It is also found in the eastern and in central parts of the graben where it corresponds to the Naskapi, Volcanic and U4 markers.

### **5.2.3 Facies C**

Facies C is characterized by low to medium amplitude, transparent, even, parallel to wavy, continuous to discontinuous reflections. It differs from facies A in having irregular reflections. This acoustic facies shows no distinctive seismic architecture: the slightly irregular discontinuous reflections suggest a low relief alluvial, deltaic or nearshore marine environment. It generally occurs between the Green marker and the U3 marker and corresponds to the lower part of the Marmora Member and to the Sable Member.

### **5.2.4 Facies D**

Facies D is characterized by low to medium amplitude, discontinuous reflections that are commonly hummocky or show systematic sigmoidal downlap. In the eastern part of the graben the discontinuous, transparent, sigmoidal architecture is more pronounced in the north-south lines. On east-west lines, this facies shows semi-continuous to continuous, subparallel, low amplitude reflections. This acoustic facies corresponds to the Marmora and Cree members of the Logan Canyon Formation. The progradational architectural character, and the fact that it corresponds to medium-coarse grained quartz-rich sandstone units according to well correlations, suggests a low relief alluvial or deltaic environment.

### **5.2.5 Facies E**

Facies E is characterized by low to medium amplitude, transparent, semi-continuous to discontinuous, subparallel to hummocky reflections. It differs from facies D in lacking organized progradational sigmoidal downlapping reflections. This acoustic facies is characteristic of the Missisauga Formation, between the U4 marker and the Mic Mac Marker and the Mic Mac and Mohican formation, below the Mic Mac marker. This acoustic facies displays more continuous, straight reflections in the north-south lines and more discontinuous, wavy, transparent reflections in the east-west lines, (i.e. the opposite of the pattern seen in facies D typical of the Cree members. The discontinuous, irregular character of this acoustic facies, given that it corresponds to a predominantly coarse to pebbly sandstone formation that is interbedded with shales and fine grained sandstones, according to well correlations, suggests abundant channeling in an alluvial or deltaic environment.

In the northeastern part of the graben this seismic facies, below the Mic Mac marker, changes to discontinuous, wavy, transparent reflections with a low amplitude and frequency and appears very similar to that of the salt acoustic facies. There is no well penetration into this change in acoustic facies and the reasons for this change are highly speculative but it is possible that this may represent a change in sedimentary facies to more homogenous or discontinuous sediments that produce fewer acoustic contrasts. It is also possible, that because this is only seen in the northern most part of the N-S trending lines, that this suggest a more proximal source for these sediments or that the shales and

limestones of the Mic Mac and Mohican formations pinch out or have become too thin to image here.

### **5.3 Salt acoustic facies and structure**

Salt is thought to be present throughout the graben. The amount of salt, however, varies greatly from line to line and from one part of the graben to another (i.e. little salt in the central and western parts of the graben vs. large diapirs of salt in the eastern parts of the graben), and its interpretation is challenging. The salt in the western part of the graben is much different from the salt in the central and eastern part of the graben, in that, based on well ties it is interbedded with dolomite, siltstone and thick beds of shale (Holser *et al.*, 1988). The Argo Formation at the Eurydice P-36 well is 1600 m thick, but of this only approximately 442 m (at the bottom of this formation) is actually salt (Figure 5.1). The Argo Formation in the western part of the graben is characterized by medium to high amplitude, parallel to subparallel reflections with a sheet like geometry. At the Eurydice P-36 well, there is a high amplitude, continuous reflection that correlates to a velocity increase at the top of salt near the base of the Argo Formation. This reflection can only be traced for a short distance. It is inferred that the salt has become mobile where the acoustic character changes from the above mentioned to chaotic and transparent reflections. However, the quality of the seismic data is very poor in this part of the graben, making it very difficult to infer how thick it is and where the salt actually is present. The acoustic character in the central and eastern parts of the graben is more typical of salt: very chaotic to transparent reflections with an uneven or wavy top. The salt has a variable shape in the central part of the graben. It varies from a wedge shape that thickens from south to north (Appendix 5 - Figure 22) to large salt diapirs with

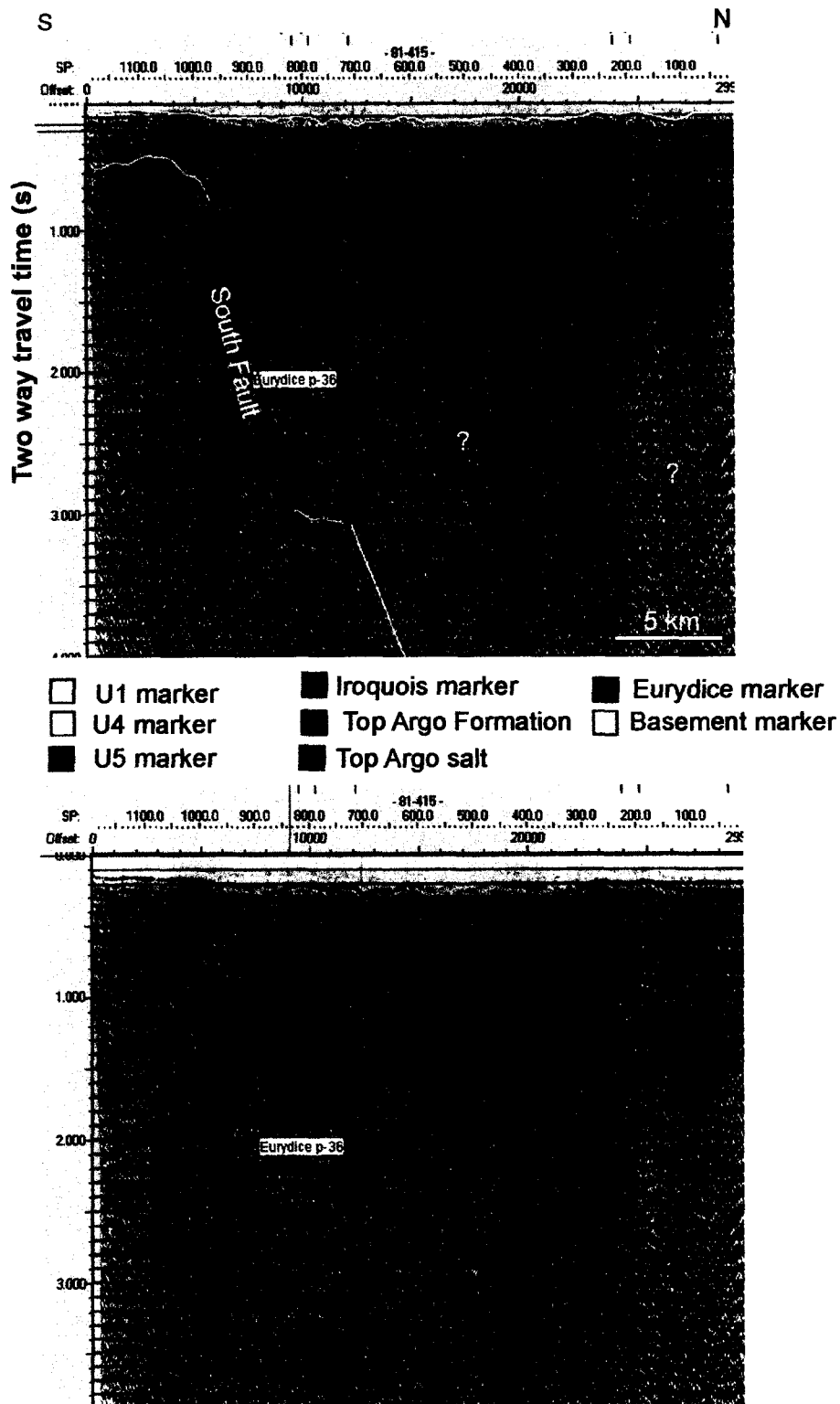


Figure 5.1. Line 81-415 shows the acoustic character of the Argo Formation below the top Argo marker. Note that the top of the Argo salt is below the top of the Argo Formation marker. The line also shows the bounding south fault (see Figure 2.1 for the location of this line).

large withdrawal minibasins to the west (Appendix 5 - Figure 10) and east (Appendix 5 - Figures 11, 13, 15, 16, 17, 23, and 24). In line 81-413 (Figure 5.2) the withdrawal minibasins are possibly filled with sediment of the Mohican and Mic Mac formations but with no ties to any wells it is possible that the Missisauga Formation may also be present in these minibasins. The salt in this profile (Figure 5.2) stopped growing (welded out against the Eurydice Formation) and moved very little since the deposition of the sediments above the U5 marker, as they are not structurally disturbed. In Figure 5.3 (line 4133-83) the salt withdrawal dominantly occurred during sediment deposition below the Mic Mac marker and has produced a salt weld (1000 sp) and one small salt structure isolated from the salt structure to the north.

Near the southern end of the central part of the graben, at the Argo F-38 well, the salt is 775 m thick and thickens northward. There is a listric fault along the south side of the graben (Appendix 5 - Figure 12) that offsets the U4 marker by about 0.4 seconds TWTT and cuts as high as the U1 marker (Figure 5.4). This profile shows that the salt in this area was withdrawing as late as the Quaternary and may still be withdrawing at present. With an offset of about 0.4 seconds TWTT we can infer that approximately 750 m of salt have been removed from this area.

Salt thickness varies greatly in the eastern part of the graben: the Jason C-20 well penetrated only 34 m and the Hercules G-15 well encountered 26 m of salt at the top of a diapir, whereas the Adventure F-80 well (drilled on the side of a diapir) encountered 948 m of salt before stopping. None of these wells drilled to the bottom of the salt so true

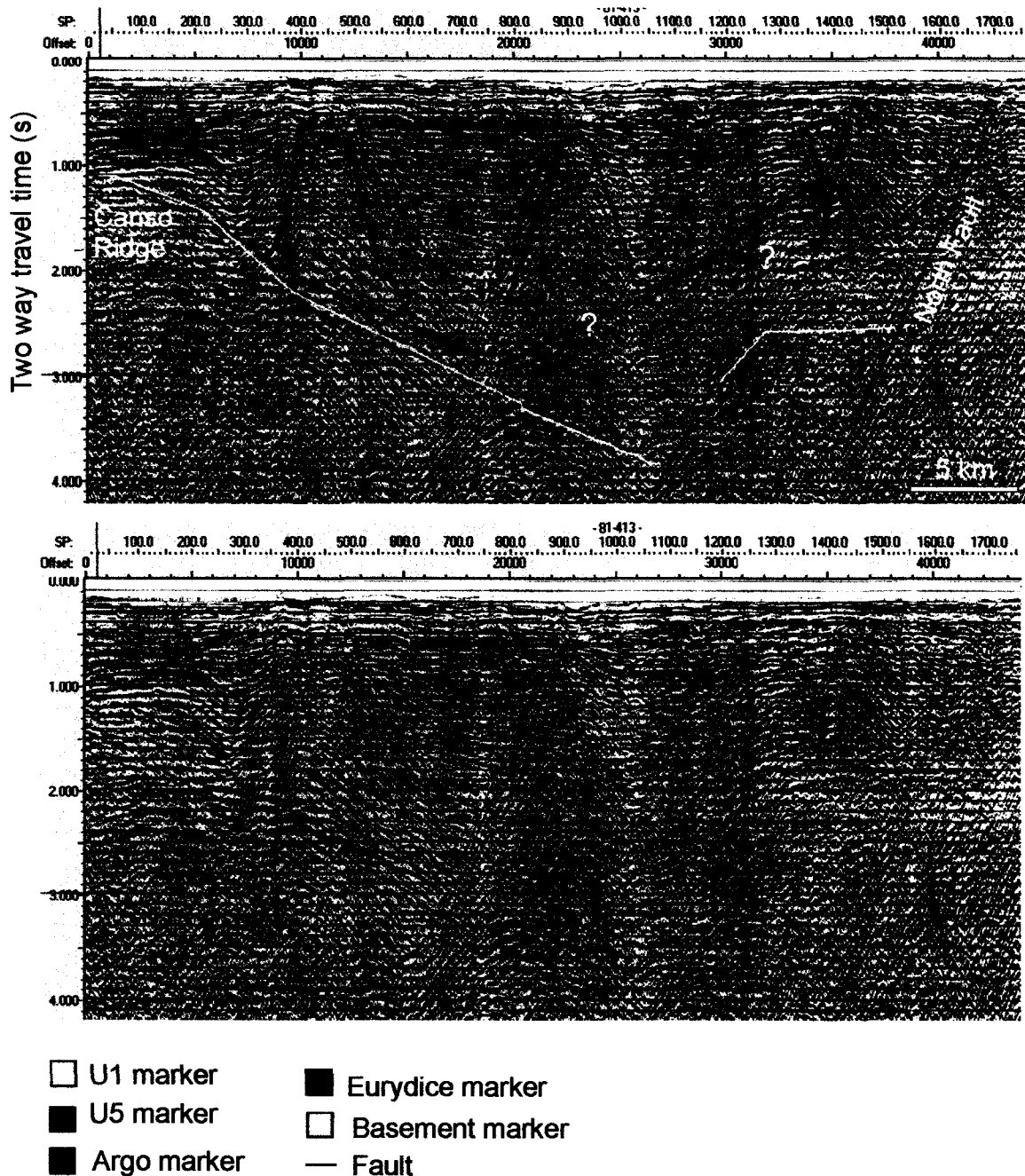
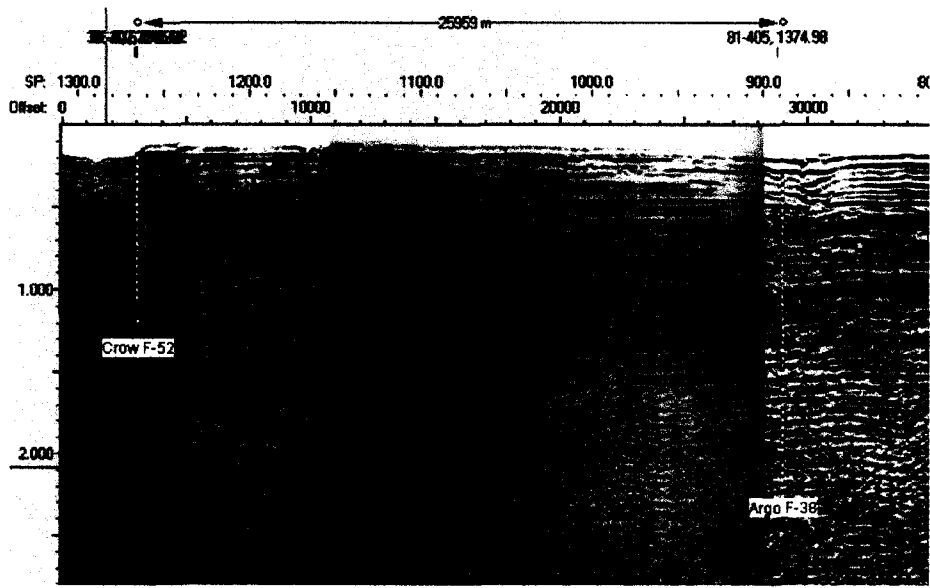
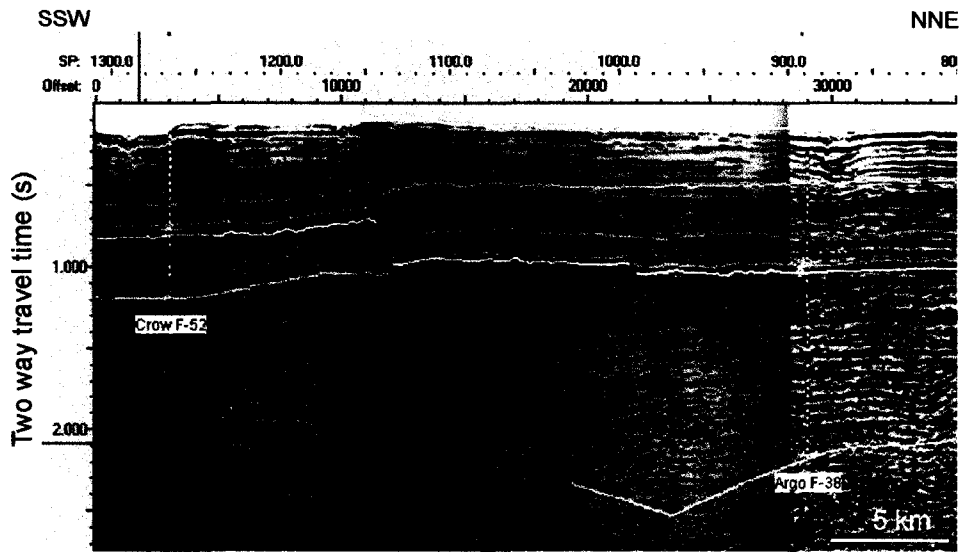


Figure 5.2. Line 81-413, showing withdrawal minibasins that are thought to be filled with sediments of the Mohican and Mic Mac formations. The exact position of the basement is the deepest part of the graben, beneath the salt is poorly constrained and speculative (see Figure 2.1 for the location of this line).





- |                   |                   |
|-------------------|-------------------|
| □ U1 marker       | ■ Mohican marker  |
| □ Petrel marker   | ■ Iroquois marker |
| ■ Green marker    | ■ Argo marker     |
| □ Cree marker     | ■ Euridice marker |
| □ U4 marker       | □ Basement marker |
| ■ Volcanic marker | — Fault           |
| ■ Mic Mac marker  |                   |

Figure 5.4. Line 390-B, showing a listric fault offsetting the seismic markers due to salt withdrawal in the north-northeast direction (to the right). The quality of seismic in this survey is significantly lower than others illustrated in Figure 5.3 and 5.4, but the interpretation is constrained by well penetrations (see Figure 2.1 for the location of this line).

thicknesses are not known. In map view, the top Argo salt marker illustrates the presence of salt throughout most of the graben (Figure 5.5). An isochron map of the top salt to the basement marker shows that the salt is probably thickest in the deepest parts of the graben (Figure 5.6) but when compared to an isochron map of the top salt marker to the Eurydice marker (Figure 5.7) the presence of large salt diapirs and withdrawal minibasins in the eastern part of the graben are better illustrated. The comparison also illustrates that in the western part of the graben the sediments of the deepest parts of the graben are filled with sediments of the Eurydice formation. In the eastern part of the graben the bottom of the salt is very speculative because of the poor seismic imaging.

#### **5.4 Faults**

There appear to be four types of faults in the Orpheus Graben, the bounding faults, faults that have not been active after the U4 or U5 markers, faults that have not been active after the U2 marker and faults related to salt tectonics (Figure 5.8). The faults that define the Orpheus Graben are primarily ENE-WSW trending en echelon faults. Crustal extension was in the northwest-southeast direction and caused basement blocks to drop down. This faulting began during the Triassic in a transtensional setting (Welsink *et al.*, 1989). The western and eastern parts of the graben have a graben structure with faults on both the north and south sides. The central part of the graben is technically a half graben structure because only the northern side is bounded by a fault (Figure 5.2). The southern side is part of the north-dipping Canso ridge and only exhibits minor faulting by comparison.

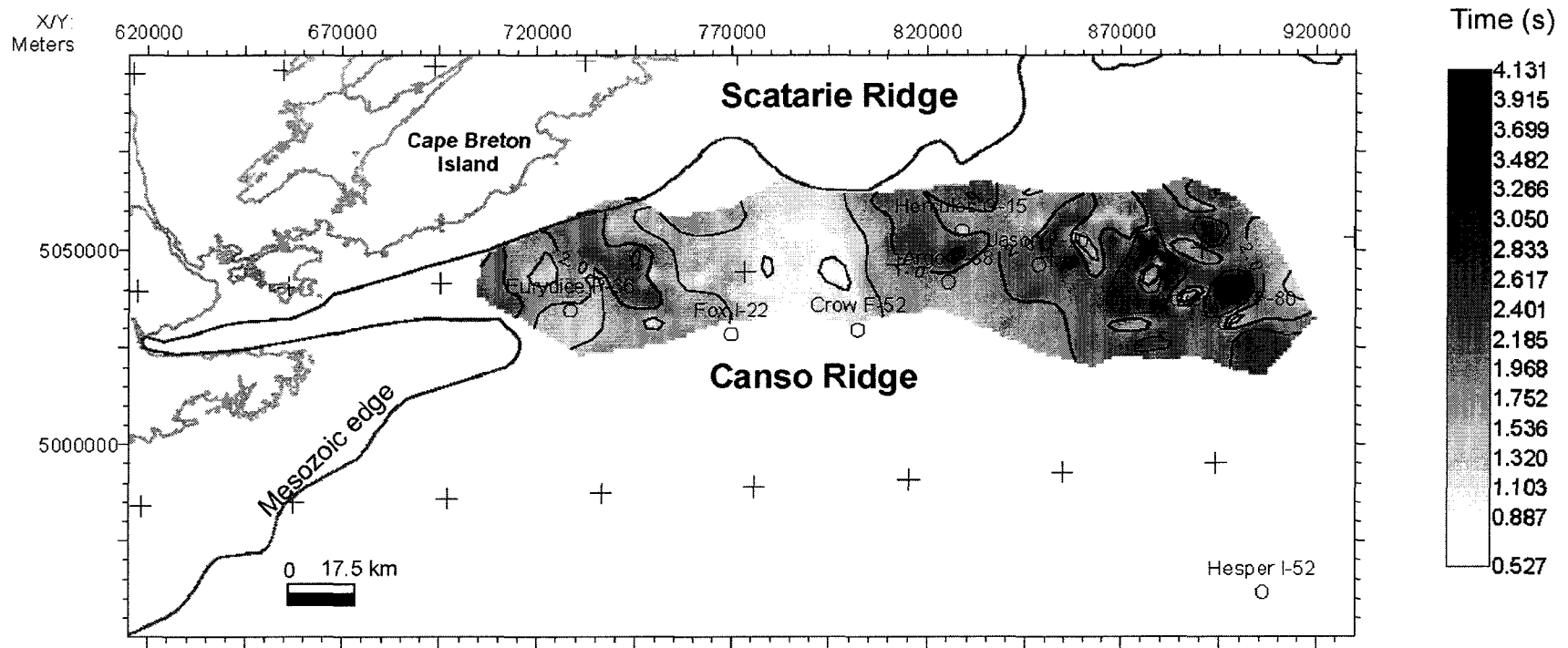


Figure 5.5. Map showing the top of Argo salt marker with contours. The contour map was generated using the inverse distance to a power algorithm with a grid spacing of 1 km, a maximum distance of 5 km, a weight of 2 and low smoothing. The Mesozoic edge are from MacLean (1991). Map plotted using The KINGDOM Suite with the UTM Zone 20N (66° W to 60° W) and WGS 1984 datum.

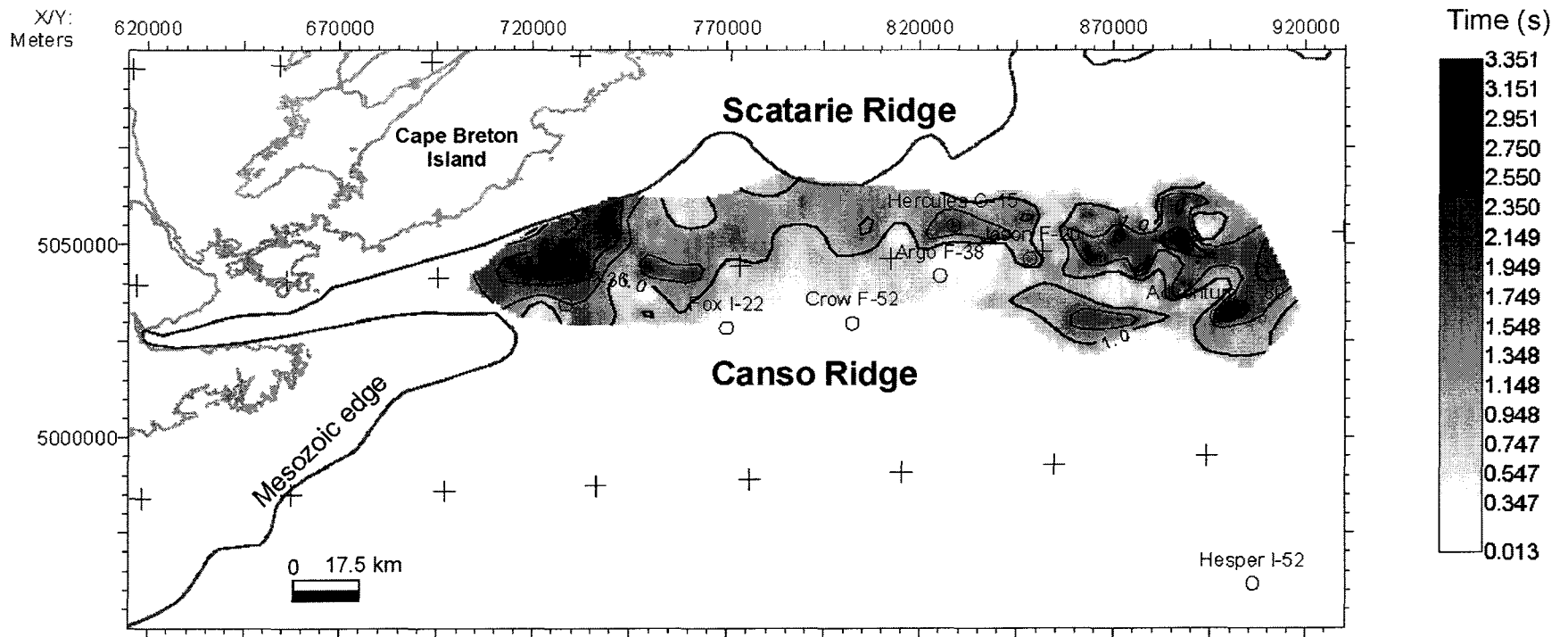


Figure 5.6. Isochron map for the Argo salt marker to the Basement marker showing the location of salt diapirs in the deepest parts of the graben. The contour map was generated using the inverse distance to a power algorithm with a grid spacing of 1 km, a maximum distance of 5 km, a weight of 2 and low smoothing. The Mesozoic edge are from MacLean (1991). Map plotted using The KINGDOM Suite with the UTM Zone 20N (66° W to 60° W) and the WGS 1984 datum.

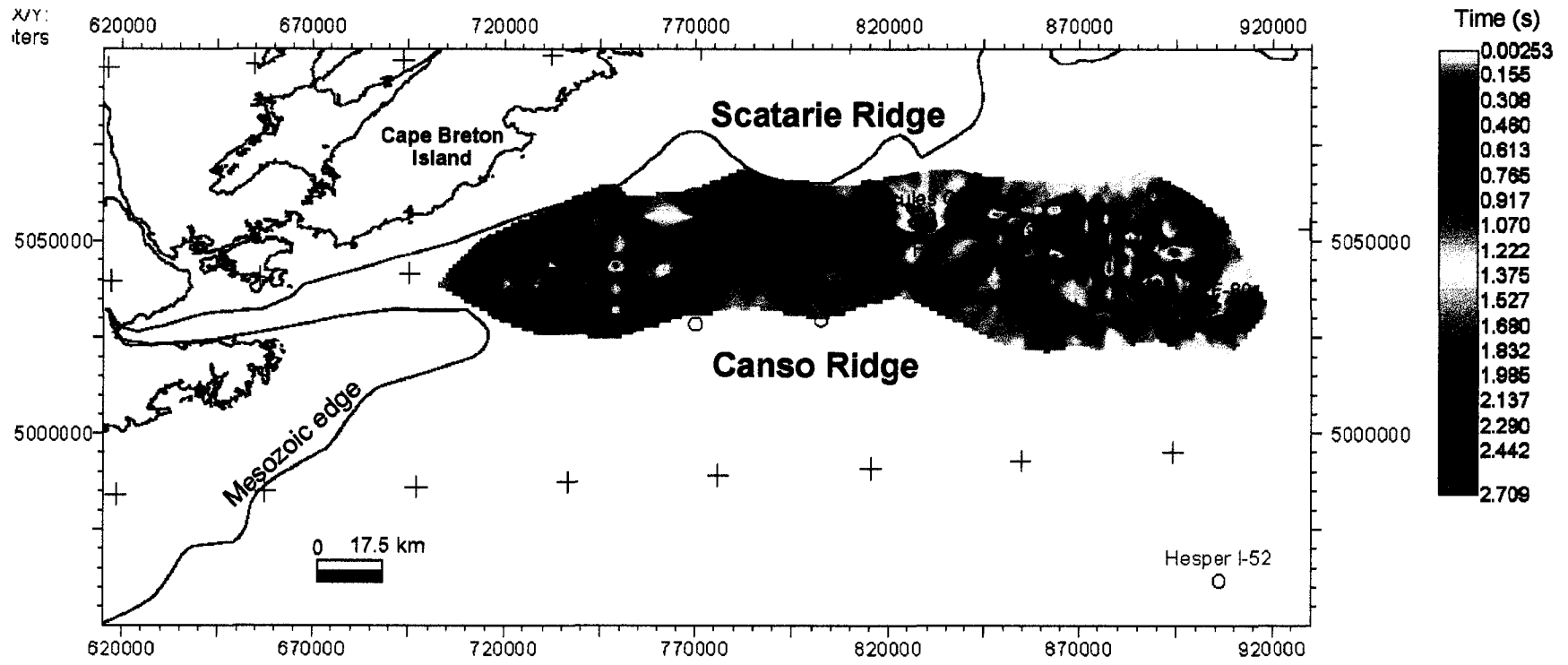


Figure 5.7. Isochron map for the Argo salt marker to the Eurydice marker showing the location of salt diapirs in the graben. The contour map was generated using the inverse distance to a power algorithm with a grid spacing of 1 km, a maximum distance of 5 km, a weight of 2 and low smoothing. The Mesozoic edge is from MacLean (1991). Map plotted using The KINGDOM Suite with the UTM Zone 20N (66° W to 60° W), WGS 1984 geodetic datum was used.

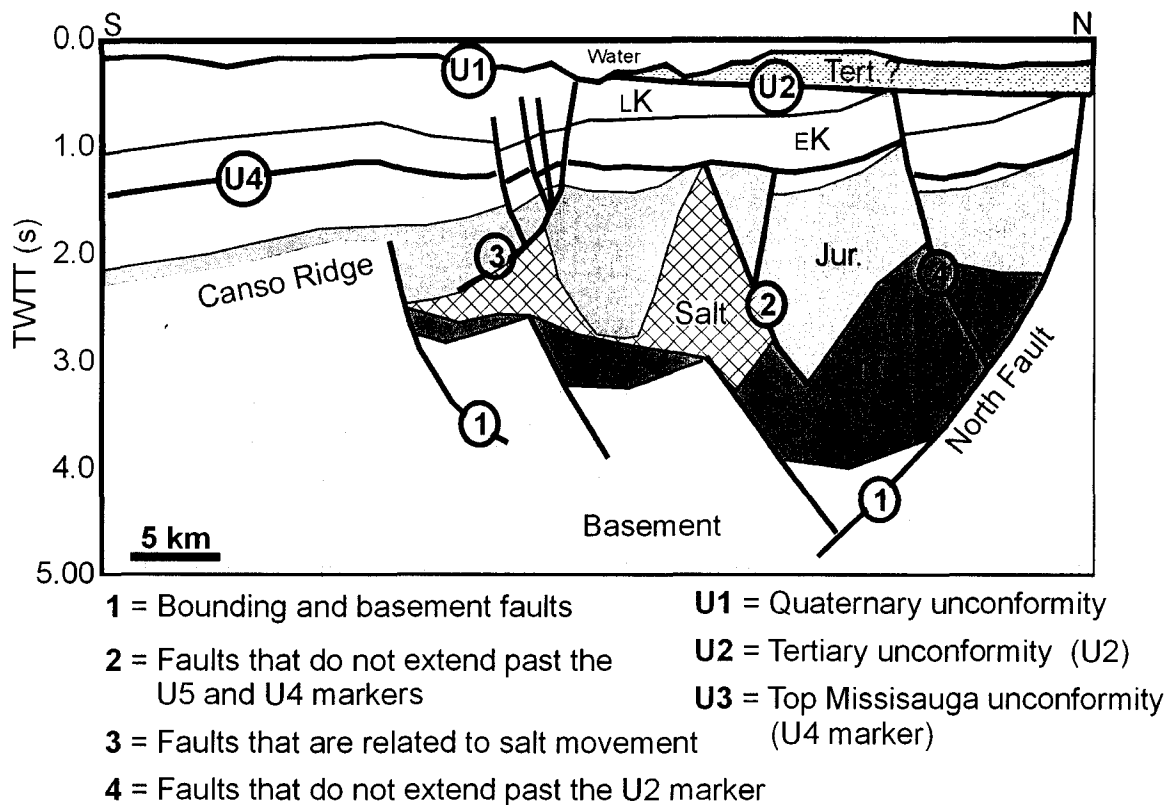


Figure 5.8. N-S Schematic cross section showing the four types of faults observed in the Orpheus Graben (scale approximates).

The seismic profiles in the western part of the graben are extremely poor but a few faults can be seen. These faults were active before the base Cretaceous unconformity (U5 marker) as they are eroded by it (Appendix 5 - Figures 10 and 20). There appears to be no faulting after this time in the western part of the graben. The quality of some of the seismic profiles is better in the central and eastern part of the graben and again faulting is dominantly before the base Cretaceous (U5) and Top Missisauga unconformities (U4 marker) and have a similar trend to the bounding faults. In the eastern part of the graben these faults have caused the basement to be broken into blocks that rotate into the graben.

Faults related to the development of minibasins due to salt withdrawal are also observed in the central and eastern parts of the graben. These are typically listric growth faults (Figure 5.4) and may have fan structures (Figure 5.3, SP 2000) where salt has withdrawn and crestal faults or parallel fault sets that occur at the top of salt diapirs. These faults generally terminate just above the Petrel marker, but some do extend to the seafloor. They are most commonly observed in both E-W and N-S trending line. ENE-WSW faulting is observed in the northeastern part of the graben as late as Early Tertiary (Figure 5.9). Faults here appear to be antithetic listric growth faults of the north bounding fault. The Tertiary unconformity (U2 marker) has not been affected by this fault.

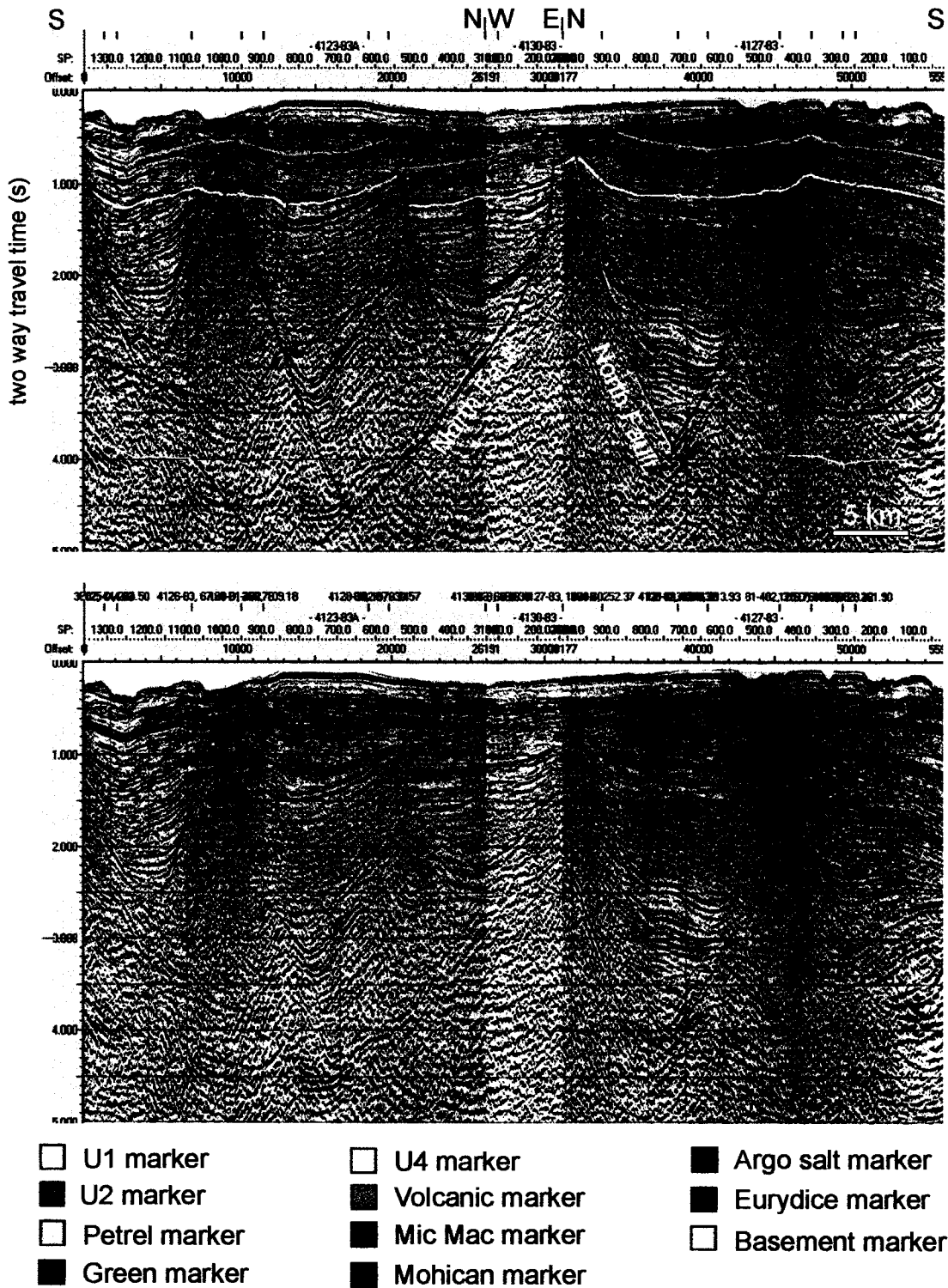


Figure 5.9. A tie line between seismic lines 4123-83A, 4130-83 and 4127-83, showing the typical fault structures observed in the northeastern most part of the graben. The exact position of the basement in the deepest part of the graben, beneath the salt is poorly constrained and speculative (see Figure 2.1 for the location of this line)

## **CHAPTER 6**

### **PETROLOGICAL STUDY**

#### **6.1 Introduction**

To better understand the lithostratigraphy of the wells in the study area, eighty-five polished thin sections of unknown cuttings, representative sandstone cuttings, and heavy mineral separation were examined. Petrographic (see Appendix 6 for the petrography of grains > 2 mm or Appendices 1-4 - Table 4 for a summary of grains > 2 mm) and electron microprobe analyses (see Appendix 1-4 - chemical analyses tables) of these thin sections have revealed stratigraphic differences in the detrital (Appendix 7 - Tables 1-5) and diagenetic mineral (Appendix 7 - Tables 10-14) assemblages including lithic clasts and heavy minerals (Appendix 7 - Tables 6-9) found in each of the wells. Differences between wells, formations and members may point to changes in provenance, depositional, and diagenetic histories. The first part of this chapter will outline the distribution and type of detrital and diagenetic minerals including lithic clasts and heavy minerals for the members of the Missisauga and Logan Canyon formations. The second part of this chapter will discuss trends seen between members and the third part of this chapter will discuss possible provenance for the heavy mineral and lithic clasts and it will also discuss the origin of important diagenetic minerals.

#### **6.2 Petrography of grains**

##### **6.2.1 Mic Mac Formation**

Detrital minerals were observed from the Mic Mac Formation in the Jason C-20 well and are quartz, K-feldspar, tourmaline, rutile, staurolite with inclusions, ilmenite (often alters to pseudorutile and rutile) with or without inclusions, and garnet. No lithic clasts are

observed. Diagenetic minerals are kaolinite, limonite, pyrite, rhodochrosite, septochlorite, quartz and siderite.

### **6.2.2 Missisauga Formation**

The most common detrital minerals in the Middle Member of this formation are quartz (some with inclusions of muscovite or rutile), feldspar, ilmenite (often altered to pseudorutile and rutile) with or without inclusions, and muscovite with lesser amounts of biotite, rutile, plagioclase, tourmaline, apatite, chromite, garnet (some with inclusions), staurolite with inclusions, K-feldspar megacryst with vermicular quartz growths, zircon and galena. Observed lithic clasts in this member are tuff, slate, chert, vein quartz, felsic plutonic rock, vein quartz containing tourmaline, and foliated felsic rock. Diagenetic minerals in this member are siderite, quartz, calcite, barite, limonite, hematite, pyrite, kaolinite, francolite, Al-phosphate, opal and illite.

The most common detrital minerals found in the Upper Member of this formation are quartz (some with inclusions of muscovite, chlorite, Ti-magnetite, siderite, K-feldspar or zircon), feldspar, and muscovite with lesser amounts of apatite, ilmenite (often altered to pseudorutile and rutile), tourmaline, zircon, rutile, plagioclase, deformed perthite and biotite. Lithic clasts of chert, vein quartz, and quartzite are also observed. Diagenetic minerals in this member are siderite, quartz, calcite, limonite, pyrite, chlorite, illite, barite, Al-phosphate and kaolinite.

Quartz granules from the Missisauga Formation are most commonly clear to white, angular to well rounded, but may be yellow angular to subrounded, grey angular to well

rounded and pink subangular to subrounded. Feldspar granules are most commonly white or pink and are angular to subangular and subangular to subrounded respectively.

### **6.2.3 Cree Member**

The most common detrital minerals of the Cree Member in the Fox I-22 well are quartz (some with inclusions of muscovite or rutile), feldspar and muscovite with lesser amounts of biotite, chromite, garnet, altered ilmenite (pseudorutile and rutile), plagioclase, rutile, tourmaline, zircon, and sphalerite. Lithic clasts identified in this member are felsic plutonic rock, quartzite, diorite, green metasandstone, vein quartz, vein quartz with tourmaline, and vein quartz with abundant euhedral rutile crystals. Siderite, calcite, ankerite, chlorite, francolite, illite, kaolinite, limonite, opal, pyrite, Al-phosphate, and glauconite diagenetic minerals are observed in this member.

Quartz granules from the Cree Member are more abundant in the lower part of the member and are dominantly white angular to well rounded with fewer yellow (angular to subrounded) and grey (subrounded to rounded) granules and very few pink (angular to rounded) granules. Feldspar granules are also more common in the lower part of this member. They are commonly both pink and white in colour and are angular to subangular. Again, in the Jason C-20 well, significantly fewer quartz granules were observed compared to the other wells.

### **6.2.4 Sable Member**

Only two samples were taken within the Sable Member from the Fox I-22 and Crow F-52 wells. This may create bias in the data when comparing this member to the others.

Detrital minerals identified from this member include quartz (some with inclusions of apatite or muscovite), K-feldspar, and muscovite with lesser quantities of ilmenite (altered to rutile), rutile, and zircon. Diorite, mica schist, green metasandstone, microgranite, felsic plutonic rock, basalt, pink granite, and felsic plutonic rock lithic clasts are also observed. Diagenetic minerals identified are siderite, illite, chlorite, kaolinite, silica and septochlorite.

### **6.2.5 Marmora Member**

Detrital minerals identified in the sandstones of the Marmora Member are quartz, K-feldspar, muscovite, and ilmenite with lesser amounts of apatite, biotite, plagioclase, rutile, tourmaline, zircon, and quartz with inclusions of chlorite, Ti-magnetite, muscovite, and magnetite partially oxidized to limonite and hematite. Lithic clasts of diorite, tuff, slate, pink granite, vein quartz, fine grained mafic igneous rock, basalt, and quartzite are observed. Diagenetic minerals identified are ankerite, siderite, chlorite, limonite, septochlorites, silica, kaolinite, illite, glauconite, francolite, and pyrite with the most common cements being calcite and siderite. One sample from Fox I-22 showed chlorite rims on quartz grains. A fragment of bone was also identified in this member (1690-1720 ft). The abundance of vascular canals and the size of the fragment suggest that the bone is probably from a dinosaur (Weir-Murphy *et al.*, submitted) (Figure 6.1).

### **6.2.6 Trends observed between wells, formations, and members**

Common detrital minerals and lithic clasts of each sampled depth are condensed into members and then grouped with the same member of the other wells to observe

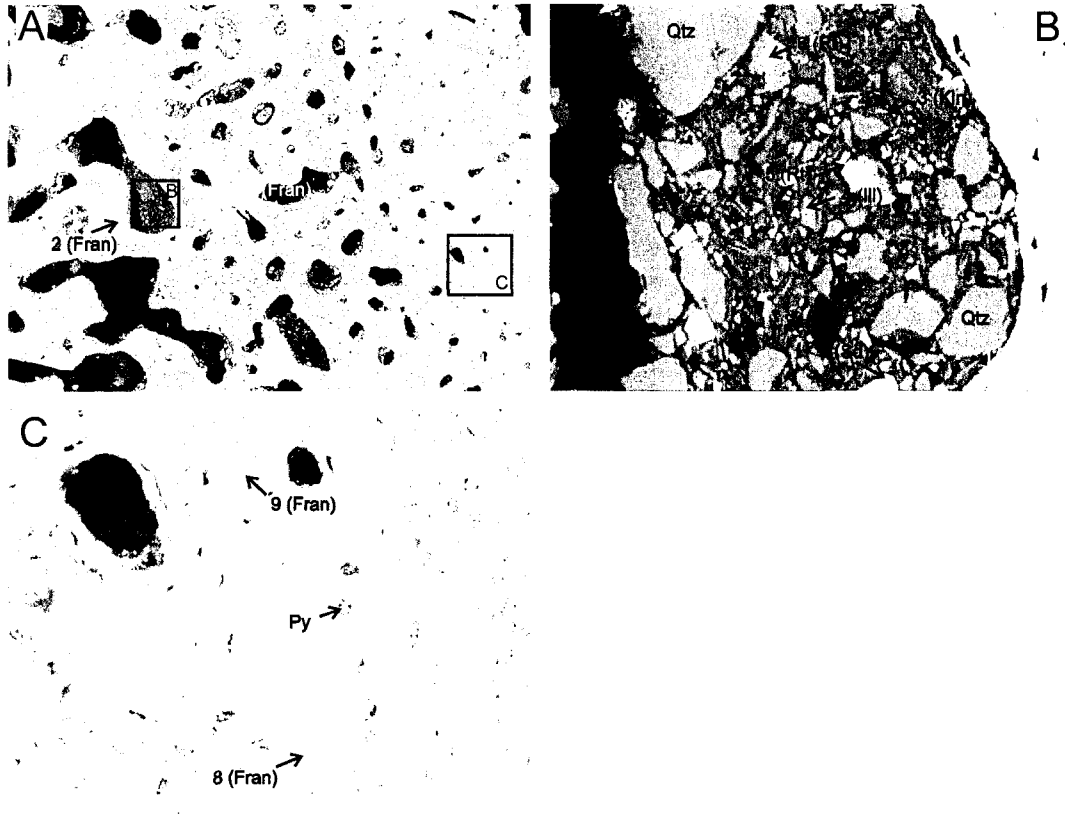


Figure 6.1. (A) Electron microprobe back-scattered electron image of the bone fragment. Numbered arrows represent locations of chemical analyses listed in Appendix 3 - Tables 6-8. Boxes show the location of Fig. 6.1B and C. Mineral abbreviations are quartz (Qtz), francolite (Fran), rutile (Rt), illite (Ill), siderite (Sd), and kaolinite (Kln). (B) Enlargement showing detrital and diagenetic minerals infilling a large Haversian canal. (C) Enlargement showing large voids produced by Haversian canals and tiny pyrite-filled osteon lacunae, labeled "Py".

differences and similarities between the members (Table 6.1). Because sandstones are not sufficiently abundant in all stratigraphic levels information on the stratigraphic variation (such as between members) in sandstone petrography may be incomplete. Biases in the observed minerals may have also been produced because some samples were examined using a binocular microscope, whereas others were examined using the electron microprobe.

Well	Member	Altered ilmenite	Apatite	Biotite	Chromite	Garnet	Ilmenite	K-feldspar	Magnetite oxidized to hematite and limonite	Muscovite	Plagioclase	Phlogopite	Quartz	Quartz w apatite inclusion	Quartz w chlorite inclusion	Quartz w muscovite inclusion	Quartz w K-feld inclusion	Quartz w rutile inclusion	Quartz w siderite inclusion	Quartz w Ti-mag inclusion	Quartz w zircon inclusion	Rutile	Sphalerite	Staurolite	Tourmaline	Zircon	Lithic clasts	
Fox	Marmora						x	x	x	x			x		x	x				x		x				x	diorite, tuff, slate vein quartz, fine grained mafic igneous, pink granite, basalt, quartzite	
Crow	Marmora		x				x	x		x	x		x									x			x	x	quartzite	
Argo	Marmora			x			x	x		x			x														-	
Fox	Sable						x	x		x			x	x		x						x				x	*1, *3, diorite, mica schist green metasandstone, microgranite, felsic plutonic rock basalt, pink granite	
Crow	Sable							x			x		x														basalt, pink granite	
Fox	Cree			x				x		x			x														*2, quartzite, *1, diorite green metasandstone, vein quartz	
Crow	Cree	x			x			x		x			x									x					vein quartz with tourmaline	
Argo	Cree					x		x		x			x		x							x					vein quartz	
Jason	Cree			x	x	x	x	x			x		x									x	x		x	x	vein quartz with rutile crystals	
Fox	Upper	x	x	x			x	x		x	x		x		x	x	x		x	x	x	x				x	x	chert, quartzite, deformed perthite, *2, vein quartz
Crow	Upper							x					x														-	
Argo	Upper							x					x														quartzite	
Fox	Middle	x					x	x		x	x		x											x	x	x	chert	
Crow	Middle	x	x				x	x		x			x									x		x		x	1*, vein quartz with tourmaline, vein quartz	
Argo	Middle		x	x			x	x		x			x		x							x		x	x		tuff, slate	
Jason	Middle	x			x	x		x		x		x	x											x	x	x	vein quartz with tourmaline, quartzite, foliated felsic rock	
Jason	Mic Mac					x		x					x		x							x		x	x		-	

\*1,\*3-clast made up of quartz and feldspar (felsic plutonic rock?)

\*2- clast made up of quartz and muscovite (quartzite?)

Table 6.1. Detrital minerals and lithic clasts identified in the members of the Logan Canyon (Marmora, Sable, and Cree) and Missisauga (Upper and Middle) formations arranged by member. Component minerals of the lithic clasts and detrital mineral grains can be found in Appendices 7, Tables 6-9.

Fox I-22 contained plagioclase with K-feldspar inclusions, quartz with inclusions of chlorite, apatite, K-feldspar, Ti-magnetite, and zircon. Fox also sampled lithic clasts of diorite, felsic plutonic rock, chert, and deformed perthite clasts. Quartz with inclusions of rutile is observed only in the Crow F-38 well. The same well contains pink granite, basalt, green metasandstone, and fine grained mafic igneous clasts. Jason C-20 showed a phlogopite grain, not observed in the other wells. Argo F-38 did not sample any detrital mineral or lithic clasts that were different from the other wells.

Some minerals such as plagioclase with inclusions of K-feldspar, quartz with inclusions of apatite, sphalerite, and magnetite partially oxidized to limonite and hematite are only observed in the Logan Canyon Formation, where as phlogopite, and staurolite with inclusions are only observed in the Missisauga Formation. Lithic clasts of diorite, basalt, pink granite, felsic plutonic rock, green metasandstone, and are only observed in the Logan Canyon Formation. Lithic clasts of chert are only identified in the Missisauga Formation.

Minerals such as ilmenite, muscovite, plagioclase, quartz, rutile, and zircon are observed in all members of the Logan Canyon and Missisauga formations. Others such as staurolite with inclusions are specific to the Middle Member of the Missisauga Formation and to the Mic Mac Formation. Garnet, ilmenite (often altered to pseudorutile and rutile) are only observed in the Cree Member of the Logan Canyon Formation and the Upper and Middle members of the Missisauga Formation. More could be given on the differences between members but this would be based on the presence of detrital minerals

found in only one of the four wells. Thus, more data is needed for a better comparison between members to see if there are any actual trends.

### **6.3 Provenance**

#### **6.3.1 Detrital mineral provenance**

The dominant detrital minerals observed in the both the Logan Canyon and Missisauga formations of all four wells are ilmenite (often altered to pseudorutile and rutile), tourmaline, and rutile. These grains are dominantly subrounded to rounded, indicating that they have undergone long transport and are likely from a distant source. Chromite is also observed in both formations. This heavy mineral is associated with ultramafic rocks (Nesse, 1991). Ultramafic rocks are found in the Baie-Verte Brompton line (a series of ophiolites between the Humber and Dunnage zones of the Taconian Orogeny) that runs from Quebec to eastern Newfoundland. Garnet (almandine and spessartine) is observed in both formations and is subangular to subrounded. Almandine is the most common garnet associated with schists and gneisses but it is also found in pegmatites, granite, and felsic volcanic rocks (Nesse, 1991). Spessartine is most commonly found in granite, pegmatite, and felsic igneous rocks but is also found in Mn-rich metamorphic rocks (Nesse, 1991).

Staurolite with inclusion is observed in the Middle Member of the Missisauga Formation. This typically occurs in metapelitic rocks which suggest a metamorphic source rock. These clasts are typically subrounded to rounded and may be first cycle or polycyclic.

### 6.3.2 Lithic clast provenance

The lithic clasts are typically larger in size (2-4 mm) than the detrital minerals and indicate a shorter transport distance. The Meguma terrane of southern Nova Scotia and the Avalon terrane of northeastern Nova Scotia are the most likely source for these clasts. Clasts such as vein quartz, vein quartz containing tourmaline, microgranite, felsic plutonic rock, vein quartz with abundant euhedral rutile crystals, slate, deformed perthite, tuff, and quartzite are common in both the Meguma and Avalon terranes, whereas clasts of basalt and chert are very rare in the Meguma terrane.

Light green metasandstone clasts observed in Crow F-52 are likely from the Goldenville Formation of the Meguma terrane. Pink granite (K-feldspar-rich) clasts observed in the Logan Canyon Formation of the Crow F-52 well resemble the Avalon terrane late Paleozoic granites, possibly such as the West Moose River (Pe-Piper *et al.*, 1991) and North River (Pe-Piper, 1991) plutons. Diorite clasts are observed in the Fox I-22 well in the Logan Canyon Formation. Diorite plutons occur in both the Meguma and Avalon terranes but are much more abundant in the Avalon terrane, especially in the Cobequid Highlands (Koukouvelas *et al.*, 2002). The largest diorite intrusion in the Meguma terrane is within the Port Mouton Pluton, located in southern Nova Scotia (Donohoe and Grantham, 1989). This is a possible source for the diorite clasts but given the size of the clasts a more proximal source, such as the diorite plutons of the Avalon terrane (Cape Breton Island) is much more likely.

#### **6.4 Diagenetic minerals**

Common diagenetic minerals identified in the Orpheus Graben are calcite, limonite, pyrite, quartz, and siderite with lesser amounts of septochlorite, glauconite, francolite, chlorite, hematite, illite, kaolinite, ankerite, barite, clay minerals, opal, silica, and rhodochrosite observed (Table 6.2). Stilpnomelane is only observed as an alteration mineral in basalt/diabase cuttings and will be discussed later in part 6.3.3 of this chapter. Siderite and calcite are observed both early and late in the diagenetic history. In many cuttings siderite is observed to alter to limonite (Appendix 4 - Figure 3). Siderite commonly occurs in two or three phases. The core phase has a normal value of  $\text{FeO}_t$  for siderite, the rim phase has  $\text{FeO}_t$  in the higher range for siderite and is normally darker in colour (in back-scattered electron images) and the intermediate phase which has  $\text{FeO}_t$  values between those of the rim and core. Glauconite grains are observed to be replaced by septochlorites (discussed in the next section) and muscovite and biotite are seen to alter to illite and chlorite (as a result it is difficult to get good electron microprobe chemical analyses of muscovite and biotite). Chlorite forms rims on quartz (Appendix 1 - Figure 36) but this is not commonly observed. Cuttings of barite cement have been identified in the heavy mineral fraction (< 2 mm) in the Jason well (4220 ft, 6480 ft) making up as much as 8 % of the total sample. It has also been identified as cement in a very fine grained quartz arenite cutting from the Fox I-22 and Crow F-52 wells (Appendix 1 - Figure 54 and Appendix 2 - Figure 40). Rhodochrosite is observed to be replacing siderite in one cutting from the Mic Mac Formation of the Jason C-20 well (Appendix 4 - Figure 43).

Well	Formation	Member	Al-P mineral	Diagenetic minerals																
				Ankerite	Barite (not drilling mud)	Calcite	Chlorite	Chlorite rims	Francolite	Glaucanite	Hematite	Illite	Kaolinite	Limonite	Opal	Pyrite	Rhodochrosite	Septochlorites	Siderite	Silica
Fox	Logan C.	Marmorora				x	x	x						x		x			x	x
Crow	Logan C.	Marmorora		x			x		x	x		x	x	x		x		x	x	
Argo	Logan C.	Marmorora							x			x	x	x		x		x	x	
Fox	Logan C.	Sable					x						x					x	x	
Crow	Logan C.	Sable				x	x					x								x
Fox	Logan C.	Cree								x										x
Crow	Logan C.	Cree		x		x			x						x			x	x	
Argo	Logan C.	Cree				x			x	x		x	x		x	x				x
Jason	Logan C.	Cree	x			x	x						x	x		x				x
Fox	Missisauga	Upper	x		x		x						x	x		x				x
Crow	Missisauga	Upper														x				x
Argo	Missisauga	Upper														x				x
Fox	Missisauga	Middle											x	x		x				x
Crow	Missisauga	Middle			x															x
Argo	Missisauga	Middle	x			x			x				x	x	x		x			x
Jason	Missisauga	Middle				x			x				x	x	x		x			x
Jason	Mic Mac	Mic Mac												x	x		x	x		x

Table 6.2. Diagenetic minerals identified in the Logan Canyon (Marmorora, Sable, and Cree members) and Missisauga (Upper and Middle members) formations arranged by member.

From Table 6.2 we see that diagenetic minerals such as siderite are observed in every depth sampled, whereas others such as glauconite, ankerite, and septochlorites are only observed in the Logan Canyon Formation. Barite and hematite are only observed in the Missisauga Formation and rhodochrosite is only observed in the Mic Mac Formation. Further distinctions can be made between members or the formations, such as chlorite is only observed in the Upper Member, whereas calcite, francolite, hematite and opal are only observed in the Middle Member of the Missisauga Formation and chlorite rims on quartz grains and unknown clay minerals are only observed in the Marmorora Member, and opal is only observed in the Cree Member. Al-phosphate is found in the Cree Member of

the Logan Canyon Formation and in the both the Upper and Middle members of the Missisauga Formation. Again, because sandstones are not sufficiently abundant in all stratigraphic levels information on the stratigraphic variation in sandstone petrography may be incomplete. Some samples were examined using a binocular microscope (see Appendix 7 - Tables 10 to 13) whereas others were examined using the electron microprobe, this may have created biases in the data.

#### **6.4.1 Francolite**

Francolite has been identified in cuttings from the Marmora and Cree member of the Logan Canyon Formation in the Crow F-52 and Argo F-38 wells and from the middle Member of the Missisauga Formation in the Argo F-38 and Jason C-20 wells. Francolite is identified as nodules (pellets?), bone (dinosaur?) fragment, coatings, ooids and as cement in silty mudstone, siltstone, and very fine grained quartz wacke cuttings. It is also found to occur together with siderite as cement (Figure 6.2C and Figures 6.4D and F) and mixed with siderite or sepioclorite in ooids (Figure 6.2B, D and F). Electron microprobe work identified quartz, K-feldspar, plagioclase, rutile, ilmenite, muscovite, biotite, altered chromite and zircon detrital minerals and siderite, calcite, chlorite, kaolinite, illite, glauconite, pyrite and sepioclorite diagenetic minerals associated with francolite (Figures 6.2 - 6.4). Francolite is also observed to infill the pores in altered ilmenite crystals. Biogenetic structures such as coal (Figure 6.4F) and foraminifera (Figure 6.3B) are also observed in cuttings. Siderite appears to have been dissolved and the void filled with francolite cement (Figure 6.4F).

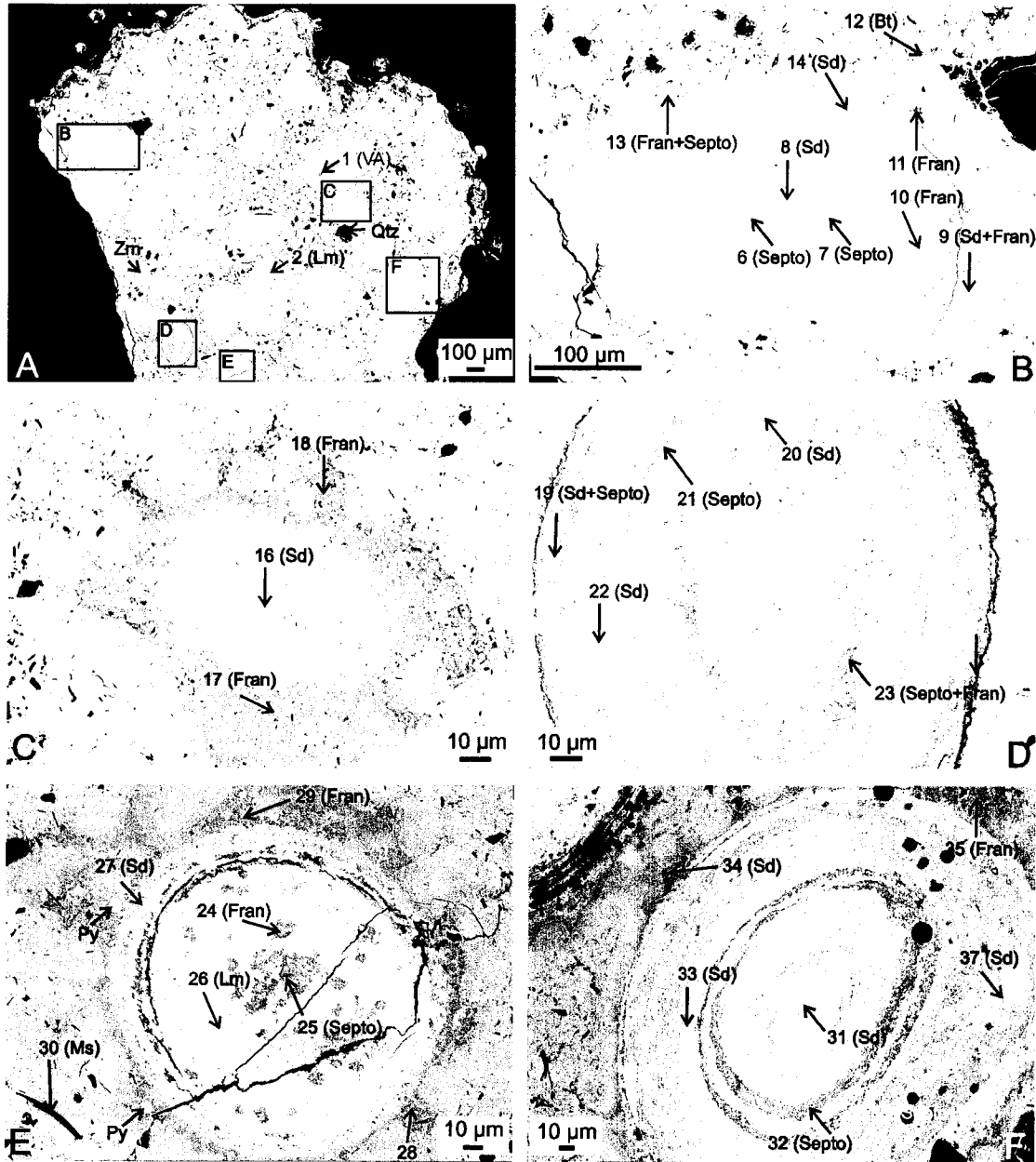


Figure 6.2. Back-scattered electron images of cuttings containing francolite from Argo F-38. Numbered arrows represent locations of chemical analyses listed in Appendix 3 - Tables 6-10. Labeled minerals are francolite (Fran), biotite (Bt), quartz (Qtz), K-feldspar (Kfs), limonite (Lm), muscovite (Ms), pyrite (Sd) siderite, (Py), septochlorite (Septo), and zircon (Zrn). (A) Ooids in siderite-cemented silty mudstone (1900-1930B-1). Black squares represent the location of Figs. 6.2B-F. (B-F) Enlargements showing compositional variations between ooids.

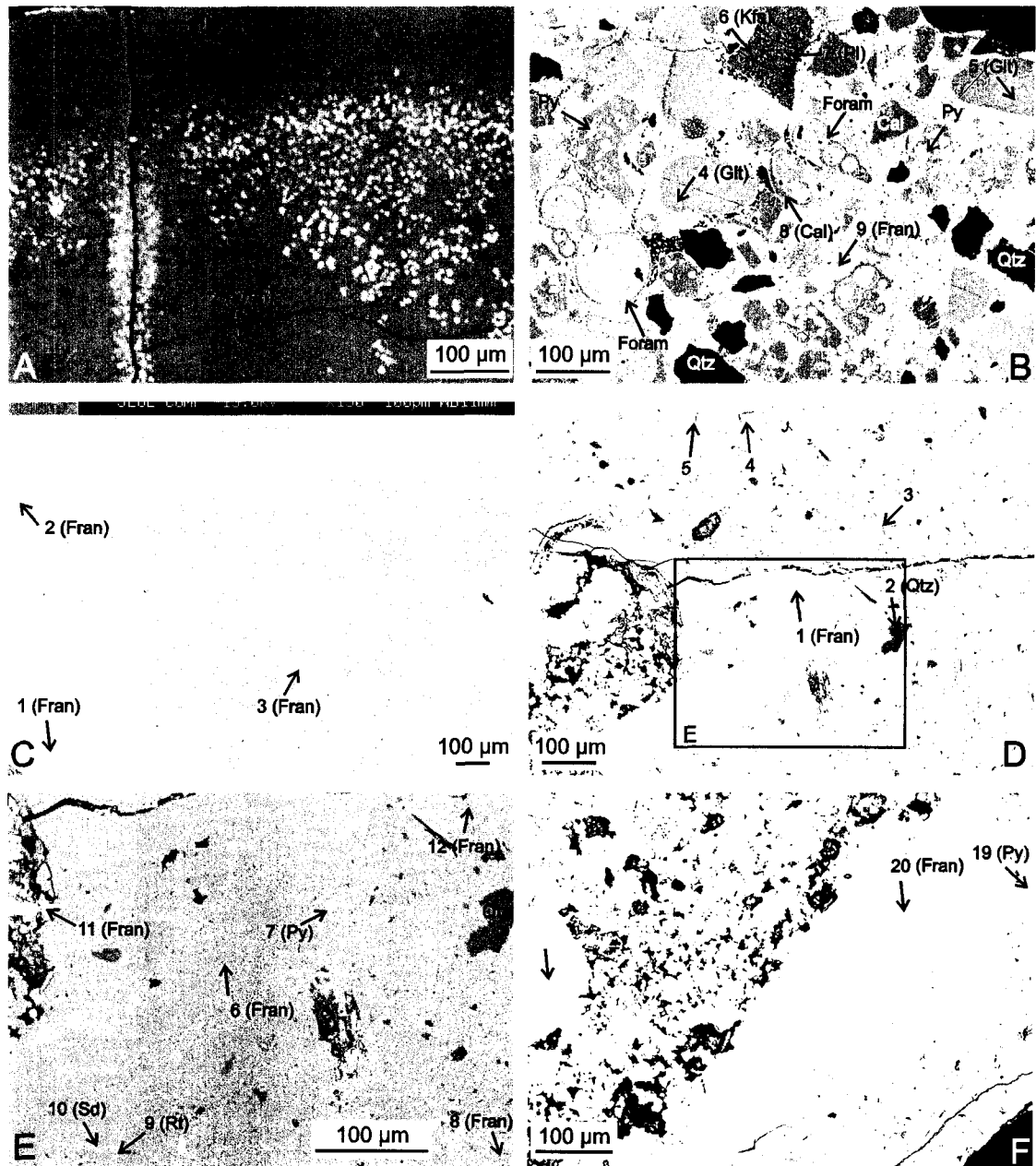


Figure 6.3. Back-scattered electron images of cuttings containing francolite from Argo F-38. Numbered arrows represent locations of chemical analyses listed in Appendix 3 - Tables 6-10. Labeled minerals are calcite (Cal), foraminifera (Foram), francolite (Fran), quartz (Qtz), K-feldspar (Kfs), glauconite (Glt), plagioclase (Pl), pyrite (Py), rutile (Rt), and zircon (Zrn). (A) Phosphate nodule (1900-1930B-3). (B) Phosphate-cemented siltstone with foraminifera and glauconite grains (3030-3060A-1). (C) Phosphate cutting (3030-3060B-1). (D) Phosphate-cemented silty mudstone with phosphate nodules (4680-4700B-2). Black square shows location of Fig. 6.4E. (E-F) Enlargement showing part of a phosphate nodule in the phosphate-cemented mudstone. (Fig. 6.3F is outside the area of Fig. 6.3D)

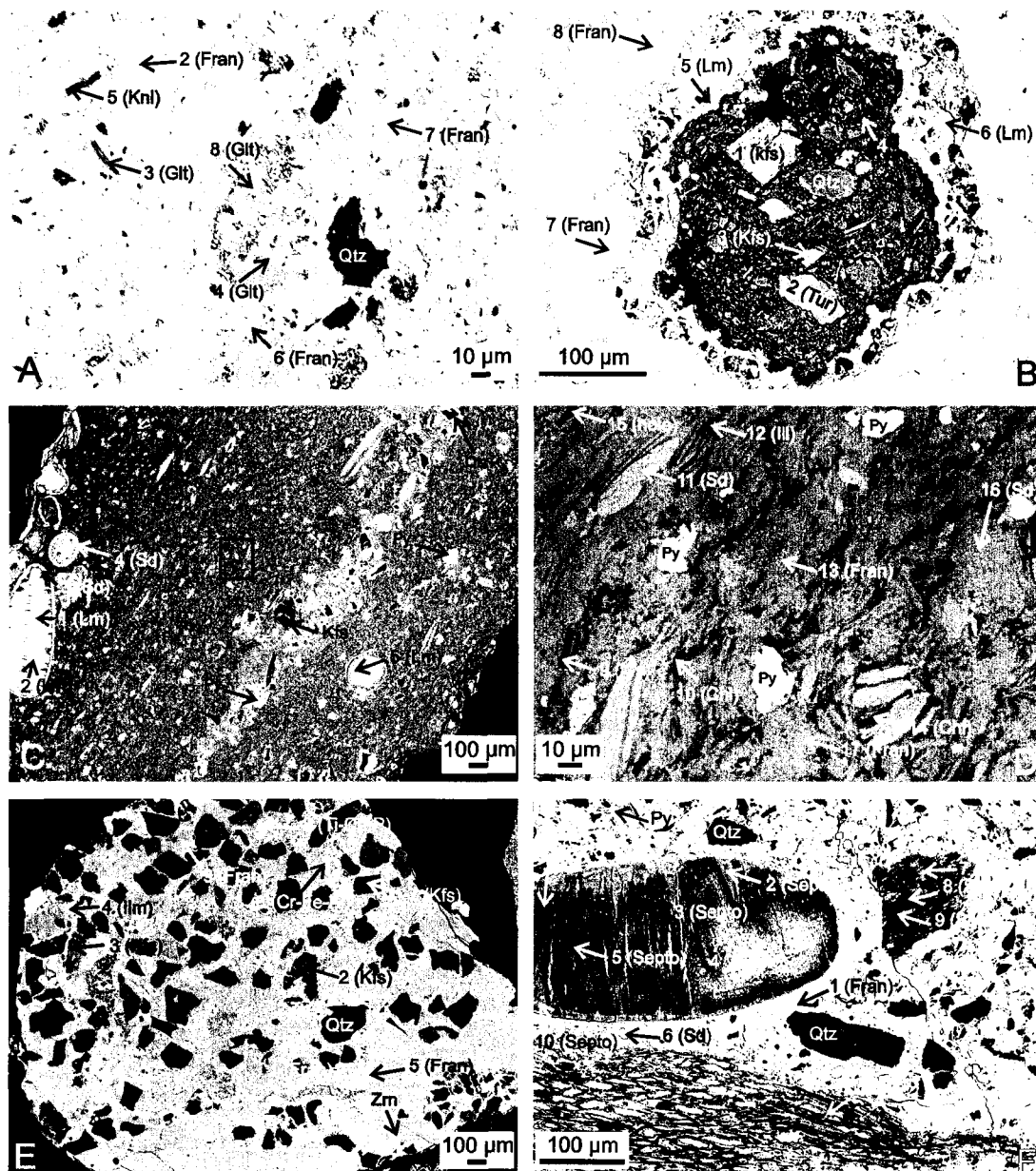


Figure 6.4. Back-scattered electron images of cuttings containing francolite from Crow F-52. Numbered arrows represent locations of chemical analyses listed in Appendix 2 - Tables 6-9. Labeled minerals are francolite (Fran), chlorite (Chl), quartz (Qtz), K-feldspar (Kfs), ilmenite (Ilm), Illite (Ill), kaolinite (Kln), limonite (Lm), glauconite (Glt), muscovite (Ms), pyrite (Py), septochlorite (Septo), tourmaline (Tur), and zircon (Zrn). (A) Phosphate-cemented silty mudstone (1430A-1). (B) Phosphate-cemented silty mudstone (showing a possible burrow-fill) (1430A-2). (C) Phosphate and siderite-cemented silty mudstone with siderite discs (1430B-3). Black square shows location of Fig. 6.4D. (D) Shows francolite cement. (E) Very fine grained phosphate-cemented quartz wacke (1610-3). (F) Phosphate- and siderite-cemented silty mudstone containing septochlorite intraclasts (probably after glauconite) (2270B-1).

### 6.4.2 Septochlorites

Septochlorite (probably berthierine) is identified in Marmora (Crow F-52 and Fox I-22), Sable (Fox I-22) and Cree (Crow F-52) members. It appears to have replaced dissolving siderite in some samples (Figure 6.5D, E and F) and replaced dissolving ankerite in others (Figure 6.5A). Septochlorite also appear to have replaced intraclasts of glauconite (?) (Figure 6.4F and Figure 6.5 B, D and E). These observations suggest that septochlorite developed mid to late in the diagenetic history. It is also found mixed with siderite and francolite forming ooids (Figure 6.2B, D, E and F). Septochlorite ooids are thought to have formed by chemical precipitation in sedimentary ironstones (Velde, 1977) and that they later alter to siderite and kaolinite (Greensmith, 1979). A cutting of tuff shows zoned rhombohedral crystals of siderite and kaolinite? being selectively replaced by septochlorite (Figure 6.6A). It appears that the siderite is replaced by septochlorite and kaolinite. Berthierine + quartz is also found to replace glass spherules in the pyroclastic unit of the Jason C-20 well (Figure 6.6B). These cuttings were found in the < 2 mm heavy mineral fraction below the unit and are interpreted as caving from the pyroclastic unit and not from the depth they are identified in.

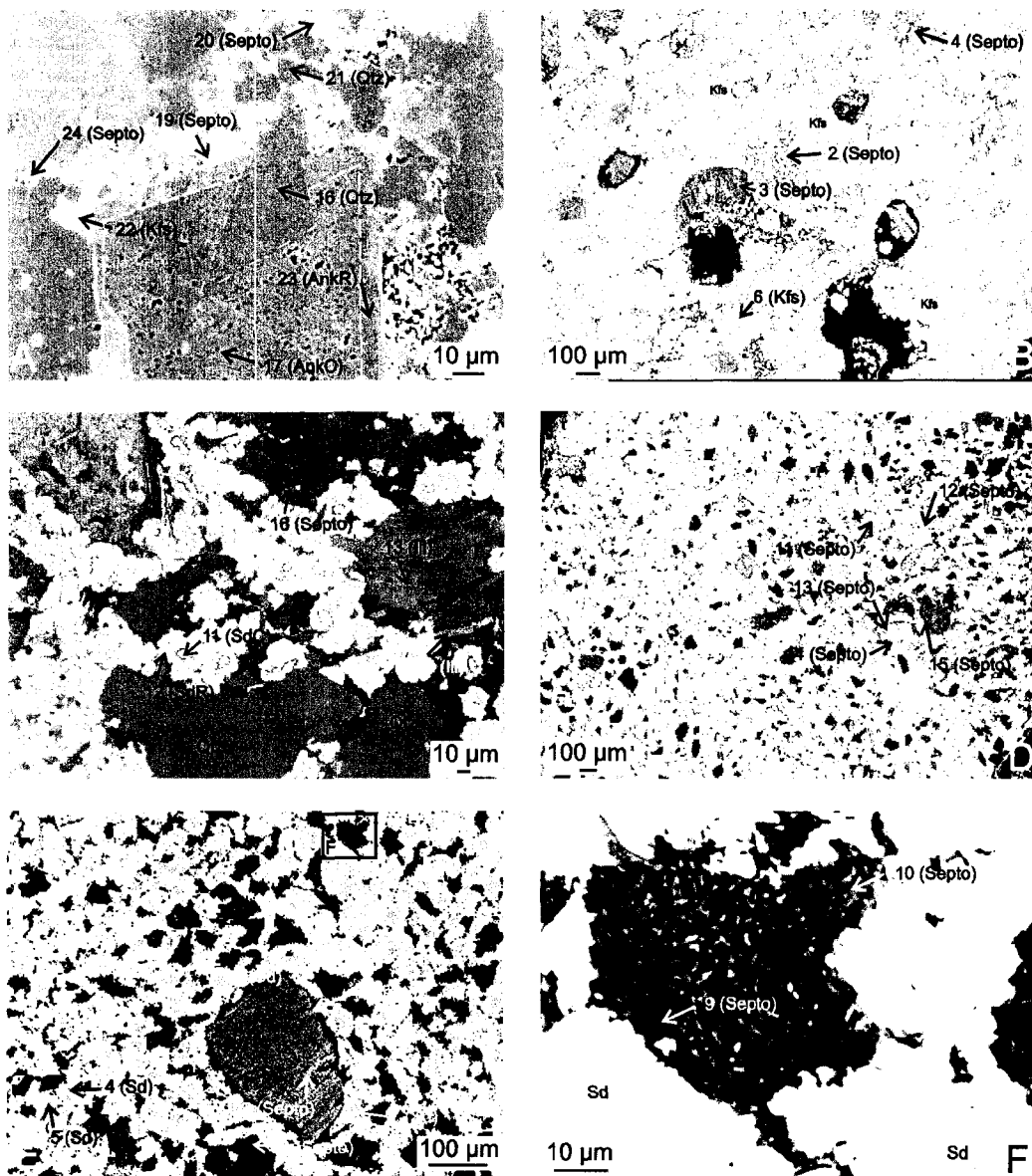


Figure 6.5. Back-scattered electron images of cuttings containing sepiochlorite. Numbered arrows represent locations of chemical analyses listed in Appendices 2-4. Labeled minerals are ankerite rim (AnkR), ankerite core (AnkC), quartz (Qtz), K-feldspar (Kfs), Illite (Ill), siderite (Sd), siderite core (SdC), siderite rim (SdR) and sepiochlorite (Septo). (A) Sepiochlorite replacing dissolved ankerite (Crow 1430B-2). (B) Sepiochlorite replacement of glauconite? grains (round to oval shape) (Crow 2480A). (C) Enlargement outside field of view of Fig.6.5B showing sepiochlorite replacing dissolving siderite (Sd), also showing zoned siderite. (D) Siderite nodule with sepiochlorite intraclasts (probably after glauconite) (Crow 2480A-2). (E) Enlargement of Fig. 6.5D (outside field of view) showing development of secondary porosity (resulting from the dissolution of siderite) and showing typical fibrous texture of sepiochlorite intraclasts. (F) Very enlarged view of Fig 6.5D (outside field of view) showing late pore filling with sepiochlorite.

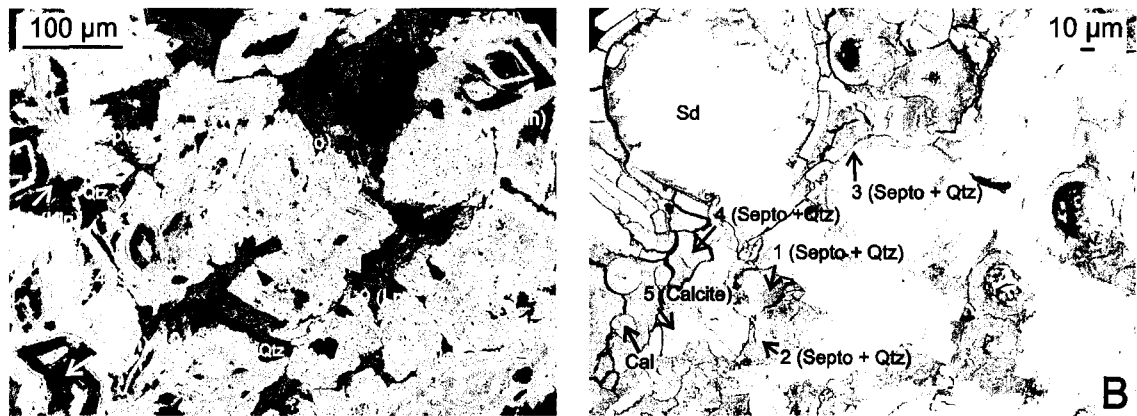


Figure 6.6. Back-scattered electron images of cuttings containing sepiochlorite diagenetic minerals. Mineral abbreviations used are quartz (Qtz), siderite (Sd), calcite (Cal), sepiochlorite (Septo), limonite (Lm) and kaolinite (Kln). (A) Altered tuff from pyroclastic unit showing zoning of rhombohedral siderite with kaolinite and sepiochlorite (Jason 6300H-1). (B) Spherulitic chloritized glass from the pyroclastic unit, replaced by siderite and sepiochlorite plus quartz and late pore filling calcite (Jason 4700F-9).

#### 6.4.3 Stilpnomelane

Some basalt/diabase cuttings in the Argo F-38 and Jason C-20 wells have altered to siderite, calcite, and stilpnomelane (Figure 6.7C, D, and E), whereas others have altered to chlorite, stilpnomelane and an unknown Si-Fe-Mg mineral in Figure 6.7. It appears that there is a difference in the resulting diagenetic minerals due to a difference in the starting minerals. In the first type, the basalt/diabase contains plagioclase (andesine and bytownite), Ti-Magnetite, apatite, ilmenite and clinopyroxene (Ti-augite) compositional minerals. The second type of basalt/diabase has plagioclase (labradorite and bytownite), Ti-magnetite, ilmenite, clinopyroxene (Ti-augite), and olivine as its original minerals. The stilpnomelane appears to be replacing the clinopyroxene minerals in the first type and the Si-Fe-Mg mineral seems to be replacing olivine in the second type. However, more work needs to be conducted to establish the relationship between the various mineral phases. Electron microprobe chemical analyses of these minerals can be found in

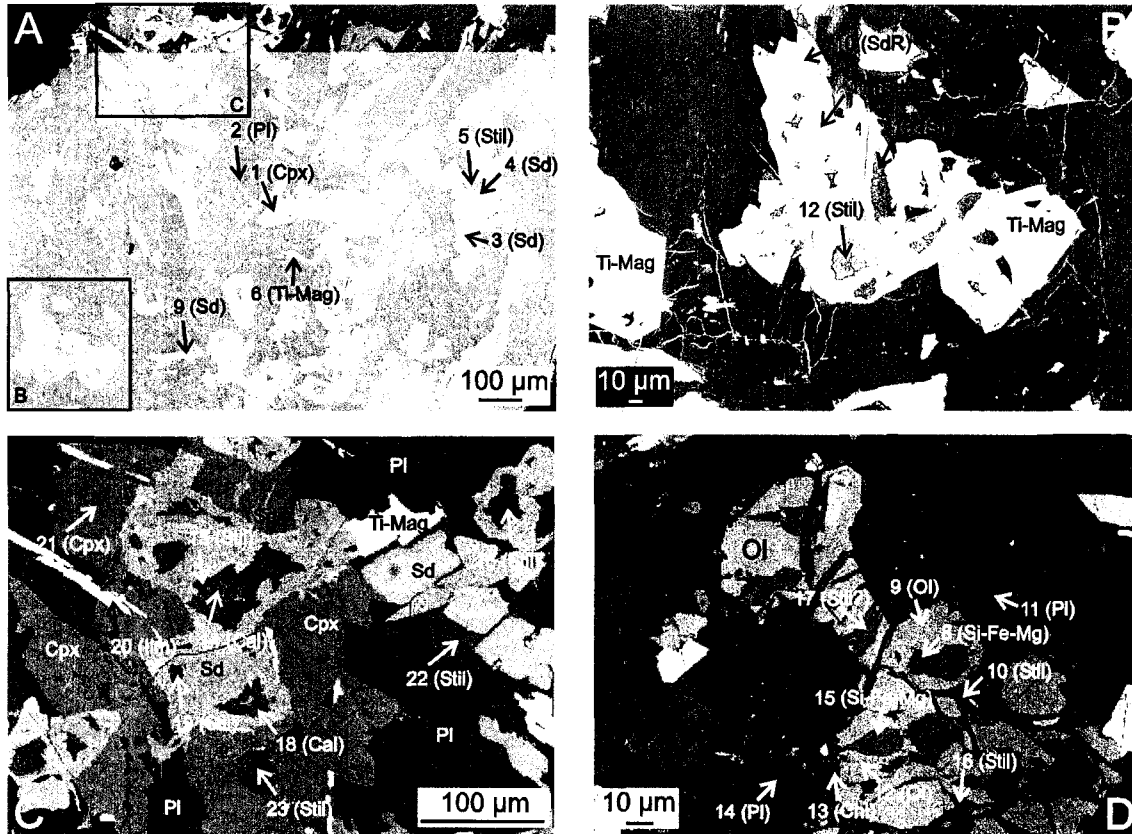


Figure 6.7. Back-scattered electron images of some cuttings containing stilpnomelane diagenetic minerals. Mineral abbreviations used are siderite (Sd), siderite core (SdC), siderite rim (SdR), ilmenite (Ilm), Ti-Magnetite (Ti-Mag), clinopyroxene (Cpx), calcite (Cal), olivine (Ol), plagioclase (Pl), stilpnomelane (Stil), chlorite (Chl), and limonite (Lm). (A) Cutting of basalt/diabase that has altered to siderite, stilpnomelane and calcite. Boxes show area of Figs. 6.7D and E. (B and C) Enlargement showing stilpnomelane replacing Cpx and later replacement of stilpnomelane by siderite and calcite. (D) Cutting of basalt/diabase that has altered to stilpnomelane, chlorite, and siderite (Jason 4700C-2).

### 6.5 Contaminants

Contaminants (Table 6.2) have been identified within the cuttings of all four wells studied (Appendix 1-4 - Table 4). In Fox I-22 well a large number of cuttings were identified as a calcareous conglomerate with granules of chert, quartz and feldspar. Examination of two of these cuttings with the electron microprobe identified hatrurite

(Appendix 1 - Table 9) as the cement, which is a synthetic ( $\text{Ca}_3\text{SiO}_5$ ) mineral and an important constituent of Portland cement (Fleischer *et al.*, 1978). Loose chert, quartz and feldspar granules in the Marmora and Sable members of the Fox well are interpreted to come from this cement and therefore are also contaminants. Similar “conglomerate” cuttings are observed in Argo F-38 (3030-3060 ft) and Jason C-20 (3530 ft) and are interpreted as well casing cement.

TS #	Well	Depth	Grain #	Component minerals							Identification
				Hatrite	Quartz	Albite	Iron	Aluminum metal	Oxidised aluminum	Limonite	
11-3	Fox	890-920A	1	x	x	x					Portland cement from well casing
11-3	Fox	890-920A	2	x	x						Portland cement from well casing
11-6	Fox	890-920B	1		x						Synthetic
11-4	Fox	1940-1970	1					x	x		Aluminum metal scrap
11-8	Fox	1040-1070	1		x					x	Chert
11-4	Fox	1940-1970	4		x						Chert
11-3	Fox	1940-1970C	6				x			x	Rusty iron

Table 6.3. Component minerals of contaminants identified in the cuttings from the Fox I-22 well.

A second type of contaminant identified in the Fox I-22 well (Figure 6.8) is an aluminum metal (partially oxidized). Six aluminum metal scraps are also identified in the Crow F-52 well (3200 ft). The third contaminant identified in the Fox I-22 well is that of a synthetic material. The binocular microscope revealed that these cuttings are black with clear, pink and blue tubes (?). The electron microprobe identify these tubes as having an organic composition. One quartz grain was also identified in this cutting. The fourth contaminant identified in the Fox I-22 well is a sliver of rusty iron found in the < 2 mm heavy mineral fraction. The second and third contaminants are thought to have entered

the samples during collection on the rig or during sub-sampling and processing and the fourth is interpreted as a possible shaving from the drill bit.

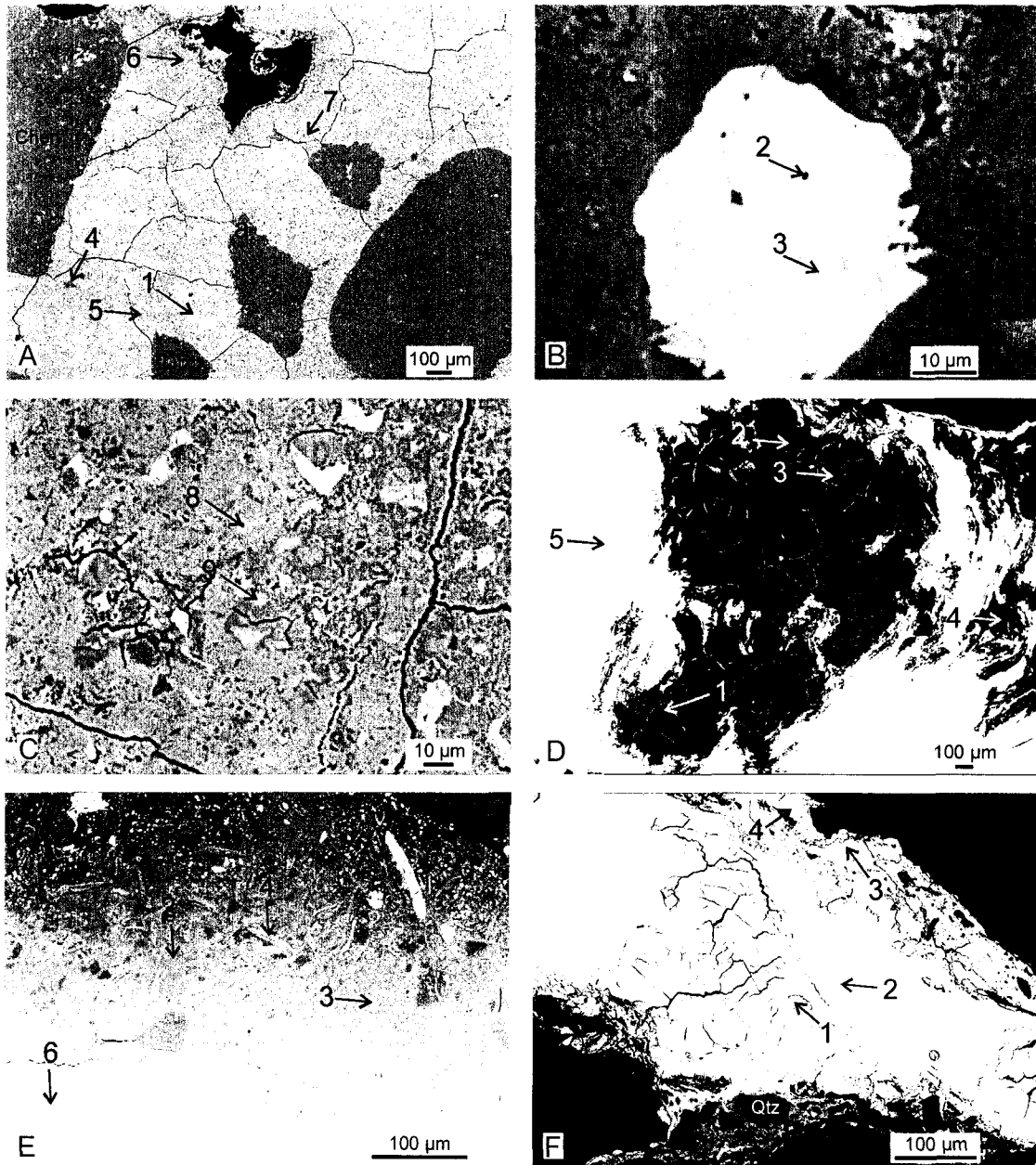


Figure 6.8. Back-scattered electron images. Numbered arrow represent locations of chemical analyses listed in Appendix 1 - Table 9. (A-C) Fox 890-920A-1 Portland cement from drill casing (1, 2 = Hatrurite; 3, 7 = unknown Al-Ca mineral; 4 = Plagioclase; 5, 6, 8, 9 = Ca-Si matrix). (D) Fox 1940-1970-1 Aluminum metal scrap (1-4 =aluminum oxide; 5 = aluminum metal). (E) Fox 890-920B-1 Synthetic (2-6 = unknowns). (F) Fox 1940-1970C-6 Rusty iron (1,3,4 = limonite; 2 = Iron).

## **CHAPTER 7**

### **DISCUSSION AND CONCLUSIONS**

#### **7.1 Introduction**

This chapter is a synthesis of seismic, lithostratigraphic and paleoenvironmental data to yield an understanding of the events in Orpheus Graben in the Cretaceous. The first part of this chapter will discuss the biostratigraphy problems observed in the Hercules G-15 well and then summarise the findings of each member of the Missisauga and Logan Canyon formations. The second part of this chapter will compare the Orpheus Graben with both the Sable Subbasin and the onshore Chaswood Formation and it discusses the tectonic evolution of the graben in relation to regional tectonic events. Figure 7.1 provides a generalized stratigraphy for the Orpheus Graben. Conclusions will be presented at the end of this chapter.

#### **7.2 Correlation between wells**

In Chapter 3 a simple correlation diagram outlined the correlation between wells at the level of formations and members. After discussing the lithostratigraphy, unconformities, salt structures, faults, and petrography, a more detailed correlation diagram for the Missisauga and Logan Canyon formations can be made (Figure 7.2 see back pocket). This figure summarizes (1) the dramatic changes in the depth of the Cretaceous sediments in the wells (shallow on the Canso Ridge or on top of salt structures and deep in the minibasins), (2) thickness variations of members between wells, (3) unconformities; and (4) sediments onlapping salt structures or the Canso Ridge basement, causing some members to be missing in some wells. Details of this correlation are

discussed in the following sub-sections.

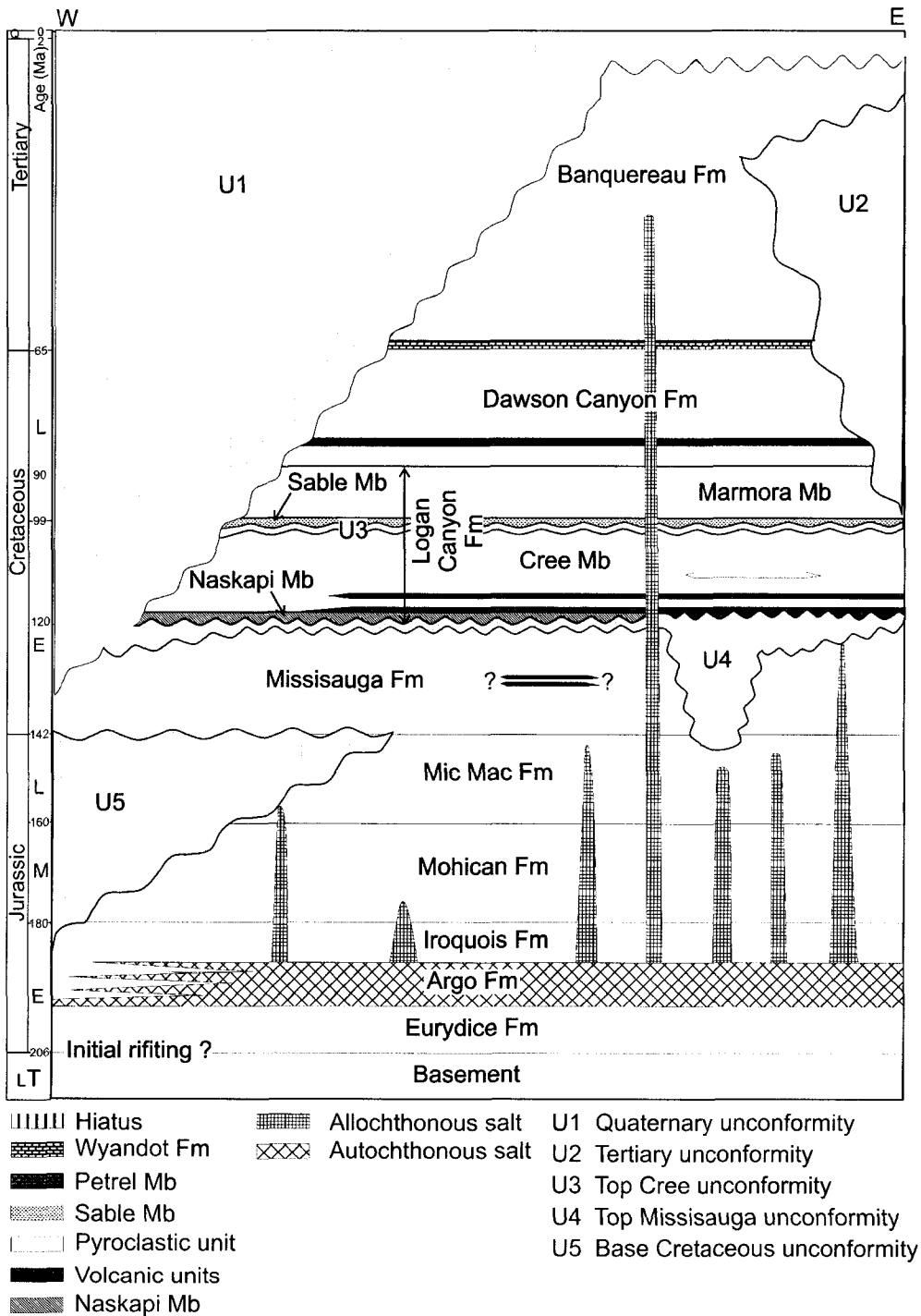


Figure 7.1. Generalized stratigraphic column based on the work of this study, and extending roughly along a W-E transverse through the Orpheus Graben. Time scale is from Gradstein and Ogg (1996). Salt of the Argo Formation is depicted in autochthonous and allochthonous modes of occurrences, with the latter schematically indicating how high the salt has migrated.

Figure 7.2  
See insert at the back

### 7.2.1 Hercules Biostratigraphy

An inconsistency in the ages of the Logan Canyon Formation at the Hercules G-15 well requires a closer examination. At Hercules, the interval from 1060 ft to 2540 ft is assigned, in this study, to the Logan Canyon Formation on the basis of lithology, wireline and seismic correlations. The Logan Canyon Formation is usually Aptian to Albian or Cenomanian in all other wells in the area. Here at Hercules, the Logan Canyon interval is assigned by Williams (in Barss *et al.*, 1979) to the Aptian near the top (1160 ft - 1280 ft) and as old as Berriasian-Hauterivian near the bottom (2060 ft - 2450 ft), a sizable discrepancy. Although the only other biostratigraphic study in this well assigns the upper part to the upper Cretaceous and Albian, the base is still as old as Upper Jurassic (Lyngberg, 1984). Some clues to the resolution of this discrepancy can be found in the details of the species found in these biostratigraphic studies.

In the interval from 1160 ft to 1280 ft, Williams (in Barss *et al.*, 1979) assigned the interval to the *Subtilisphaera perlucida* – *Systematophora schindewolfi* Zone (Aptian) and also lists the occurrence of the palynomorphs *Cleistosphaeridium polypes* (now known as *Kiokansium williamsii* with a top in the Cenomanian (A. MacRae, pers. comm., 2004)) and *Rugubivesiculites rugosus*. Williams (in Barss *et al.*, 1979) interpreted these two species as cavings from higher in the well. Lyngberg (1984) recorded additional palynomorph species, some from the same interval: *Paleohystrichophora infusorioides* (approx. 1160 ft to 1240 ft), *Cyclonephelium vannophorum* (approx. 1380 ft), *Canningia colliveri* (approx. 1460 ft) and *Spinidinium vestitum* from 1850 ft. All are typical of Upper Cretaceous or Albian. Lyngberg (1984) interpreted these palynomorphs to be in

place rather than cavings, assigning an Albian age. If this in-place interpretation is accepted, the biostratigraphy is consistent with the correlation proposed in this study, at least to a depth of 2040 ft according to Lyngberg (1984). There may be additional issues at this well, such as reworking, that hinder the interpretation of the biostratigraphy at deeper levels. This interval should be studied further.

### **7.2.2 Base Cretaceous unconformity (U5)**

The Base Cretaceous unconformity (U5) is thought to be present throughout most, if not the entire Orpheus Graben, and corresponds, in part, to the “Avalon Unconformity”. This unconformity initiated from a combination of transform fault motion and the progressive rifting between the Grand Banks and Iberia (Wade and MacLean, 1990). This unconformity is actually a multi-phased event with four erosional events identified in the Jeanne d’Arc Basin (Grant and McAlpine, 1990). These unconformities merge towards the southern Grand Banks to form one large unconformity that can reflect up to 50 to 60 Ma of deformation, uplift, and erosion.

The base Cretaceous unconformity (U5) most likely corresponds to the fourth erosional event (Berriasian-Tithonian boundary) depicted by Grant and McAlpine (1990, their figure 6.5). The U5 marker is clearly imaged in the western part of the graben where it truncates the Mic Mac, Mohican and Iroquois formations. Here the unconformity is shallow and only the sediments of the Missisauga Formation overlie it. Just to the east of this study area MacLean and Wade (1992) report that the unconformity separates faulted and rotated blocks below and relatively unfaulted and flat -lying strata above. This is

also observed in the western part of the study area but the unconformity is not clearly imaged in all parts of the graben because of younger salt movement.

### **7.2.3 Missisauga Formation**

The Missisauga Formation is found in six of the seven wells drilled in the Orpheus Graben, the exception being the Adventure F-80 well, which was drilled on the side of a salt diapir (Appendix 5 – Figures 16 and 17). Here the sediments of the Missisauga Formation appear to have abutted against or overlapped the structure, as the sediments of this formation and those of the lower Logan Canyon Formation were being deposited at the same time as salt growth here. The age of the Missisauga Formation in the Orpheus Graben is Berriasian to Barremian (Barss *et al.*, 1979). The Lower Member is absent within the graben, as in much of the rest of the Scotian Basin (Wade and MacLean, 1990). The Middle Member of the Missisauga Formation is characterized by thick beds of dominantly coarse to pebbly, mature, quartz-dominated sandstones that are interbedded with thin beds of shale, very fine grained sandstones, marl and limestone. The Upper Member of the Missisauga Formation consists of beds of medium to coarse grained, quartz-rich sandstones with thin beds of silty mudstone and very fine to fine grained sandstones. This member is found in four of the six wells that encountered the formation. The exceptions are Jason C-20 and Hercules G-15 (Appendix 5, Figures 13 and 14), where the top Missisauga Formation unconformity (U4) has completely eroded the Upper Member and possibly part of the Middle Member.

Mostly non-marine palynomorphs have been identified in this interval, but occasionally Lower Cretaceous dinoflagellates are present, suggesting either a marginal marine

environment with strong terrestrial influences, or a predominantly non-marine environment with minor episodes of marine conditions (Barss *et al.*, 1979). The second interpretation is preferred, given the lithostratigraphy of this formation, the presence of marls, and its blocky log response (fluvial channels?), showing mature sands with no obvious internal trend, interbedded with shale and very fine grained sandstones.

The average penetrated thickness of the Missisauga Formation is approximately 670 m (about 0.4 seconds of TWTT). This thickness varies from 269 m (at Eurydice P-36) in the western end of the Graben, to 106 m (about 0.05 seconds of TWTT) at the Fox I-22 well, where it appears to be its thinnest due to onlap onto the Canso Ridge, and approximately 1500 m or more (about 1.15 seconds of TWTT) in a salt withdrawal minibasin (Appendix 5 - Figure 14). The seismic data show that the Missisauga Formation thickens away from the Canso Ridge both northward and southward and this may suggest that at the time of deposition the Canso Ridge was either a paleo-relief feature or that sediments were infilling the Orpheus Graben and not being deposited on the Canso Ridge.

Among the detrital minerals present in the Missisauga, several were not found in the detrital minerals of the Logan Canyon Formation and suggest some change in sources and/or preservation. Those present in the Missisauga Formation and not in the Logan Canyon Formation include: staurolite crystals with inclusions, quartz crystals with zircon inclusion, and quartz crystals with chlorite inclusions. A greater quantity of altered ilmenite (altered to pseudorutile and rutile) with inclusions is also observed in the

Missisauga Formation. Mineral grains found exclusively in this formation are deformed perthite crystals, and a feldspar megacryst with vermicular quartz inclusions. All observed detrital lithic clasts could be derived from the Meguma and Avalon terranes (see Chapter 6). Fewer quartz granules and no feldspar granules are found in the Missisauga Formation of the Jason C-20 well, in comparison to the other wells, which may suggest smaller channels delivered sediment to this area, that this area was more distal to the sediment source, or that the depositional or diagenetic environment affected preservation of some minerals.

Seismic facies E corresponds to the Missisauga Formation and is seen as low to medium amplitude, transparent, semi-continuous to discontinuous, subparallel to hummocky reflections. This seismic facies displays more continuous, straight reflections in the north-south lines and more discontinuous, wavy, transparent reflections in the east-west lines of the same survey (project 8624-P028-068E). This may be indicative of anisotropy to the bedding surfaces generating the acoustic contrasts in this interval, such as fluvial channels aligned N-S, and generating more continuous reflections in that orientation than in E-W sections which cut orthogonally to the channel forms. This may hint at more N-S paleocurrent orientations, but because channels were not individually imaged, it is a speculative interpretation. The observation is also limited by the availability of suitably oriented, better-quality sections.

There are a few continuous seismic reflections within the Missisauga Formation, which are thought to correlate to thin marl and limestone beds inferred from the identification of

these cuttings in the Middle Member of the formation. The log response in the Middle Member is blocky and is thought to reflect fluvial channels switching their course among finer delta plain deposits. The presence of marl and limestone suggests that there were intermittent ocean flooding events. The depositional environment was most likely that of an upper delta plain, which experienced a few episodes of marine incursions. The Upper Missisauga Formation is finer grained than the Middle Member, suggesting either that sediment supply was not as great during the time of deposition or that there was a shift in the depositional environment to the lower delta plain or delta front, where shoreface environments would be prevalent and would better sort the sand. Thin coal beds indicate intermittent swamp environments on the delta plain.

In the Argo F-38 well, a volcanic interval within the Missisauga Formation is observed. Two volcanic units, each approximately 6 m in thickness, are identified from the wireline response and the abundances of basalt/diabase in the cuttings below these intervals (Table 1.1). The Missisauga volcanic interval does not produce a distinct high amplitude reflection like the Cree interval and was not traced seismically. Spores below this interval are notably darker in colour, but not above, suggesting that this may be a flow rather than a sill (Lyngberg, 1984).

#### **7.2.4 Top Missisauga unconformity (U4)**

The top Missisauga unconformity (U4) is traceable throughout the central and eastern parts of the Orpheus Graben. Like the base Cretaceous unconformity (U5) this unconformity most likely also corresponds to one of the several events comprising the “Avalon Unconformity”. This unconformity most likely corresponds to the third

erosional event (Barremian-Aptian boundary) depicted by Grant and McAlpine (1990, their figure 6.5). A Barremian - Aptian unconformity with a volcanic interval overlying it has been previously observed by Wade and MacLean (1990, their figure 5.21) on the eastern Scotian Shelf and most likely is the top Missisauga unconformity (U4) and the Cree volcanic interval of this study.

The Top Missisauga unconformity is not imaged in the western part of the graben because it is either too close to the seafloor or it has been eroded by a later unconformity. In the central part of the graben (at the Fox I-22, Crow F-52 and Argo F-38 wells) the transgressive, shale-dominated Naskapi Member of the Logan Canyon Formation overlies the top Missisauga unconformity, which truncates the underlying strata. In the eastern part of the graben (at the Hercules G-15 and Jason C-20 wells) the Naskapi Member is absent and the lower volcanic unit of the Cree Member overlies this unconformity. In some lines (i.e. 81-402A, 125-D) the unconformity can be clearly and easily traced. In these lines the unconformity creates distinct diffractions (suggesting an irregular erosion surface) below a negative, high amplitude reflection. In other lines (i.e. 364-B, 362-B, 360-B, 135-D, 133-D, 137-D and E2-14) a positive high amplitude reflection that truncates the underlying reflections is seen as directly underlying the Volcanic marker. In these lines, as in most, the unconformity is planar but in others (Appendix 5 – Figures 22 and 23) it is discontinuous and uneven, which may be related to the underlying salt, or may indicate local channeling or at least suggests an irregular erosional surface. Immediately below the top Missisauga unconformity at the Fox I-22

well (1940-1970 ft and 2030-2060 ft) there is an increase in abundance of the diagenetic mineral kaolinite, probably due to subsurface weathering.

In the central part of the graben, where both the U5 marker and U4 marker are thought to be present, some faults appear to have not disrupted the U4 marker. Line quality, and the closeness of these two unconformities makes it unclear if these faults do not extent past the U5 marker or U4 marker (Figure 5.2). In the eastern part of the graben, some faults are clearly imaged to not to extent past the U4 marker (Figure 5.8) or just slightly above (Figures 5.3 and 5.4). Faulting related to salt tectonics is very common in the eastern part of the graben and in many places other faults disrupt the Top Missisauga unconformity (U4 marker) (Figures 5.3, 5.4 and 5.8).

### **7.2.5 Naskapi Member**

The Naskapi Member has been identified in three of the seven wells (Fox I-22, Crow, F-52, and Argo F-38). It has been eroded in the western part of the graben and is absent in places in the eastern part of the graben (Jason C-20, Hercules G-15), but whether this is due to later erosion or non-deposition is unclear. In the northeastern Sable Subbasin, it was interpreted by MacLean and Wade (1993) to be interbedded with the volcanic unit, as in the Hesper P-52 and Hesper I-52 wells. Where it is present in the graben, the Naskapi Member is composed of alternating light grey to medium grey shales (with mm scale laminations) interbedded with silty mudstone and fine to very fine grained sandstones. The age of the Naskapi Member in the Orpheus Graben was determined to be Aptian (Barss *et al.*, 1979) as in the rest of the Scotian Basin (Wade and MacLean,

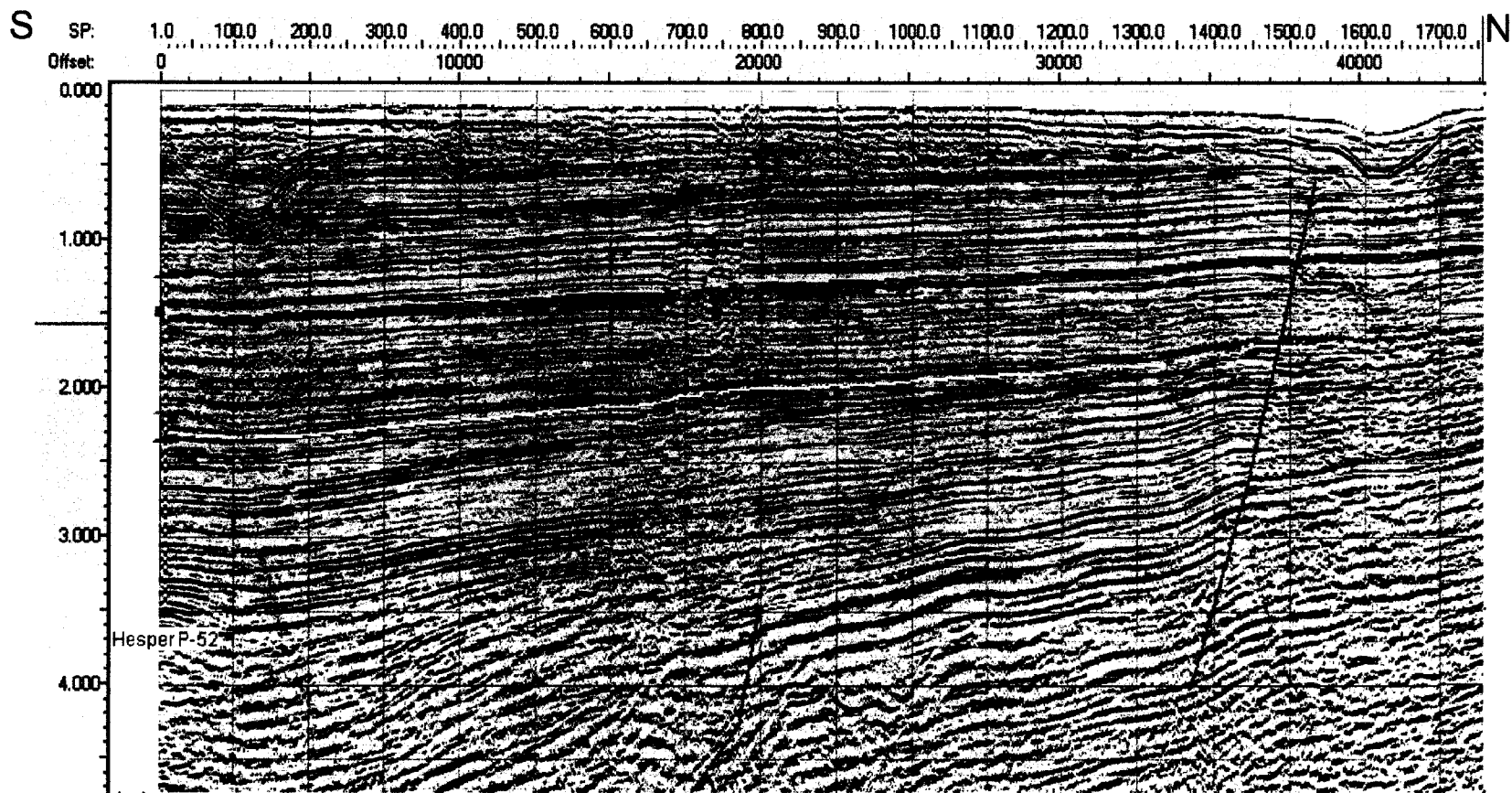
1990). In the Fox I-22 well, near the top of the Naskapi Member, there is evidence of either a brackish water or open shelf environment, because this is the only interval (1808 ft) within the well where dinoflagellate cysts were recovered; the rest of the well only encountered non-marine palynomorphs (Barss *et al.*, 1979). The Naskapi Member in the Argo F-38 well is also within an interval (3665 ft to 1570 ft) that saw an increase in marine palynomorph diversity (Barss *et al.*, 1979). In the Fox I-22 well, the succession is cleans upwards at the top of the member, as indicated by a decreasing upward gamma log response. In the Argo F-38 and Crow F-52, wells the gamma ray log response remains strong throughout the Naskapi Member. This data, combined with the lithostratigraphic data, suggest that the member was deposited in an open marine environment, fining eastward and shallowing upwards.

Seismically, the Naskapi marker, an event near the top of the Naskapi Member, can not be followed far from the wells before being lost, because the thickness of this member is near the resolution limits of the data. This reflection is of low to high amplitude, semi-continuous and wavy at the wells where it is found. The Naskapi marker (at the top of the Naskapi Member) in the Fox I-22 and Crow F-52 wells is at the same stratigraphic level as the Volcanic marker (near the base of the Cree Member) in the Hercules G-15, Argo F-38, and Jason C-20 wells, so that mapping the extent of this member is very difficult, because it is so thin, and because the top Naskapi Marker creates a similar reflection character as the Volcanic marker. The thickness of the Naskapi Member encountered in the wells varies from 43 m to 14 m depending on the well.

### **7.2.6 Volcanic interval of the Cree Member**

Volcanic intervals are found within three wells in the Orpheus Graben (Argo F-38, Hercules G-15 and Jason C-20) and in the Hesper I-52 and Hesper P-52 wells (Figure 7.3) just to the south of the graben in the Abenaki Subbasin. Seismically, the volcanic marker at the Hesper wells can be traced to the volcanic marker of the Cree Member in the Orpheus Graben, suggesting they correspond to the same volcanic event. In all three wells in the Orpheus graben the volcanic interval occurs near the base of the Cree Member of the Logan Canyon Formation. The volcanic interval was interpreted to be within the Naskapi shale at the Hesper I-52 well (Jansa and Pe-Piper, 1985). The lower unit of the Cree volcanic interval, in the Orpheus Graben, separates the Aptian Naskapi Member (in the Argo F-38 and Jason C-20) from clastics of the Albian Cree Member. The age of the volcanic interval at the Hesper wells is likely to be Aptian (the age of the Missisauga Formation just below the volcanic interval is Hauterivian to Barremian (Ascoli, 1990)). It is possible that the volcanic interval is in the Naskapi Member at the Hesper wells because the boundary between the Naskapi Member and the Cree Member is diachronous.

The Cree volcanic interval appears to be flows rather than sills because it does not cut across strata and it appears in the same stratigraphic location in the wells of the Orpheus Graben. This interpretation is strengthened by the fact that immediately below the Cree volcanic interval in the Jason C-20 and Hercules G-15 the spores are notably darker in colour, but not darkened above (Lyngberg, 1984). The seismic correlation of the Cree



- |  |   |  |  |
|--|---|--|--|
| <input type="checkbox"/> U1 marker                 | <input type="checkbox"/> Petrel marker              | <input type="checkbox"/> U4 marker             | <input checked="" type="checkbox"/> Mic Mac marker |
| <input checked="" type="checkbox"/> Wyandot marker | <input checked="" type="checkbox"/> Volcanic marker | <input checked="" type="checkbox"/> "O" marker | <input type="checkbox"/> Basement marker           |

Figure 7.3. Line 3604-1 showing the location of the volcanic interval at the Hesper P-52 well, south of the Orpheus Graben.

Volcanic marker to volcanic marker at the Hesper wells suggests they are part of the same flows. On the other hand, the coarse texture of the basalt and lack of extrusive lithologies at the Hesper I-52 well led Jansa and Pe-Piper (1985) to interpret it as a sill or dike and not a flow. Although no source for the volcanic intervals was imaged in the seismic data, there are large gaps in the seismic coverage of the area and a volcanic cone or fissure may remain undetected.

The basal Cree volcanic interval in the Orpheus Graben is made up of two basalt/diabase units with the upper unit (2 m to 8 m) thinner than the lower unit (9 m to 18 m). The basalts/diabase cuttings analysed are composed of plagioclase, K-feldspar, Ti-magnetite, ilmenite, clinopyroxene, apatite, and olivine. Some of these minerals have altered to siderite, chlorite, stilpnomelane, calcite, pseudorutile, and rutile. The alteration of olivine to stilpnomelane may indicate that the volcanic rocks were extruded into, or had contact with, sea water. Palynology studies from all three wells suggests that the Cree volcanic interval was deposited in a marine environment (Barss *et al.*, 1979; Lyngberg, 1984)

In the two wells in the northeastern part of the graben (Hercules G-15 and Jason C-20) there is also a thick pyroclastic unit. In the Hercules G-15 well this unit is approximately 76 m thick and at the Jason C-20 well it is approximately 72 m thick. This pyroclastic unit is not found in the Argo F-38 well. From the seismic data it appears that this unit may stop at a fault that cuts the volcanic interval but not the overlying U3 marker, implying that the fault created relief at the time of deposition. The pyroclastic unit consists of pyroclastic and volcanoclastic rocks in which volcanic tephra, including glass,

is mixed with quartz rich sediments that are interbedded with thin lava flows (Jansa and Pe-Piper, 1988). Cutting analyses from this interval (or cavings from this interval) were found to be altered tuffs and spherulitic chloritized glass, partially replaced by siderite and calcite.

Seismically the lower unit of the Cree volcanic interval appears to be more laterally continuous than the upper unit and it corresponds to a high amplitude, continuous reflection that, in most parts of the graben, can be easily traced. The reflection occurs a short distance above the top Missisauga unconformity (U4 marker) and when traced westward in the graben the reflection character changes to a variable amplitude, semi-continuous, wavy reflection. Where the reflection intersects the Fox I-22 and Crow F-52 wells, it corresponds to the top of the Naskapi Member. To the east of the study area of this thesis (in the STP lines of MacLean and Wade, 1992) the Volcanic marker correlates to the KIO reflection, which MacLean and Wade (1992) thought corresponded to the “O” marker of the Missisauga Formation. The KIO reflection is also commonly directly above an unconformity, termed the “Avalon unconformity” by MacLean and Wade (1992). Figure 7.2 shows that the “O” marker is eroded out by the top Missisauga unconformity (U4 marker) on the southeastern flank of the Canso Ridge. The KIO reflection of MacLean and Wade (1992) may in fact be the volcanic interval and not the “O” marker and their “Avalon unconformity” may actually correspond to the top Missisauga unconformity (U4 marker), matching what is seen in this study. This unconformity might also be an amalgamation of the U5 and U4 markers. Mapping the full extent of the Volcanic Marker is very difficult because the reflection is at the same

position stratigraphically as the KIO reflection and the Naskapi marker. Figure 4.4 shows the mapped extent of the volcanic marker. It may also extend farther eastward but future work and better data coverage will need to be done to verify this.

### **7.2.7 Cree Member**

The Cree Member is interpreted to be in five of the seven wells, the exceptions being the Eurydice P-36 and Adventure F-80 wells (where it likely onlaps against a salt diapir). This member has been eroded in the western part of the graben by the Quaternary (?) unconformity (U1). The age of the member has been determined to be Albian by palynology studies in the Fox I-22 (Barss *et al.*, 1979), Argo F-38 (Barss *et al.*, 1979), Hercules G-15 (Lyngberg, 1984), and Jason C-20 (Lyngberg, 1984) wells, although preliminary work by Shell (1971b) suggested a Cenomanian age in the Crow F-52 well. The Cree Member consists of thick beds of medium to coarse grained quartz rich sandstones interbedded with thin beds of very fine to fine grained sandstones, silty mudstone and marl. The upper part of this member has fine to medium grained sandstones that are interbedded with very fine to fine grained sandstones and silty mudstone beds. The thickness of this member does not appear to vary greatly throughout the graben, with an average thickness of 184 m. Petrographically the Cree Member differs from the rest of the Logan Canyon Formation in that sphalerite and garnet grains were identified (see Chapter 6, section 6.2.3).

Seismically, the Cree Member corresponds to seismic facies D (Chapter 5, section 5.2.4), low to medium amplitude, discontinuous reflections that are commonly hummocky. In the eastern part of the graben the discontinuous, transparent, sigmoidal architecture is

more pronounced in the north-south lines. On east-west lines, this facies shows semi-continuous to continuous, subparallel, low amplitude reflections. As in the interval corresponding to the Missisauga Formation (see section 7.2.3 of this chapter) this may suggest that the paleocurrent orientations was dominantly from north to south, with the hummocky reflections produced as the result of coastal progradation but this interpretation is speculative given the resolution of the data.

The depositional environment inferred from the palynological information is a mix of non-marine in the central part of the graben (Fox I-22; Barss *et al.*, 1979) to marine in the east (Argo F-38, Hercules G-15, and Jason C-20; Lyngberg, 1984). Several thin marl beds are found within the Cree Member, which may indicate minor episodes of marine incursions. The wireline logs are irregular and show no systematic pattern within the Cree Member. The hummocky character of the seismic facies, which correspond to medium-coarse grained quartz rich sandstone interbedded with thin beds of marl, suggests a low relief deltaic environment, probably lower delta plain to shoreface. Thin coal beds may indicate a local swamp development on the delta plain.

### **7.2.8 Top Cree Unconformity**

The U3 unconformity (Chapter 4) correlates to the top of the Cree Member and most likely corresponds to the second erosional event at the Aptian – Albian boundary depicted by Grant and McAlpine (1990, their figure 6.5). This unconformity is observed in the eastern and parts of the central graben and is interpreted as a transgressive surface with minor erosion beneath, because it is seen as a sub-planar reflection that occasionally truncates underlying reflections. The reflection of this unconformity is positive, low to

high, wavy to planar, and semi-continuous. The wavy nature of this reflection may indicate minor channeling or simply discontinuous bedding continuity. The underlying seismic reflections are subparallel to parallel where they are not truncated by the unconformity, implying little or no tectonic activity at the time of formation of the unconformity.

### **7.2.9 Sable Member**

The Sable Member is found in five of the seven wells of the Orpheus Graben, the exceptions being the Eurydice P-36, where it was either not deposited or has been eroded, and Adventure F-80, where the member onlaps against a salt diapir. The reported age of this member ranges from Aptian to Cenomanian although an Albian age is most likely. Palynological studies from the Fox I-22 (Barss *et al.*, 1979), Argo F-38 (Barss *et al.*, 1979), Jason C-20 (Lyngberg, 1984), and Hercules G-15 (Lyngberg, 1984) wells indicated an Albian age. A Cenomanian age was reported for Crow F-52 (Shell, 1971) and an Aptian age for Jason C-20 (Lyngberg, 1979). This member is characterized by a predominantly shaly interval interbedded with very fine to fine grained sandstones. The average thickness of this member is 46 m and it does not appear to vary much in the seismic profiles. The Fox I-22 and Crow F-52 wells have cutting samples from only one interval within this member. Petrographically this member differs from the rest of the Logan Canyon Formation by having grains of quartz with inclusions of apatite and muscovite but lacking grains of tourmaline. None of the diagenetic minerals found in the other member of the Logan Canyon Formation, such as glauconite, pyrite, limonite, ankerite, barite, kaolinite, and phosphorite were identified, although this might be a consequence of the small number of samples.

Seismically the top of this member was not traced throughout the graben. The depositional environment inferred from the palynological information varies from non-marine in the central part of the graben (Fox I-22 (Barss *et al.*, 1979)) to marine in the east (Argo F-38, Hercules G-15, and Jason C-20 (Lyngberg, 1984)). Wireline log patterns in this member are a mixture of bell and funnel shapes suggesting a proximal delta front to shallow to open marine environment. The gamma ray logs at the Argo F-38 and Hercules G-15 both have sharp bases and funnel patterns and may suggest that these relatively close wells may have a slightly different depositional environment from the other wells.

#### **7.2.10 Marmora Member**

The Marmora Member of the Logan Canyon Formation is interpreted to be present in six of the seven wells, the exception being the Eurydice P-36 well where it has been eroded at an unconformity. This member is composed of very fine to fine sandstones interbedded with fine to medium grained sandstone, silty mudstone, and shale beds. Thin marl and coal beds are also seen in this member. The Marmora Member has been eroded in the western and parts of the central graben as well as in the north eastern parts of the graben at the Quaternary (U1) and Tertiary unconformities (U2) respectively. The reported age of this member varies from Turonian to Albian, being reported as Cenomanian-Albian (Barss *et al.*, 1979) at Fox I-22, Cenomanian (Shell, 1971c) at Crow F-52, Turonian-Cenomanian (Barss *et al.*, 1979) and Cenomanian (Lyngberg, 1984) at Argo F-38, middle Albian (Union, 1975) and Albian (Lyngberg, 1984) at Jason C-20, and Cenomanian (Barss *et al.*, 1979) at Adventure F-80. The thickness of the member does not appear to vary where it has not been affected by erosion or by salt growth or withdrawal. It has an

average thickness of 235 m and is thinnest where it has been eroded (Fox I-22, 185 m thick) and where there is salt growth (Adventure F-80, 132 m) and thickest where salt appears to have withdrawn (Argo F-38, 348 m). Petrographically the Marmora Member differs from the other members of the Logan Canyon Formation in that it contains grains of plagioclase with K-feldspar inclusions, Ti-magnetite, and hematite. This upper part of this member is unique in that it has a large number of phosphatic nodules and phosphate-cemented cuttings in the Fox I-22, Crow F-52 and Argo F-38 wells. A probable Cretaceous dinosaur bone was also found in this member in the Argo F-38 well (Weir-Murphy *et al.*, submitted to *Atlantic Geology*).

Seismic facies A and C correspond to this member. The reflections in the upper part of this member are more planar and continuous whereas the lower part of this member has reflections that are wavy and semi-continuous and more transparent. The wireline logs in the Marmora Member frequently show small scale (10-20 m) fining upward, cleaning upward and bell shaped patterns. The palynology for the Fox I-22 well did not show any marine palynomorphs but the Argo F-38 well shows an increasing diversity in marine palynomorphs from the Cree Member upwards. The above, combined with the observation of phosphorites and glauconite grains in the upper part of this member, suggest that the lower part was initially deposited in an upper shoreface, deltaic environment that became progressively deeper as sea level continued to rise and the upper part of this member was deposited in a lower shoreface or open shelf environment.

### **7.3 Comparison with the Sable Subbasin and the onshore Chaswood Formation**

#### **7.3.1 Comparison with the Chaswood Formation onshore**

The Chaswood Formation is located onshore Nova Scotia, with the largest occurrence along strike, in central Nova Scotia (Figure 1.1 in Chapter 1). It has deposits of terrestrial facies, principally fluvial sands and gravels, overbank kaolinitic clays with paleosols, lacustrine shales, and lignite deposits representative of swamps (Stea and Pullan, 2001). The age of these deposits is mostly Albian to Aptian with local deposits of Neocomian age (Valanginian – Barremian) (Stea and Pullan, 2001). Most of the Chaswood Formation is therefore probably a proximal equivalent of the Logan Canyon Formation in the Orpheus Graben.

The detrital minerals of the Chaswood Formation sands are similar to those found in the Orpheus Graben (Gobeil, 2002). However some of the detrital minerals in the Chaswood Formation have a low textural maturity, suggesting a local source, whereas the textural maturity of the detrital minerals observed in the Orpheus Graben is much higher and suggests a more distant source. The detrital minerals andalusite, monazite, and cassiterite are also observed in the Chaswood Formation (Gobeil, 2002) and not in the Orpheus Graben. Aluminophosphate diagenetic minerals are observed in both the Chaswood Formation and Orpheus Graben.

### **7.3.2 Comparison with the Sable Subbasin**

The Sable Subbasin is located approximately 150 km south of the Orpheus Graben. The sediments of the Late Jurassic to Early Cretaceous were deposited in a deltaic environment (Drummond, 1992). Both the Sable Subbasin and the Orpheus Graben show similar stratigraphic units, however the sediments of the Missisauga and Logan Canyon Formation have a lower sand: shale ratio in the Sable Subbasin. This suggests that the Orpheus Graben is a more proximal equivalent of the eastern Sable Subbasin. There is also no base Cretaceous (U4 marker) nor top Missisauga unconformity (U5 marker) recognized in the Sable Subbasin, such as is observed in the Orpheus Graben. The Sable Subbasin is dominated by listric-normal, down-to-basin faulting whereas the Orpheus Graben is dominated by east-west normal faulting, with a strike-slip component (i.e. transtensional). No volcanic rocks are observed in the Sable Subbasin, with the exception of the Hesper (I-52 and P-52) wells. As mentioned earlier, these rocks correlate seismically to the volcanic rocks of the Orpheus Graben, suggesting that they are part of the same volcanic episode.

Detrital grains found in the Glenelg N-49 and Alma K-85 wells are different from the Orpheus Graben in that the sandstones at Glenelg N-49 and Alma K-85 are principally quartz arenites with minor subarkoses (Pe-Piper, 2002), with 8 to 10% feldspar (Ingram, 2002). In contrast, Orpheus Graben sands are dominantly quartz arenite and quartz wacke and typically have < 3 % feldspar. Detrital mineral grains of chromite and garnet are common in both the Sable Subbasin (Ingram, 2002) and Orpheus Graben. Detrital minerals such as zircon, tourmaline, K-feldspar with perthitic texture and quartz with

inclusions of zircon are observed in the Peskowsk A-99 and Dauntless D-35 wells (Shannon, 2003) and in the Orpheus Graben. Late Jurassic to Early Cretaceous sediments are thought to have been delivered to the Sable Subbasin by an ancient Saint Lawrence River, providing sediments from as far as the Precambrian Canadian shield and the Paleozoic metamorphic sequences in Nova Scotia (Drummond, 1992; Zentilli and Grist, 2003).

#### **7.4 Tectonic evolution**

The Scotian Basin developed during the Triassic when the super continent of Pangaea began to break up, creating a complex of northeast- and east-trending horsts, grabens and half-grabens (MacLean and Wade, 1992) (Figure 7.4). The Break-up unconformity corresponds to this event. A continued rifting event in the Late Jurassic - Lower Cretaceous, culminating in the separation of the Grand Banks from Iberia, was involved in the formation of the “Avalon Unconformity”. This unconformity is actually a multi-phase event with four erosional events identified in the Jeanne d’Arc Basin (Grant and McAlpine, 1990). The last three erosional events are thought to be present in the Orpheus Graben (see sections 7.22, 7.24 and 7.28).

The sediments of the Orpheus Graben appear to be divisible into two distinct sections, before and after the Late Jurassic. These two sections are divided by the base Cretaceous unconformity (U5 marker) in the west and the Top Missisauga unconformity (U4 marker) in the east. Below these unconformities there are large minibasins in the eastern part of the graben (a couple are also present in the western part of the graben) that are filled with large amounts of sediments that are deformed, steeply dipping, and faulted dominantly in

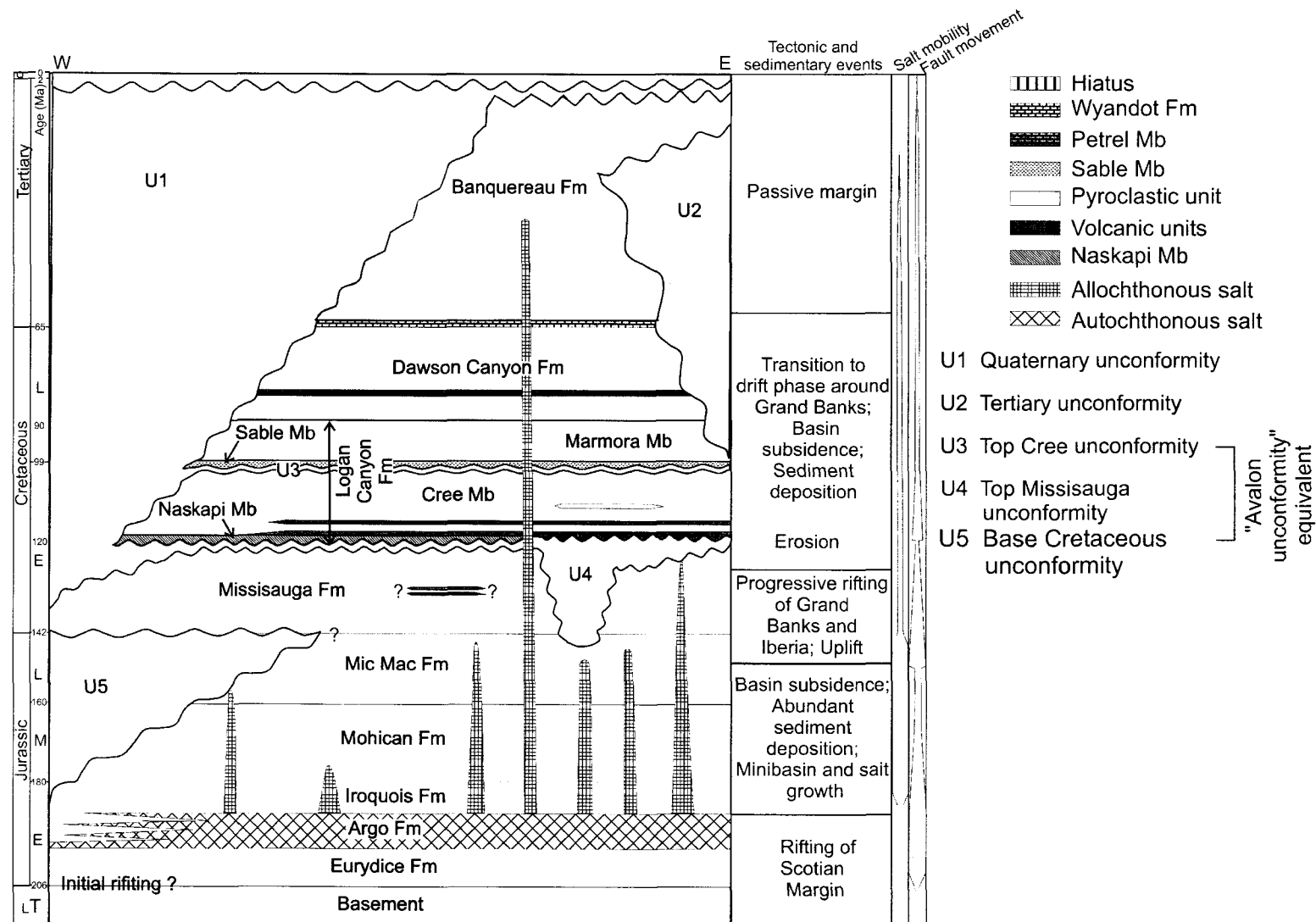


Figure 7.4. Generalized W-E stratigraphic column with an interpretation of the tectonic evolution and timing of fault and salt movement within the Orpheus Graben based on the work of this study. Time scale from Gradstein and Ogg(1996). Tectonic events modified from Grant and McAlpine (1996).

an ENE-WSW direction (Figure 7.5). Above the unconformities the sediments are comparatively flat and faulting appears to be the continuation of preexisting faults related to the growth of minibasins or salt tectonics (Figure 7.6). Salt and fault activity is much less after the Top Missisauga unconformity (U4 marker).

The dominantly ENE-WSW trending bounding faults of the Orpheus Graben probably experienced periodic motion along the Cobequid-Chedabucto-SW Grand Banks fault system (Figures 7.7 and 7.8). Motion along this fault during the renewal of extension between the Grand Banks and Iberia (Valanginian-Barremian) may have been involved in the production of the volcanic rock of the Missisauga Formation observed in the Argo F-38 well. Motion during this time and later may have also created the oldest Chaswood Formation basins and facilitated the volcanism observed on the SW Grand Banks and Fogo Seamounts (Pe-Piper and Piper, in press; Piper and Pe-Piper, 2004). The Aptian volcanic interval (Cree Member) observed in the Orpheus Graben may have resulted from motion during the Aptian-Cenomanian (Pe-Piper and Piper, in press). A mid Cretaceous (Aptian?) unconformity is observed in the Chaswood Formation, Orpheus Graben (U4 marker) and on the southwest Grand Banks (Pe-Piper et al., 1994). This unconformity is not observed in the Sable Subbasin. The presence of the shaly Naskapi and Sable members in both the Sable Subbasin and Orpheus Graben suggest a regional sea level rise that encompassed the entire Scotian Shelf or basin subsidence.

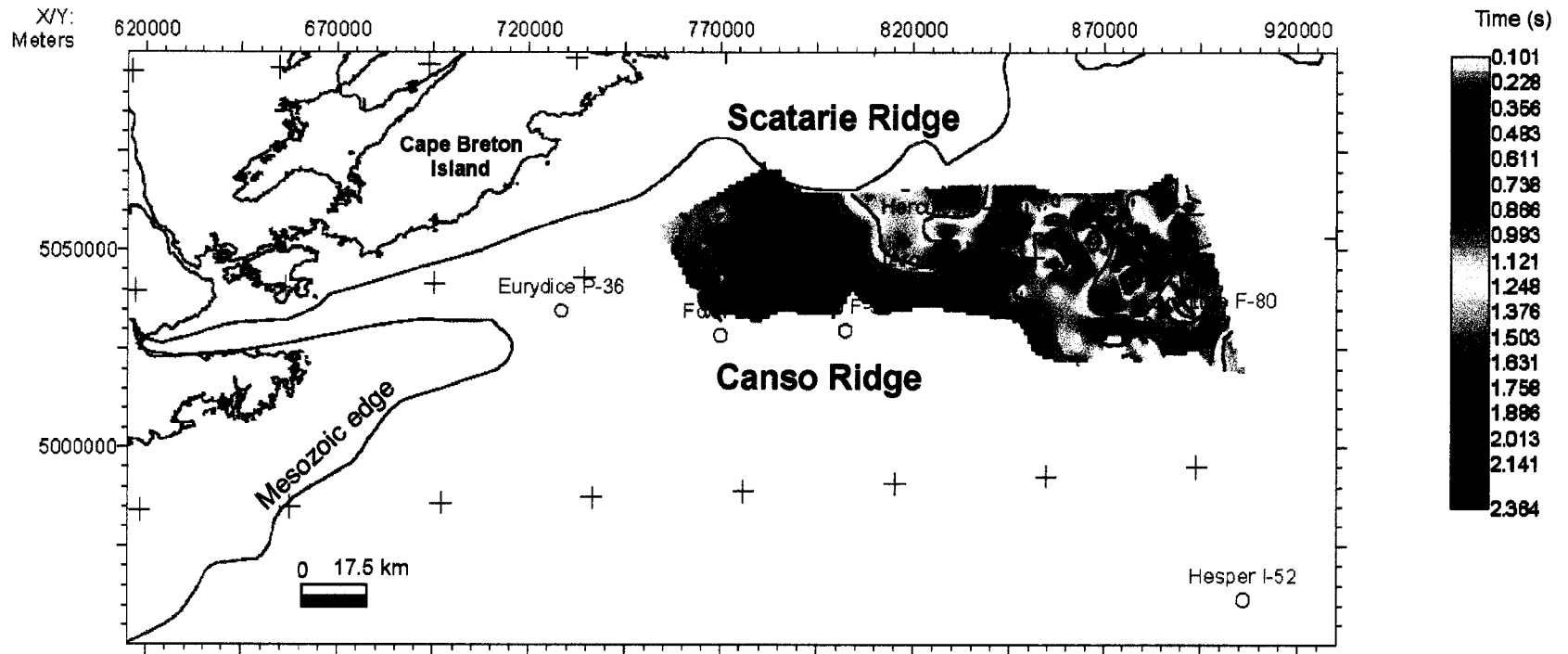


Figure 7.5. Isochron map for the U4 marker to top of Argo salt marker showing that minibasin growth was very active before the U4 marker. Contours were generated using algorithm inverse distance to a power with a grid spacing of 1 km, maximum distance of 5 km, weight of 2 and low smoothing. Mesozoic edge are from MacLean (1991). Map plotted using The KINGDOM Suite with UTM Zone 20N (66° W to 60° W) and WGS 1984 datum.

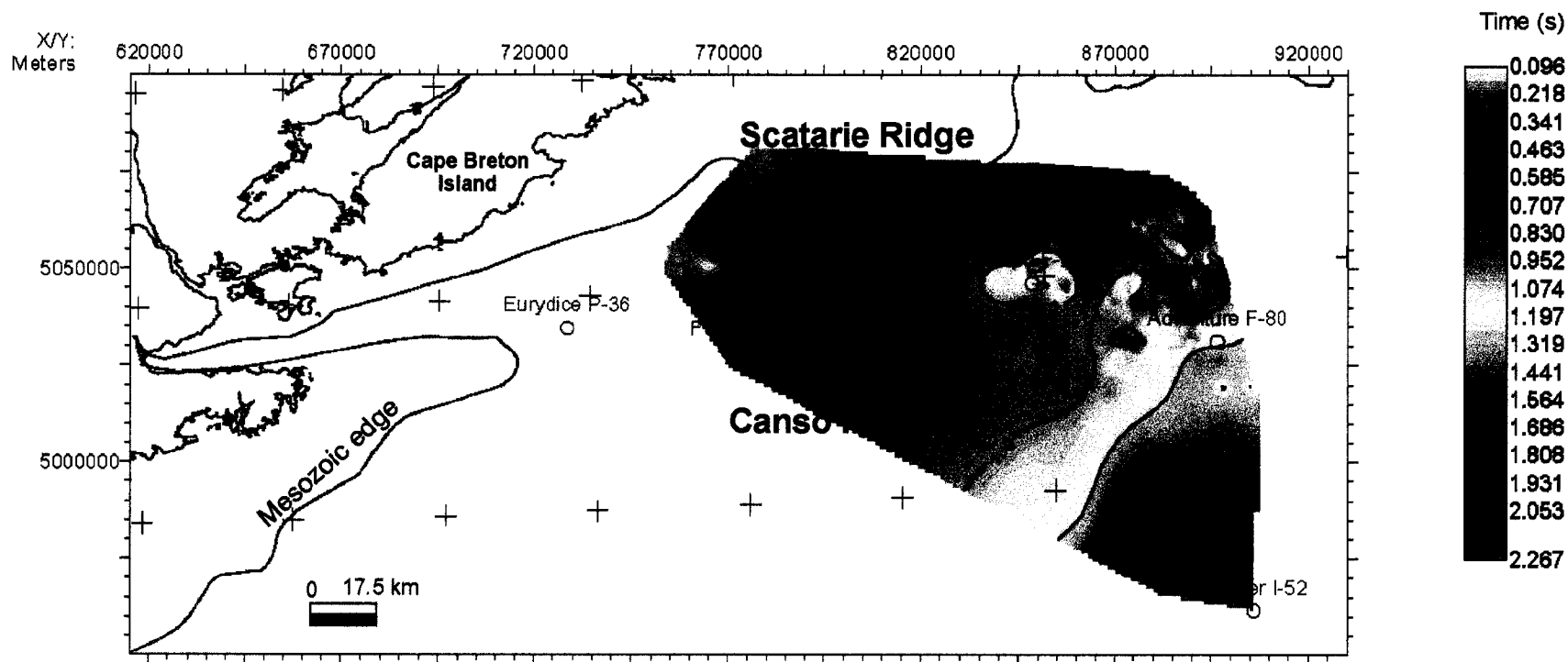


Figure 7.6. Isochron map for the U1 to U4 marker showing that there was very little minibasin growth after the U4 marker. Contours were generated using inverse distance to a power algorithm with a grid spacing of 1 km, maximum distance of 5 km, weight of 2 and low smoothing. Mesozoic edge are from MacLean (1991). Map plotted using The KINGDOM Suite with UTM Zone 20N (66° W to 60° W) and WGS 1984 datum.

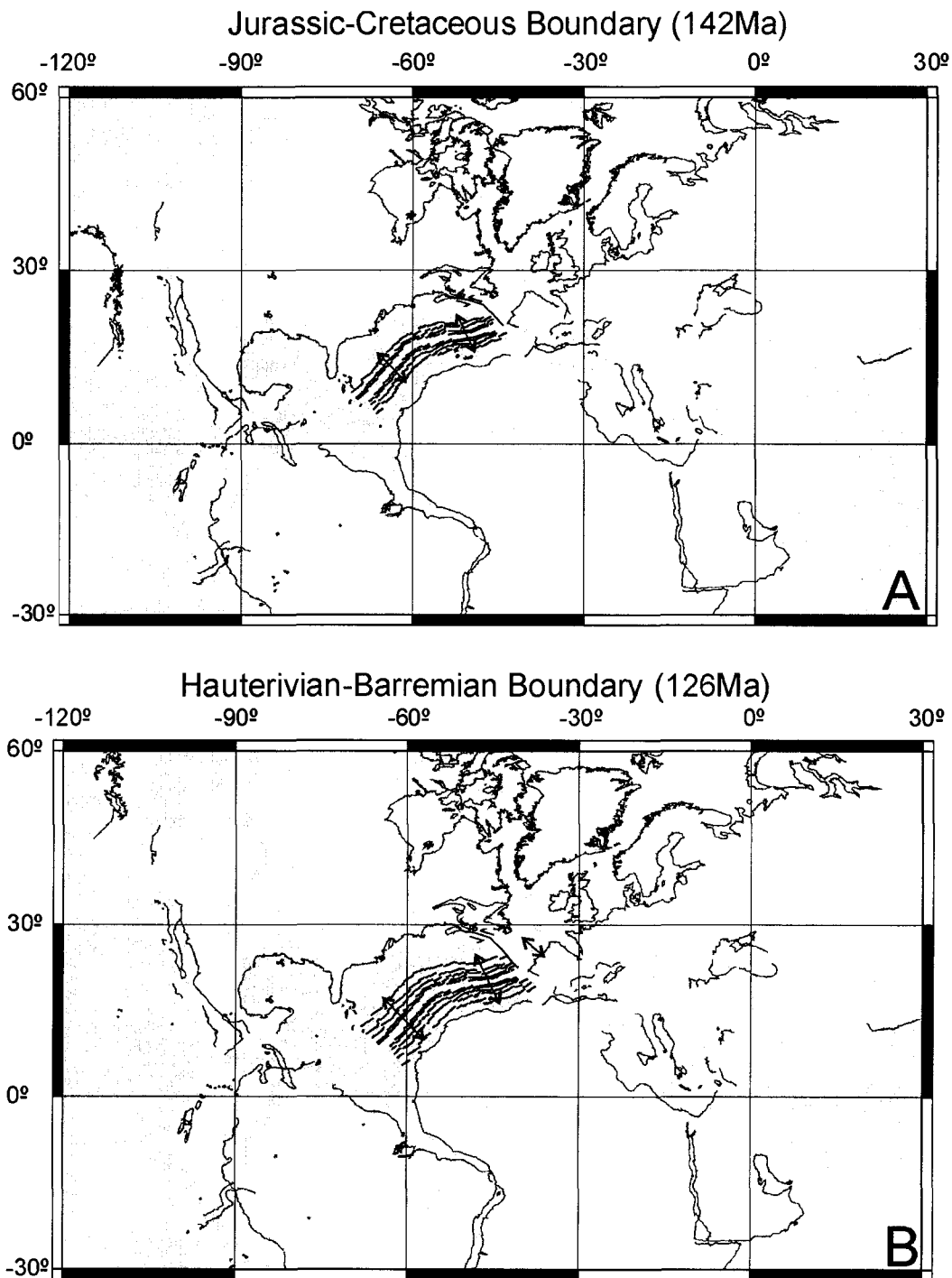
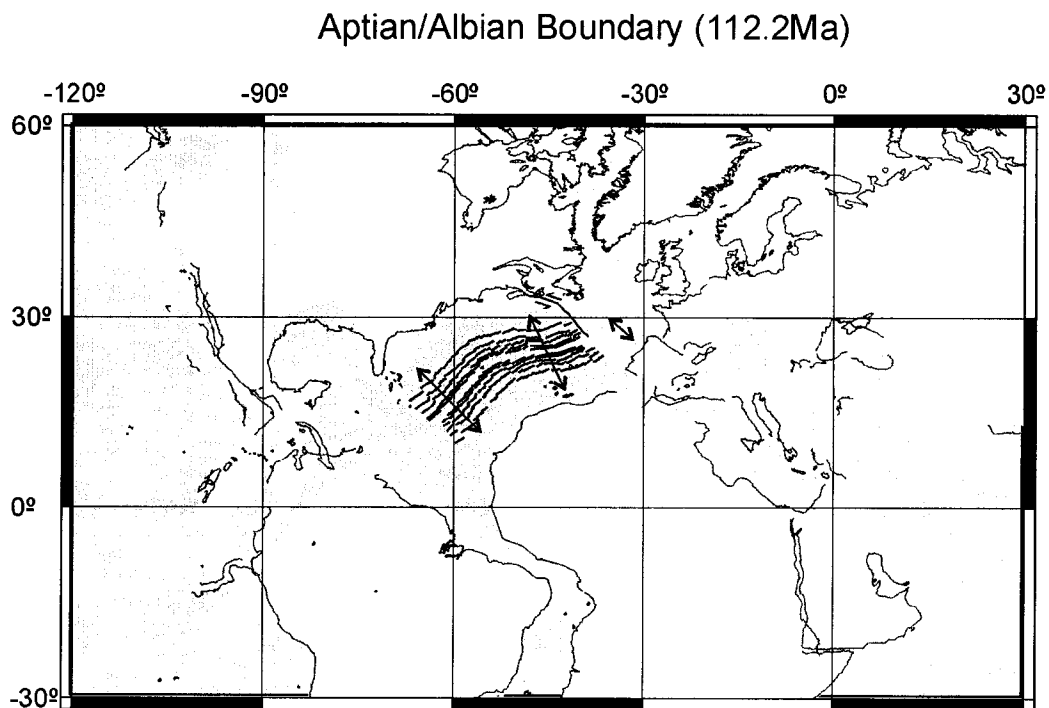
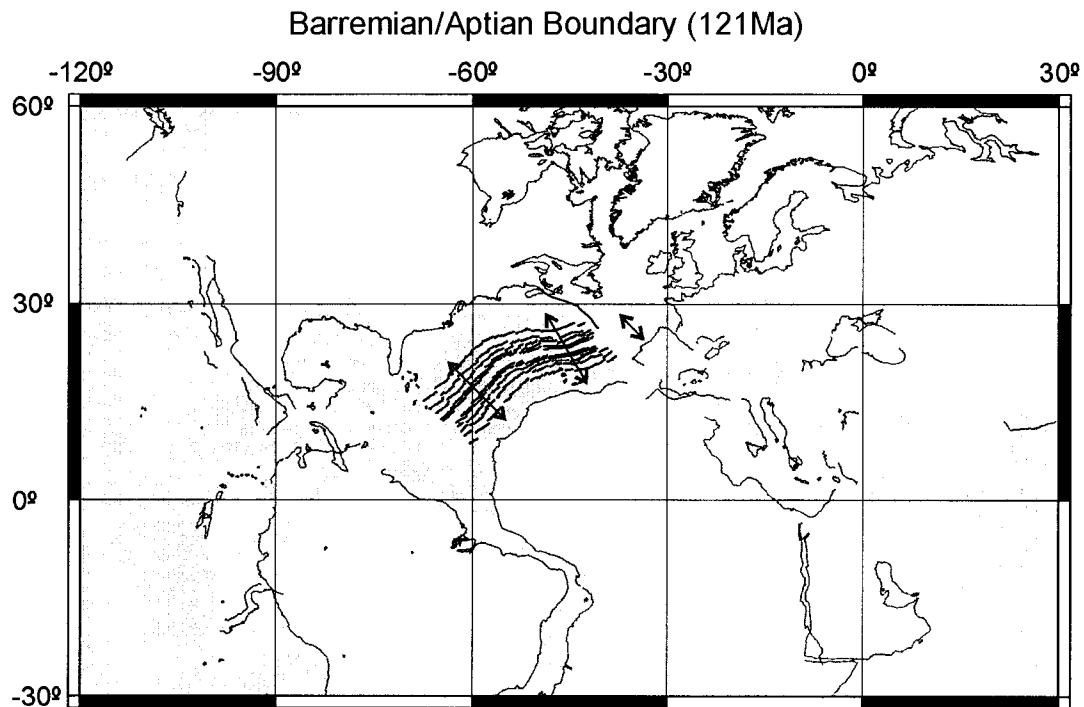


Figure 7.7. Plate tectonic map showing the Scotian margin (A) before the rifting between Grand Banks and Iberia and (B) in the initial stages of rifting between Grand Banks and Iberia. This map was made from the data files used for the publication of Hay et al., (1999) and use the paleomagnetic reference frame for North America of Harrison and Lindh (1982) and the timescale of Gradstein and Ogg (1996). (Refer to <http://www.odsn.de/odsn/services/paleomap/paleomap.html>). Maps were plotted using Generic Mapping Tools (GMT) by Wessel and Smith (1992).



7.8. Plate tectonic map showing the position of the Grand Banks and Iberia at the (A) Barremian/Aptian Boundary (121Ma) and (B) Aptian/Albian Boundary (112.2Ma). This map was made from the data files used for the publication of Hay et al., (1999) and use the paleomagnetic reference frame for North America of Harrison and Lindh (1982) and the timescale of Gradstein and Ogg (1996). (Refer to <http://www.odsn.de/odsn/services/paleomap/paleomap.html>). Maps were plotted using Generic Mapping Tools (GMT) by Wessel and Smith (1992).

Basement faulting in the northeastern part of the graben occurred as late as early Tertiary (Figure 5.8). A Tertiary (Oligocene-Miocene?) unconformity removed approximately a minimum of 0.022 s (about 45 m) of sediments and may have removed up to as much as 0.5 s (about 1000 m) of sediments (values above this are within minibasins and not included) (Figure 7.8). This unconformity is thought to possibly be the result of either sinistral motion on the E-W fault segment or dextral motion on the SSE-NNW trending SW Grand Banks Fault (Pe-Piper and Piper, in press). This unconformity may have resulted from uplift and may also account for erosion of at least 700 m of inferred sediment overlying the Chaswood Formation in the onshore areas (Grist and Zentilli, 2003).

## **7.5 Conclusions**

1. Meeting the short-term objectives of this thesis has resulted in a new understanding of the lithostratigraphy of the Orpheus Graben.

- The Logan Canyon Formation in the Orpheus Graben is divisible into the Naskapi, Cree, Sable and Marmora members and the Missisauga Formation is divisible into its Middle and Upper members.
- The Middle Member of the Missisauga Formation is characterized by thick beds of dominantly coarse to pebbly, mature, quartz-dominated sandstones that are interbedded with thin beds of shale, very fine grained sandstones, marl and limestone. The depositional environment was most likely that of an upper delta plain, which experienced a few episodes of marine incursions.

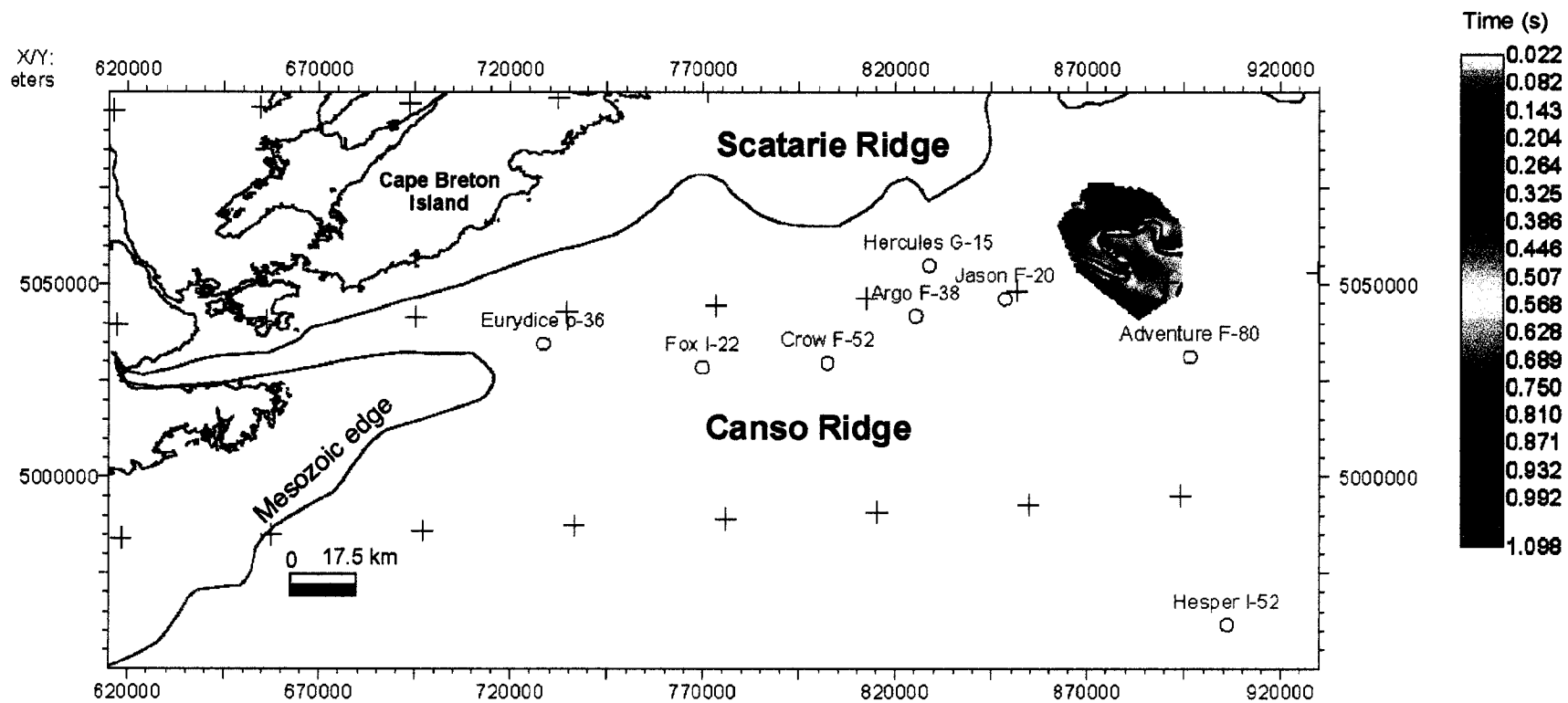


Figure 7.9. Isochron map for the U2 marker to Volcanic marker. Contours were generated using algorithm inverse distance to a power with a grid spacing of 1 km, maximum distance of 5 km, weight of 2 and low smoothing. The Mesozoic edge is from MacLean (1991). Map plotted using The KINGDOM Suite with UTM Zone 20N (66° W to 60° W) and WGS 1984 datum.

- The Upper Member of the Missisauga Formation is slightly finer grained than the Middle Member with beds of medium to coarse grained, quartz-rich sandstones that are interbedded with thin beds of silty mudstone and fine to very fine grained sandstones. The depositional environment is interpreted to be that of a lower delta plain, delta front or possible shoreface.
- The Naskapi Member is composed of alternating light grey to medium grey shales with mm scale laminations interbedded with silty mudstone and very fine to fine grained sandstones. The Naskapi Member was deposited in an open shelf environment.
- Two volcanic intervals are observed in the Orpheus Graben, one in the Missisauga Formation (in the Argo F-38 well) and one at the base of the Cree Member, overlying the top Missisauga unconformity (U4).
- The Cree Member is divisible into a lower and upper part. The lower part consists of thick beds of medium to coarse grained, quartz rich sandstones interbedded with thin beds of very fine to fine grained sandstones, silty mudstone and marl. The upper part has fine to medium grained sandstones that are interbedded with very fine to fine grained sandstones and silty mudstone beds. The sediments were probably deposited in a low relief deltaic environment, probably lower delta plain to shoreface.
- The Sable Member is characterized by a predominantly shaly interval interbedded with very fine to fine grained sandstones. Like the Naskapi Member it was deposited in an open shelf environment.

- The Marmora Member is composed of very fine to fine sandstones interbedded with fine to medium grained sandstone, silty mudstone, shale, marl and coal beds. Phosphorites and glauconite are also observed in the upper part of this member. The lower part was initially deposited in an upper shoreface, deltaic environment that became progressively deeper as sea level continued to rise and the upper part of this member was deposited in a lower shoreface or open shelf environment.
- Seismic facies possibly suggest a dominantly N-S paleocurrent direction for the Missisauga Formation and for the Cree members of the Logan Canyon Formation.

2. Three long term objectives were identified in this thesis.

- (a) The paleofluvial relationship of the Orpheus, Chaswood Formation and Sable Subbasin, can only be tentatively interpreted from the detrital petrology presented here. All observed detrital lithic clasts of both formations in Orpheus Graben could have been derived from the both Meguma and Avalon terranes. The detrital mineral grains of ilmenite (altered to pseudorutile and rutile), tourmaline, staurolite, rutile and chromite are dominantly subrounded to rounded, suggesting that they are likely from a distant source. Chromite is possible associated with ultramafic rocks that run from Quebec to eastern Newfoundland. Rather different detrital petrology in the Chaswood Formation and Sable Subbasin suggesting they had a different fluvial supply. The sediments of the Orpheus Graben are interpreted to have an important local provenance originating from the North of

the graben with an additional source from metamorphic rocks of the Taconic Orogen and Canadian Shield.

- (b) This study has shown that thick sandstones are present in both the Missisauga and Logan Canyon Formations, principally in alluvial or deltaic facies. Marine transgressions are recognized in both formations. There are many salt and fault structures in the eastern part of the graben that may be suitable for trapping hydrocarbons. Jurassic source rocks are much thicker and deeper in the eastern parts of the graben. Maturation levels were found to be higher above salt structures (Lyngberg, 1984) and the presence of many salt structures in this part of the graben and the depth of source rocks may have been enough for these rocks to have experienced thermal maturation. No further study of reservoir properties was made.
- (c) Local tectonic events can be related to the multi-phase “Avalon Unconformity”. Resulting from a combination of motion along the transform fault and the progressive rifting of Iberia and the Grand Banks.
- At least five unconformities are observed in the Orpheus Graben. The base Cretaceous unconformity (U5) near the Berriasian-Tithonian boundary, the top Missisauga Formation unconformity (U4) near the Barremian-Aptian boundary and the top Cree unconformity (U3) near the Aptian-Albian boundary are thought to correspond to the last three erosional events that make up the multi-phase “Avalon Unconformity”.

- There appears to be four types of faults in the Orpheus Graben, bounding ENE-WSW trending faults; faults possibly associated with the breakup of the Grand Banks and Iberia that do not extend above the U5 or U4 markers; ENE-WSW trending faults in the northern most part of the northeastern section of the graben that have not extend above the U2 marker; and faults related to salt tectonics that were often extend above the Petrel marker.

## REFERENCES

- Ascoli, P., 1990. Report on the biostratigraphy (Foraminifera and Ostracoda) and depositional environments of the Husky-Bow Valley *et al.* Hesper P-52 well, Scotian shelf, from 2990 to 5679 m (T.D. 5679 m) Report No.BAS-PAL.2-90PA, 5p.
- Ascoli, P., 1976. Foraminiferal and ostracod biostratigraphy of the Mesozoic-Cenozoic, Scotian Shelf, Atlantic Canada. Maritime Sediments Special Publication No.1, pp.653-771.
- Ascoli, P., 1973. Revision of the foraminiferal and ostracod biozonation of the Scotian Shelf (wells Sable Island C-67, Oneida O-25, Naskapi N-30 and Mohawk B-93); Geological Survey of Canada, Internal Report, ESGS-PAL.18-73A.
- Barss, M. S., Bujak, J.P., and Williams, G.L., 1979. Palynology zonation and correlation of sixty-seven wells, eastern Canada; Geological Survey of Canada, Paper 78-24, 118p.
- Bujak, J.P., 1976. Palynological analysis of Shell Argo F-38, Scotian Shelf, Geological Survey of Canada, Internal Report, EPGS-PAL.27-76JPB.
- Cohen, J.K. and Stockwell, Jr. J.W., 2003, CWP/SU: Seismic Unix Release No.37: a free package for seismic research and processing, Center for Wave Phenomena, Colorado School of Mines. (<http://www.cwp.mines.edu/cwpcodes/>)
- Donohoe, H.V., and Grantham, R.G., 1989. Geological Highway Map of Nova Scotia, second edition, Atlantic Geoscience Society, Halifax, AGS Special Publications No.1.
- Drummond, K.J., 1992. Geology of Venture, a geopressured gas field, offshore Nova Scotia, (ed.) M.T. Halbouty, *in* Giant oil and gas fields of the decade 1978-1988: AAPG Memoir 54, pp.55-71.
- Fleischer, M., Cabri, L.J., Cho, G.Y., and Pabst, A., 1978. New mineral names. American Mineralogist, v.63, pp.424-427.
- Franke, R., and Nielson, G., 1980. Smooth Interpolation of Large Sets of Scattered Data. International Journal for Numerical Methods in Engineering, 15, pp.1691-1704.
- Given, M.M., 1977. Mesozoic and Early Cretaceous geology of offshore Nova Scotia. Bulletin of Canadian Petroleum Geology, v.25, pp.63-91.

- Gobeil, J., 2002. Stratigraphy, sedimentology, and provenance of the Chaswood Formation, West Indian Road pit, Shubenacadie, Nova Scotia. Masters Thesis, Dalhousie University, 205p.
- Gradstein, F., and Ogg, J., 1996. A Phanerozoic time scale, episodes, v.19, nos.1 & 2.
- Grant, A.C., and McAlpine, K.D., 1990. The continental margin around the Newfoundland, Geological and historical perspective, Chapter 6, (ed.) M.J. Keen and G.L. Williams, *in* Geology of the Continental Margin of Eastern Canada, Geological Survey of Canada, Geology of Canada, no.2 pp.239-292 (also Geological Society of America, The Geology of North America, v.I-1)
- Greensmith, J.T., 1978. Petrology of the sedimentary rocks, 6<sup>th</sup> ed., George Allen & Unwin, London, 241p.
- Grist, A.M. and Zentilli, M., 2003. Post-Paleocene cooling in the south Canadian Atlantic region: evidence from apatite fission track models. *Canadian Journal of Earth Science*, v.40, pp.1279-1297.
- Harrison, C. G. A., and Lindh, T., 1982, A polar wandering curve for North America during the Mesozoic and Cenozoic: *Journal of Geophysical Research*, v.87, pp.1903-1920.
- Hay, W.W., DeConto, R., Wold, C.N., Wilson, K.M., Voigt, S., Schulz, M., Wold-Rossby, A., Dullo, W.-C., Ronov, A.B., Balukhovskiy, A.N. and Soeding, E., 1999. Alternative global Cretaceous paleogeography, (ed.) Barrera, E. and Johnson, C., *in* The Evolution of Cretaceous Ocean/Climate Systems, Geological Society of America Special Paper 332, pp.1-47.  
(<http://www.odsn.de/odsn/services/paleomap/paleomap.html>)
- Holser, W.T., Clement, G.P., Jansa, L. F., and Wade, J.A., 1988. Evaporite deposits of the North Atlantic rift; in Triassic-Jurassic rifting: continental breakup and the origin of the Atlantic Ocean and passive margins, (ed.) W. Manspeizer; *Developments in Geotectonics* 22, Part B, pp.525-556.
- Ingram, S., 2002. Lower Cretaceous lithofacies, syn-sedimentary deformation, and petrology of Glenelg (N-49) and Alma (K-85), Scotian Basin. Honours Thesis, Saint Mary's University, Halifax, Nova Scotia, 50p.
- Jansa, L.F., and Wade, J.A., 1975a. Geology of the continental margin off Nova Scotia and Newfoundland, (ed.) W.J.M. van der Linden and J.A. Wade, *in*: Offshore Geology of Eastern Canada, v.2, Regional geology, Geological Survey of Canada, Paper 74-30, v.2, pp.51-106.
- Jansa, L.F., and Wade, J.A., 1975b. Paleogeography and sedimentation in the Mesozoic and Cenozoic, southeastern Canada, (ed.) W.J.M. van der Linden and J.A. Wade,

In: Canada's Continental Margins and Offshore Petroleum Exploration. Canadian Society of Petroleum Geologists, Memoir 4, pp.79-102.

Jansa L.F. and Pe-Piper, G., 1985. Early Cretaceous volcanism on the northeastern American margin and implications for plate tectonics. Geological Society of America Bulletin, v.96, pp.83-91.

Jansa L.F., and Pe-Piper, G., 1988. Middle Jurassic to Early Cretaceous igneous rocks along eastern North American continental margin. The American Association of Petroleum Geologists Bulletin, v.72, No.3(March), pp.347-3661.

Jenkins, W.A.M., Ascoli, P., Gradstein, F.M., Jansa, L.F., and Williams, G.L., 1974. Stratigraphy of the Amoco IOE A-1 Puffin B-90 well, Grand Banks of Newfoundland; Geology survey of Canada, Paper74-61, 12p.

King, L.H., and MacLean, B.C., 1970. Continuous seismic reflection study of Orpheus gravity anomaly. The American Association of Petroleum Geologists Bulletin, v.54, No.11, pp.2007-2031.

Koukouvelas, I., Pe-Piper, G., and Piper, D.J.W., 2002. The role of dextral transpressional faulting in the evolution of an Early Cretaceous mafic-felsic plutonic and volcanic complex; Cobequid Highlands, Nova Scotia, Canada. Tectonophysics, v.348, pp.219-246.

Lynberg, E., 1984. The Orpheus Graben, offshore Nova Scotia: palynology, organic geochemistry, maturation and time-temperature history. Masters Thesis, University of British Columbia, 159p.

MacLean, B.C., and Wade, J.A., 1993. Seismic markers and stratigraphic picks in the Scotian Basin wells: East coast basin atlas series. Geological Survey of Canada. 276p.

MacLean, B.C., and Wade, J.A., 1992. Petroleum geology of the continental margin south of the islands of St. Pierre and Miquelon, gulf of St. Lawrence; Canadian Society of Petroleum Geologists Bulletin, v.40, pp.222-253.

MacLean, B.C., 1991. Structure and isopach 1: depth to pre-Mesozoic basement and oceanic layer 2; in East Coast Basin Atlas Series: Scotian Shelf; Atlantic Geoscience Centre, Geological Survey of Canada, p.75.

Magnusson, D.H., 1973. The Sable Island deep test of the Scotian Shelf; ed. P.J. Hood; in Earth Science Symposium on Offshore Eastern Canada, Geological Survey of Canada, Paper71-23, pp.253-266.

McIver, N.I., 1972. Cenozoic and Mesozoic stratigraphy of the Nova Scotia shelf; Canadian Journal of Earth Science, v.9, pp.54-70.

- Mobil Oil Canada, 1975. Mobil Tecto Gulf Adventure F-80: well history report; National Energy Board, Calgary, Alberta.
- Nesse, W.D., 1991. Introduction to optical mineralogy, second ed. Oxford University Press, New York. 335p.
- Pe-Piper G., and Piper, D.J.W., in press. The effects of strike-slip motion along the Cobequid-Chedabucto-SW Grand Banks fault system on the Cretaceous – Tertiary evolution of Atlantic Canada. *Canadian Journal of Earth Science*.
- Pe-Piper, G., 2002. Progress report on Chaswood Formation and its relevance to the Scotian Basin. For: Petroleum Research Atlantic Canada (SOEI), 70p.
- Pe-Piper, G., and Jansa L.F., 1999. Pre-Mesozoic basement rocks offshore Nova Scotia, Canada: New constraints on the accretion history of the Meguma terrane. *Geological Society of America Bulletin*, v.111, no.12, pp.1773-1791.
- Pe-Piper, G., Jansa L.F., and Palacz, Z., 1994. Geochemistry and regional significance of the Early Cretaceous bimodal basalt-felsic associations on Grand Banks, eastern Canada. *Geological Society of America Bulletin*, v.106, pp.1319-1331.
- Pe-Piper, G., 1991. Granite and associated mafic phases, North River Pluton, Cobequid Highlands, Nova Scotia, *Atlantic Geology*, v.27; 1, pp.15-28.
- Pe-Piper, G., Piper, D.J.W., and Clerk, S.B., 1991. Persistent mafic igneous activity in an A-type granite pluton, Cobequid Highlands, Nova Scotia. *Canadian Journal of Earth Science*, v.28, pp.1058-1072.
- Pe-Piper, G., and Jansa L.F., 1987. Geochemistry of late Middle Jurassic-Early Cretaceous igneous rocks on the eastern North American margin. *Geological Society of America Bulletin*, v.99, pp.803-813.
- Pe-Piper, G., and Jansa L.F., 1985. Early Cretaceous volcanism on the northeastern American margin and implications for plate tectonics. *Geological Society of America Bulletin*, v.96, pp.83-91.
- Piper D.J.W., and Pe-Piper, G., 2004. The effects of strike-slip motion along the Cobequid-Chedabucto-SW Grand Banks fault system on the Cretaceous – Tertiary evolution of Atlantic Canada. Abstracts from the Atlantic Geoscience Society, January 30-31, 2004, Moncton, New Brunswick, Canada.
- Pettijohn, F.J., 1987. Sand and sandstone. Springer-Verlag, New York, 553p.

- Shannon, J., 2003. Lower Cretaceous lithofacies and petrography of Peskowsk A-99 and Dauntless D-35 wells, Scotian Basin. Honours Thesis, Saint Mary's University, Halifax, Nova Scotia, 121p.
- Shell Canada Limited, 1972. Eurydice P-36 well history report, National Energy Board, Calgary, Alberta.
- Shell Canada Limited, 1971a. Shell Argo F-38: well history report; National Energy Board, Calgary, Alberta.
- Shell Canada Limited, 1971b. Shell Crow F-52: well history report; National Energy Board, Calgary, Alberta.
- Shell Canada Limited, 1971c. Shell Fox I-22: well history report; National Energy Board, Calgary, Alberta.
- SMT, 2003. Seismic Micro-technology. <http://www.seismicmicro.com>
- Stea, R.R., and Pullan S.E., 2001. Hidden Cretaceous basins in Nova Scotia. *Canadian Journal of Earth Science*, v.38, pp.1335-1354.
- Union Oil Company of Canada, 1975. Union et al. Hercules G-15: well history report, National Energy Board, Calgary, Alberta.
- Union Oil Company of Canada, 1974. Union et al. Jason C-20: well history report, National Energy Board, Calgary, Alberta.
- Velde, B., 1977. *Clays and clay minerals in Natural and synthetic systems*: Elsevier, Amsterdam, 218p.
- Wade, J.A., and MacLean, B.C., 1990. The geology of the southeastern margin of Canada, Chapter 5, (ed.) M.J. Keen and G.L. Williams, *in* *Geology of the Continental Margin of Eastern Canada*, Geological Survey of Canada, *Geology of Canada*. no.2, pp.167-238 (also *Geological Society of America, The Geology of North America*, v.I-1).
- Wade, J.A., MacLean, B.C., and Williams, G.L., 1995. Mesozoic and Cenozoic stratigraphy, eastern Scotian Shelf: new interpretations. *Canadian Journal of Earth Science*, v.32, pp.1462-1473.
- Weir-Murphy, S.L., MacRae, A., and Pe-Piper, G., submitted. A probable dinosaur bone from the Cretaceous upper Logan Canyon Formation, Orpheus graben, offshore Nova Scotia. *Atlantic Geology*.
- Welsink, H.J., Dwyer, J.D., and Knight, R.J., 1989. Tectono-stratigraphy of passive margins off Nova Scotia, Chapter 14, (ed.) A.J. Tankard and H.R. Balkwill, *in*

Extensional Tectonics and Stratigraphy of the North Atlantic Margins; American Association of Petroleum Geologists, pp.215-231.

Wessel, P., and Smith, W.H.F., 1991. Free software helps map and display data. Eos, Transactions, American Geophysical Union, v.72, no.41, pp.441, 445-446, 08 Oct 1991.

Williams, G. L., 1975. Dinoflagellate and spore stratigraphy of the Mesozoic-Cenozoic, offshore eastern Canada, (ed.) W.J.M. van de Linden and J.A Wade, *in* Offshore Geology of Eastern Canada; v.2, Regional geology; Geological Survey of Canada, Paper74-30, v.2, pp.107-161.

Williams, G.L., 1973. Palynological analysis of Shell Fox I-22, Geological Survey of Canada, Internal Report, EPGs-PAL19-73GLW.